

University of Cincinnati

Date: 7/14/2016

I, Alireza Nemati, hereby submit this original work as part of the requirements for the degree of Doctor of Philosophy in Electrical Engineering.

It is entitled:

Designing, Modeling and Control of a Tilting Rotor Quadcopter

Student's name: Alireza Nemati

This work and its defense approved by:

Committee chair: Manish Kumar, Ph.D.

Committee chair: Ali Minai, Ph.D.

Committee member: Raj Bhatnagar, Ph.D.

Committee member: Kelly Cohen, Ph.D.

Committee member: Rui Dai, Ph.D.



22187

Designing, Modeling and Control of a Tilting Rotor Quadcopter

A Dissertation submitted to the
Graduate School
of the University of Cincinnati
in partial fulfillment of the
requirements of the degree of

Doctor of Philosophy

in the Department of Electrical Engineering and Computing Systems
of the College of Engineering and Applied Sciences

by

Alireza Nemati

M.S. Shahrood University of Technology

August 2007

Committee Chair: Manish Kumar, Ph.D.

Ali Minai, Ph.D.

An Abstract of
Designing, Modeling and Control of a Tilting Rotor Quadcopter
by
Alireza Nemati

Submitted to the Graduate Faculty as partial fulfillment of the requirements for the
Doctor of Philosophy Degree in Electrical Engineering

University of Cincinnati
March 2016

The aim of the present work is to model, design, control, fabricate and experimentally study quadcopter with tilting propellers. A tilting quadcopter is an aerial vehicle whose rotors can tilt along axes perpendicular to their respective axes of rotation. The tilting rotor quadcopter provides the added advantage in terms of additional stable configurations, made possible by additional actuated controls, as compared to a traditional quadcopter without titling rotors. The tilting rotor quadcopter design is accomplished by using an additional motor for each rotor that enables the rotor to rotate along the axis of the quadcopter arm.

Conventional quadcopters, due to limitation in mobility, belong to a class of under-actuated robots which cannot achieve any arbitrary desired state or configuration. For example, the vehicle cannot hover at a defined point at a tilted angle. It needs to be completely horizontal in order to hover. An attempt to achieve any pitch or roll angle would result in forward (pitch) motion or lateral (roll) motion. This proposed tilting rotor concept turns the traditional quadcopter into an over-actuated flying vehicle allowing us to have complete control over its position and orientation.

In this work, a dynamic model of the tilting rotor quadcopter vehicle is derived for flying and hovering modes. The model includes the relationship between vehicle orientation angles and rotor tilt-angles. Furthermore, linear and nonlinear controllers have been designed to achieve the hovering and navigation capability while having any desired pitch and/or roll orientation. In the linear approach, the four independent speeds of the propellers and their rotations about the axes of quadcopter arms have been considered as inputs. In order to start tracking a desired trajectory, first, hovering from the initial starting point is needed. Then, the orientation

of the vehicle to the desired pitch or roll angle is obtained. Subsequently, any further change in pitch or roll angles, obtained using a linear controller, result in motion of the quadcopter along the desired trajectory.

The dissertation then presents a nonlinear strategy for controlling the motion of the quadcopter. The overall control architecture is divided into two sub-controllers. The first controller is based on the feedback linearization control derived from the dynamic model of the tilting quadcopter. This controls the pitch, roll, and yaw motions required for movement along an arbitrary trajectory in space. The second controller is based on two Proportional Derivative (PD) controllers which are used to control the tilting of the quadcopter independently along the pitch and the yaw directions respectively. The overall control enables the quadcopter to combine tilting and movement along a desired trajectory simultaneously.

Furthermore, the stability and control of tilting-rotor quadcopter is presented upon failure of one propeller during flight. On failure of one propeller, the quadcopter has a tendency of spinning about the primary axis fixed to the vehicle as an outcome of the asymmetry about the yaw axis. The tilting-rotor configuration is an over-actuated form of a traditional quadcopter and it is capable of handling a propeller failure, thus making it robust in one propeller failure during the flight. The dynamics of the vehicle once the failure accrued is derived and a controller is designed to achieve hovering and navigation capability.

The dynamic model and the controller of the vehicle were verified with the help of numerical studies for different flight scenarios as well as failure mode. Subsequently, two different models of the vehicle were designed, fabricated and tested. Experimental results have validated the dynamical modeling and the flight controllers.

Copyright 2016, Alireza Nemati

This document is copyrighted material. Under copyright law, no parts of this document may be reproduced without the expressed permission of the author.

Acknowledgments

First and foremost, I would like to express my sincere gratitude to my advisor Professor Manish Kumar for the continuous support of my Ph.D. study and related research, for his patience, motivation, generosity, enthusiasm and immense knowledge. I appreciate all his contribution of time, ideas, encouragement and financial support that he provided. His continuous guidance helped me carry out research and write this thesis. During my study, he was not only a great advisor for problems related to my work, but also an exceptional consultant for other situations I faced.

I wish to express my sincere thanks to Professor Ali Minai, my thesis advisor, for his valuable guidance and encouragement extended to me. I am thankful to Dr. Kelly Cohen for all his motivations he gave not only to me but also to the other members of our team, for his guidance and suggestions.

Besides my advisors, I would like to thank Professor Raj Bhatnagar, and Professor Rui Dai, for their insightful comments, assistance and encouragement throughout my project.

In addition, a thank you to Younes Kheradmand, who was my boss before I started my Ph.D. for 5 years. I really appreciate all the advise he provided me like a father and encouragements he gave like a friend during my career. A thank you also to professor Abdullah afjeh who has inspired me the professionalism.

My appreciation also extends to my fellow lab mates. Balaji R Sharma, Baisravan Homchaudhuri and Ruoyu Tan who helped me settle in the lab for first couple of months. I would like to thank my friends at the Cooperative Distributed Systems Laboratory for the wonderful times, long meetings and exciting brainstorming discussions we had. Two of my colleagues cannot remain nameless, Mohammad Sarim and Mohammadreza Radmanesh for the stimulating discussions, for the sleepless nights we were working together before competitions and deadlines, for the travels we made for different conferences and for all the fun we had in the

last couple years.

The final words in acknowledgments are usually reserved to those dearest to the author. I do not wish to break this tradition. Without the love and support from my family, I would not have come this far.

Table of Contents

Abstract	iii
Acknowledgments	v
Contents	vii
List of Tables	x
List of Figures	xi
List of Abbreviations	xiv
1 Introduction	1
1.1 Objectives	1
1.2 Approaches	1
1.3 Motivation for this work	2
1.4 Contribution	5
1.5 Publications	5
1.6 Organization of Thesis	7
2 History of the Quadcopters	9
2.1 A Brief History of Quadcopters	9
2.1.1 The Early History of Quadcopters	9
2.1.2 History of Tilt Rotor Vertical Takeoff Vehicles	12
2.1.3 History of Tilt Rotor Quadcopter	16
2.2 Current Quadcopters	18
2.2.1 Quadcopters with Tilting Mechanism	20

3	Dynamic Modeling	27
3.1	Traditional Quad-rotor	27
3.2	Tilting Rotor Quadcopters	30
4	Control System	35
4.1	Linear Controller Design	35
4.1.1	Proportional Derivative Control	35
4.2	Nonlinear Control	41
4.2.1	Feedback Linearization	42
4.2.2	PD Based Tilting Angle Controller	47
4.3	Stability Analysis	48
5	Fault Tolerant Flight	54
5.1	Introduction	54
5.2	Fault Detection	56
5.3	Dynamic Modeling	56
5.3.1	Tilting Rotor Quadcopters with One Propeller Failure	57
5.4	Controller Design	61
5.5	Linearization and Stability Analysis	63
6	Hardware design	70
6.1	Description of the Prototype	70
6.1.1	Central body	71
6.1.2	Tilting Mechanism	71
6.2	Drive System	77
6.2.1	Motors	77
6.2.2	Batteries	78
6.3	Avionics	78
6.3.1	Control Board	78
6.3.2	Communications	79

7 Numerical Simulations and Experimental Results	80
7.1 Numerical Simulations	80
7.1.1 Simulation set-up	80
7.1.2 Tilt-Rotor Quadcopter Simulation results	81
7.1.3 Feedback Linearization Numerical Simulation	84
7.1.4 Fault Tolerant Numerical Simulation	87
7.1.4.1 Hover Flight	87
7.1.4.2 Tracking a Trajectory	90
7.2 Preliminary Experimental Results	94
7.2.1 Hovering on the spot	94
7.2.2 Trajectory	96
7.2.2.1 Line	96
7.2.2.2 Box	98
8 Conclusions and future work	101
8.1 Conclusions	101
8.2 Future Works	102
References	104

List of Tables

6.1	Specifications of the Prototype	73
6.2	Vehicle's component mass details.	74
6.3	Power output from ESC, 4S LiPo, 10x47 Propeller.	78

List of Figures

2-1 Gyroplane.	10
2-2 The Oemichen2	10
2-3 De Bothezat	11
2-4 Convertawings, Model A	12
2-5 George Lehbergers 1930 tilting propeller vertical take-off “flying machine”	13
2-6 Three-view drawing of the Focke-Achgelis FA-269 convertiplane	14
2-7 The Bell XV-3, during flight testing.	15
2-8 XV-15 taking off	15
2-9 The V-22 Osprey, during transition flight	16
2-10 X-19 in hovering flight	17
2-11 Bell X-22A	17
2-12 The Quad-TiltRotor concept, University of Patras.	20
2-13 CAD design of the CQTR, Istanbul Commerce University.	21
2-14 The Configuration of the QTR UAV under research a) Quadcopter mode b) Flying wing mode, Beihang University.	22
2-15 CQTR with integrated actuators in different flight configurations.	23
2-16 Overview of developed CQTR, Nihon University.	24
2-17 CAD model of the quadcopter with tilting propellers, Max Planck Institute.	25
2-18 Vehicle prototype on the ball joint rig flight test, Cranfield University.	26
3-1 Schematic diagram showing the coordinate systems and forces acting on the quad-rotor	29
3-2 Coordinate Frames and Free body diagram of Tilting Quadcopter	31
4-1 The block diagram of position and orientation control algorithm	36

4-2	Hovering with tilted arms	38
5-1	Free body diagram of tilt-rotor quadcopter upon propeller failure	58
5-2	Vehicle's Position	69
5-3	Vehicle's Orientation	69
6-1	The CAD model of the tilting quadcopter	70
6-2	HS-5087MH HV Digital Micro Servo.	72
6-3	The CAD model of components of the tilting mechanism.	72
6-4	The real model of the first model of tilting Quadcopter.	73
6-5	The CAD model of transparent tilting mechanism	75
6-6	The CAD model of tilting mechanism mounted on the arm with the servo and the motor	76
6-7	The CAD and the actual model of the prototype.	76
6-8	850 kv brushless DC motors	77
7-1	The reference (commanded) pitch and roll angle	81
7-2	The actual trajectory followed by the UAV in 3-dimensions	81
7-3	The actual orientation of the vehicle in 3 directions	82
7-4	The angle of each arm during simulation	82
7-5	The speed of each rotor	83
7-6	The enlarged view of the figure 8	84
7-7	Quadcopter trajectory in three-dimensional space	85
7-8	Position and orientation of the quadcopter: altitude vs. time (top left), x-position vs. y-position (top right), pitch vs. time (bottom left), and yaw vs. time (bottom right).	85
7-9	The reference roll (bottom) and actual roll angle (top) during the flight.	86
7-10	Inputs generated by the proposed feedback linearization method.	86
7-11	The actual trajectory followed by the UAV in 3- dimensions	88
7-12	Vehicle's trajectory in X,Y and Z	89
7-13	Vehicle's trajectory in X,Y and Z	89

7-14 The actual orientation	90
7-15 The actual trajectory followed by the UAV in 3- dimensions	91
7-16 Vehicle's trajectory in X,Y and Z	91
7-17 Vehicle's trajectory in X,Y and Z	92
7-18 The actual orientation	93
7-19 Angular velocity around Z axis	93
7-20 Snapshot of the hovering with the tilted angle	94
7-21 Vehicle's trajectory in 3-dimension	95
7-22 The actual orientation of the vehicle along the three directions	95
7-23 Vehicle's trajectory in 3-dimension	96
7-24 The actual orientation	97
7-25 Vehicle's position versus time graph along the 3 directions	97
7-26 Vehicle's trajectory in 3-dimension	98
7-27 The actual orientation	99
7-28 Vehicle's position versus time graph along the 3 directions	99

List of Symbols

ACAH	Attitude Command Attitude Hold
ESC	Electronic Speed Controller
FEM	Finite Element Method
FPGA	Field Programmable Gate Array
IMU	Inertial Measurement Unit
MV	Measured values
PWM	Pulse Width Modulation
RC	Remote Control
rpm	Revolutions per minute
Rx	Receive
Tx	Transmitt
SP	Setpoints for the controller
UART	Universal Asynchronous Receiver/Transmitter
GW	Gross Weight
lipo	lithium polymer
3D	Three dimensional
QTW	Quad Tilt Wing
QTR	Quad Tilt Rotor
UAV	Unmanned Air Vehicle
VTOL	Vertical TakeOff and Landing
V/STOL	Vertical/Short TakeOff and Landing

Chapter 1

Introduction

This chapter discusses the objectives, approaches, applications and contributions of the research. The list of publications resulting from the present work are also provided.

1.1 Objectives

The primary objective of this work is to model, design, control, fabricate and experimentally study quadcopter with tilting propellers. The tilting propellers are expected to result in more stability as well as the ability to follow any arbitrary trajectory in a smoother manner as compared to the conventional quadcopters and also add the capability to continue the mission in the case of one propeller failure.

In addition to this advantage, the tilting mechanism turns the conventional quadcopter, which is an under-actuated vehicle, to an over-actuated robot which allows full control over a wide range of state-space. In order to incorporate this new mechanism, which makes the dynamics of the quadcopter highly nonlinear, this research focuses on developing novel control mechanisms in order to achieve the desired flight requirements as well as make the vehicle robust to one propeller failure during the flight.

1.2 Approaches

In order to accomplish the objectives set forth for this study, the new equations of motion for the tilting quadcopter are first derived mathematically. The derived equations is used to design

a linear and nonlinear controller. The numerical simulation of the platform is programmed in both Simulink and MATLAB for solving the highly nonlinear dynamic equations of motion. The simulation environment is then used to verify the performance of the developed control mechanisms. Once the simulation results indicate achievement of desired performance after running with different flight situations, a 3D model of the new platform is designed using SolidWorks. The designed 3D model is used to make and 3D print different parts and fabricate the vehicle. Several attempts are made to improve the platform design. Each attempt focused on factors such as the weight, the robustness and the functionality of the platform. Several set of real-world flight tests are carried out to evaluate the capability of the platform in different flight conditions. The actual flight tests have validated the derived equations for the dynamic model as well as the designed control systems.

1.3 Motivation for this work

Quadcopters are one of the most popular designs for miniature aerial vehicles (MAVs) [56] due to their vertical take-off and landing capability, simplicity of construction, maneuverability, and ability to negotiate tight spaces making it possible for use in cluttered indoor areas. Due to these capabilities, quadcopters have recently been considered for a variety of applications both in military and civilian domains [21, 49, 18, 12]. In particular, quadcopter MAVs have been explored for applications such as surveillance and exploration of disasters [11, 33, 67] (such as fire, earthquake, and flood), search and rescue operations [17, 73], monitoring of hazmat spills [2], and mobile sensor networks [19, 72].

Blimps [91], fixed-wing planes, single rotor helicopters, bird-like prototypes [28], coaxial dual rotor helicopters [53], quad-rotors [68, 69, 70, 71] and tilting rotor quadcopters [51, 55, 54, 26, 61, 78] are examples of different configurations and propulsion mechanisms that have been developed to allow 3D movements in aerial platforms. Each of these has advantages and drawbacks. This dissertation focuses on quadcopters or quad-rotors which consist of four rotors in total, with two pairs of counter-rotating, fixed-pitch blades located at the four corners of the aircraft. This kind of design has two main advantages over the comparable vertical takeoff and

landing (VTOL) Unmanned Aerial Vehicles (UAVs) such as single rotor helicopters. Firstly, quad-rotors do not require complicated mechanical linkage for rotor actuation. Quad-rotors utilize four fixed pitch rotors the variations of whose speeds form the basis of the control. It results in simplified design and maintenance of the quad-rotors. Secondly, the use of four individual rotors results in their smaller diameters as compared to the similar main rotor of a helicopter. The smaller the rotors the less is stored kinetic energy associated with each rotor. This diminishes the risk posed by the rotors if it comes in contact with any external object. Furthermore, by securing the rotors inside a frame, the protection of rotors during collisions is achieved. It allows indoor flights in obstacle-dense environments with lower risk of quad-rotor damage, and higher operator and surrounding safety. These benefits have resulted in safe test flight by inexperienced pilots in indoor environments and recovery time in case of collisions. In particular, vertical, low speed, and stationary flight are well-known characteristics of a quad-rotors. Structurally, quad-rotors can be made in a small size, with a simple mechanics and control. Though, as a main drawback, the high energy consumption can be mentioned. However, the trade-off results are very positive. This configuration can be attractive in particular for surveillance, for imaging dangerous environments, and for outdoor navigation and mapping.

Conventionally, the quad-rotor attitude is controlled by changing the rotational speed of each motor. The front rotor and back rotor pair rotates in a clockwise direction, while the right rotor and left rotor pair rotates in a counter-clockwise direction. This configuration is devised in order to balance the moment created by each of the spinning rotor pairs. There are basically four maneuvers that can be accomplished by changing the speeds of the four rotors. By changing the relative speed of the right and left rotors, the roll angle of the quad-rotor is controlled. Similarly, the pitch angle is controlled by varying the relative speeds of the front and back rotors, and the yaw angle by varying the speeds of clockwise rotating pair and counter-clockwise rotating pair. Increasing or decreasing the speeds of all four rotors simultaneously controls the collective thrust generated by the robot.

One of the basic limitations of the classical quad-rotor design is that by having only 4 independent control inputs, i.e., the 4 propeller spinning velocities, the independent control of the six-dimensional position and orientation of the quad-rotor is not possible. For instance, a

quad-rotor can hover in place only and if only when being horizontal to the ground plane or it needs to tilt along the desired direction of motion to be able to move. Tilting rotor quadcopter concept has evolved to solve these basic limitations of a quad-rotor.

Tilt-design makes the dynamics of the quadcopter more complex, and introduces additional challenges in the control design. However, tilting rotor quadcopter, designed by using additional four servo motors that allows the rotors to tilt, is an over-actuated system that potentially can track an arbitrary trajectory over time. It gives the full controllability over the quad-rotor position and orientation providing possibility of hovering in tilted configuration.

Another application of the tilting platform lies in its ability to recover during a failure situation. In conventional quadcopters, if one of the propellers fails, due to its inherent dependency on the symmetry of the platform, the vehicle becomes entirely uncontrollable. However, in the proposed platform, if one of the motors completely fail, by using the tilt mechanism of one of the three remaining motors, the unbalanced momentum can be compensated. Moreover, providing additional actuation would make the quadcopter more robust to disturbances which can be rejected more effectively because of the enhanced maneuverability of the quadcopter with tilting design.

There is a lot of interest recently in developing small aerial vehicles that can carry humans for transportation in an autonomous manner. To have the quadcopter to be operational for such purposes, it needs to be scaled up to be able to carry more payloads. Due to safety issues of the human passenger, it should be robust to external disturbances and unpredictable situations. To reject external disturbances, agility becomes an important issue. The problem with scaled up quadcopter is the heavy weight. Once the weight scales up, the inertia will increase and larger moments will be needed to create the same angular acceleration on a lighter vehicle. As a consequence, longer propellers would be needed. Therefore, a stronger motor is required to rotate the new propellers which add more weight to the vehicle. This would make the vehicle to become more sluggish. Although the tilting mechanism can not make a big difference in throttle, it is expected that the orientation agility can be increased in big size vehicles due to the tilting mechanism.

1.4 Contribution

This dissertation focuses on designing, fabricating, modeling and controlling a quadcopter with tilting propellers. The contribution of the work lies in following:

- The mathematical representation of the quadcopter dynamics with tilting rotors has been derived in order to be used in system analysis and control design.
- Appropriate control techniques have been designed for highly nonlinear dynamics of the quadcopter with tilting propellers.
- Based on the dynamic equation of motion of tilting rotor quadcopter, the dynamic model of quadcopter with one motor failure has been derived and the control technique has been designed in order not only to maintain the stability of the vehicle after the failure, but also to continue flight mission.
- Two different platforms have been fabricated for the quadcopter which were designed in SolidWorks environments and some parts have been printed by using 3D printer.
- The numerical simulations and experimental results have validated the mathematical representation as well as designed control techniques.

1.5 Publications

Journals

- Alireza Nemati and Manish Kumar. Control of Microcoaxial Helicopter Based on a Reduced-Order Observer, *Journal of Aerospace Engineering*, 04015074, 2015.
- Mohammadreza Radmanesh, Manish Kumar, Alireza Nemati and Mohammad Sarim. Dynamic Optimal UAV Trajectory Planning in the National Airspace System via Mixed Integer Linear Programming, *Proceedings of the Institution of Mechanical Engineers, Part G: Journal of Aerospace Engineering*, 0954410015609361, 2015.

- **Alireza Nemati** and Manish Kumar. Dynamic Modeling and Control of a Quadcopter with Tilting Rotors, submitted to *IEEE Transactions Aerospace and Electronic Systems*, 2015.

Book Chapters

- Manish Kumar, Mohammad Sarim and **Alireza Nemati**. Autonomous Navigation and Target Geolocation in GPS Denied Environment, *Multi-Rotor Platform Based UAV Systems*. *Wiley Publishing*,
- Manish Kumar, **Alireza Nemati**, Anoop Sathyan and Kelly Cohen. Real-time Video and FLIR Image Processing for Enhanced Situational Awareness, *Multi-Rotor Platform Based UAV Systems*. *Wiley Publishing*,

Proceedings

- **Alireza Nemati** and Manish Kumar. Modeling and Control of a Single Axis Tilting Quadcopter, *American Control Conference (ACC)*, pp. 3077–3082. IEEE, 2014.
- **Alireza Nemati** and Manish Kumar. Non-Linear Control of Tilting Quadcopter Using Feedback Linearization Based Motion Control. *Dynamic System and Control Conference (DSCC)*, pp. V003T48A005-V003T48A005, ASME, 2014.
- Mohammadreza Radmanesh, **Alireza Nemati**, Mohammad Sarim and Manish Kumar. Flight Formation of Quad -copters in Presence of Dynamic Obstacles using Mixed Integer Linear Programming, *Dynamic Systems and Control Conference. ASME* , 2015.
- **Alireza Nemati**, et al. Autonomous Navigation of UAV through GPS-Denied Indoor Environment with Obstacles, *American Institute of Aeronautics and Astronautics, AIAA SciTech*, DOI: 10.2514/6.2015-0715, 2015.
- Mohammad Sarim, **Alireza Nemati** and Manish Kumar. Autonomous Wall-Following Based Navigation of Unmanned Aerial Vehicles in Indoor Environments. *American Institute of Aeronautics and Astronautics, AIAA SciTech*, DOI: 10.2514/6.2015-0715, 2015.

- Mohammad Sarim, **Alireza Nemati**, Manish Kumar and Kelly Cohen. Extended Kalman Filter based Quadrotor State Estimation based on Asynchronous Multisensor Data, *Dynamic Systems and Control Conference. ASME* , 2015.
- Mohammadreza Radmanesh, Manish Kumar, **Alireza Nemati** and Mohammad Sarim. Solution of Traveling Salesman Problem with Hotel Selection in the Framework of MILP-Tropical Optimization, accepted in *American Control Conference (ACC)*, IEEE, 2016.
- **Alireza Nemati**, Neal Soni, Mohammad Sarim, and Manish Kumar. Design, fabrication and control of a tilt rotor quadcopter. In ASME 2016 Dynamic systems and control conference. American Society of Mechanical Engineers, 2016.
- **Alireza Nemati**, Rumit Kumar, and Manish Kumar. Stabilizing and control of tilting-rotor quadcopter in case of a propeller failure. In ASME 2016 Dynamic systems and control conference. American Society of Mechanical Engineers, 2016.

Intellectual property

- **Alireza Nemati**, Mehdi Hashemi and Manish Kumar, “ World Frame Based Radio Controller(RC) for Multi-copter UAVs” *Filed for provisional patent*, October 2015
- **Alireza Nemati**, Manish Kumar and Rumit Kumar. Fault Tolerance Quadcopter . *Provisional Patent Has Been Filed by University of Cincinnati*, February 2016.

1.6 Organization of Thesis

This dissertation consists of eight chapters. This includes “Introduction” as the first chapter. Chapter 2 is a literature review that provides a brief history of the conventional as well as tilting quadcopters. Chapter 3 reports on the dynamic model of the tilting quadcopter and considers the nonlinearities that add to the equation due to additional control inputs. Chapter 4 presents a combined linear and nonlinear controller which is used to control desired orientation during the flight. The dynamic model of the vehicle and the proposed control technique once the failure occurs is presented in chapter 5.

The hardware design process is described in detail in Chapter 6. Results from numerical simulation and experimental studies carried out to verify the modeling and control of tilting rotor quatcopters following a reference trajectory with simultaneous control of both pitch and roll angles are discussed in Chapter 7. The conclusions and future works are presented in Chapter 8. This chapter summarizes the dissertation, discusses the contributions and also outlines directions for future works to be pursued.

Chapter 2

History of the Quadcopters

2.1 A Brief History of Quadcopters

2.1.1 The Early History of Quadcopters

A Quadcopter or Quadrotor is multi-rotor mechatronic device capable of Vertical Takeoff and Landing (VTOL) that is lifted or propelled by four independently rotating rotors. The idea behind Quadcopters was first developed in the early 1900s. There were very few unique and momentous quadcopter designs developed throughout the 20th century. The earliest ideas for a quadcopter were designed and test piloted by Louis Breguet, Etienne Oemichen, George DeBothezat, and D.H. Kaplan. The first successful flight of a quadcopter aerial vehicle was in 1907. This device, named the Gyroplane (Figure (2-1)¹), was built by Breguet brothers and consisted of a 55hp Renault engine and two forward-tilting 2-blade rotors. It was reported to have multiple successful flights during the summer of 1908. However it's mobility and range of flight were very limited.

¹<https://en.wikipedia.org/wiki/Breguet-Richet-Gyroplane>

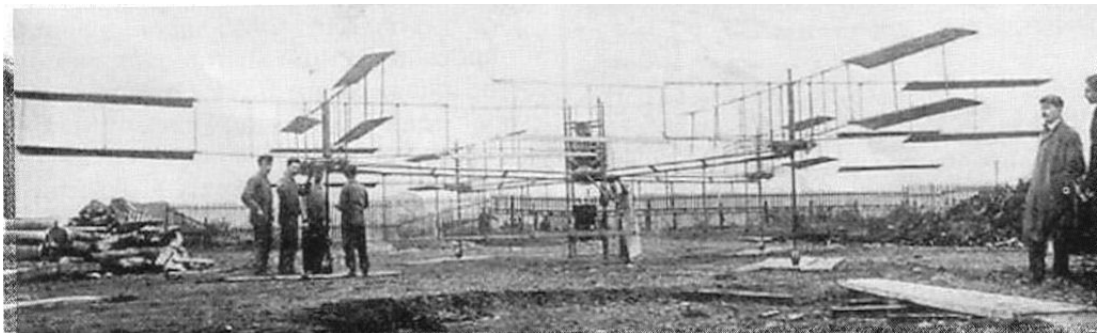


Figure 2-1: Gyroplane.

In the 1920s, Etienne Oemichen, was able to construct the first stable VTOL quadcopter which he named Oemichen *II* (Figure (2-2) ²). It consisted of a single 180hp Gnome engine powering four rotors, a complex steel-tube framework of cruciform layout, five smaller propellers mounted horizontally to provide lateral stability, and an additional pair of propellers that were mounted to the nose of the craft for steering. The last pair of propellers provided forward thrust. This design made thousands of successful flights during the mid 1920s and even established a world record of flying one kilometer in seven minutes and forty seconds. Almost all quadcopters in the 1920s were unable to sustain a controlled flight and had to use the Ground Effect to sustain flight limiting these designs to stay low to the ground.

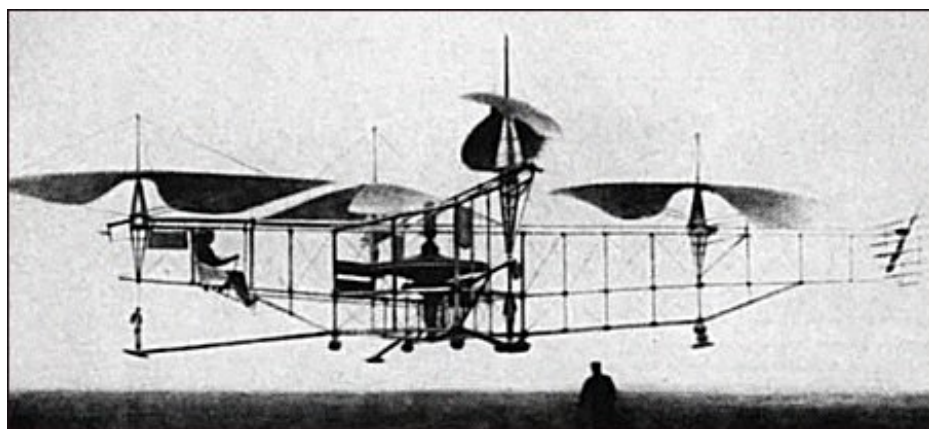


Figure 2-2: The Oemichen2

Around the same time, George DeBothezat designed and built the Flying Octopus (Figure (2-3) ³ for the United States Army Air Corps. The 1678kg "X" shaped structure supported

²<https://en.wikipedia.org/wiki/C389tienne-Oehmichen>

³<https://en.wikipedia.org/wiki/Pescara-Model-3-Helicopter>

four 8.1m diameter six-blade rotors; one on each end of the 9m long arms. At each end of the lateral arms, two smaller propellers with variable pitch supplied thrust and enabled yaw control. After working on his design for a little over two years, DeBothezat was able to develop a fairly capable quadcopter. This design was able to carry a payload of up to 4 people including the pilot. However, the design was considered to be flawed as it was under-powered, unresponsive and very fragile. The craft was only capable of reaching an altitude of around 5m rather than the 100m desired by the army.

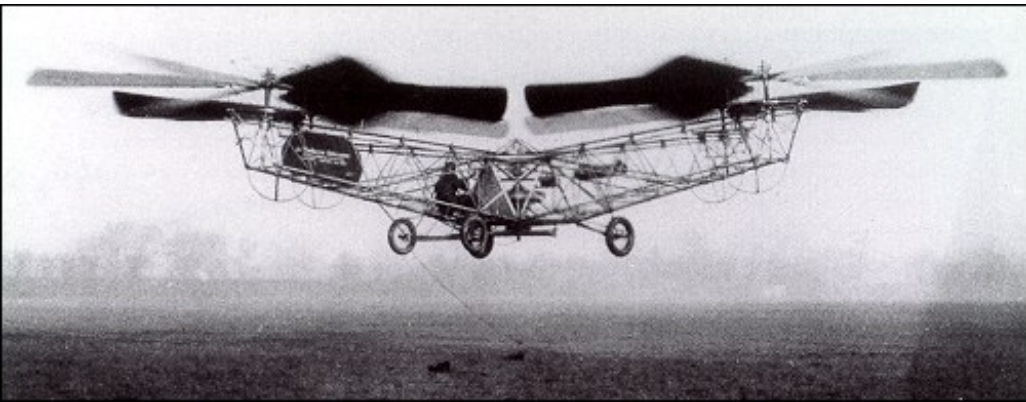


Figure 2-3: De Bothezat

Early quadcopters typically contained a single engine positioned in the center of the fuselage that drove the four rotors via belts or shafts. These belts and shafts were heavy and more importantly broke down often. In addition, the four rotors of the quadcopter were ever so slightly different from one another, so the quadcopter was not naturally stable during flight. Running all rotors at the same speed did not produce a stable flight and each rotor had to be constantly adjusted to sustain a stable flight. In the early 1900s, with the absence of any digital computers or sensors, flying a quadcopter required a monumental workload for the pilot making the early quadcopters very inefficient and not practical for transportation. These early quadcopters designs also included multiple additional rotors located on different locations of the quadcopter for additional stability, making these designs not true quadcopters. As materials and engineering practices evolved over the century, numerous improvements were made by both increasing the power of the motors and reducing the overall weight of the designs. During the early 1950s, D.H. Kaplan, worked on and test piloted the Convertawings Model A

Quadcopter (Figure (2-4)⁴). Kaplan's design featured four rotors and had a two motor layout with the rotors positioned in an H configuration. Kaplan's machine may be considered the first true quadcopter as it was capable of sustaining a controlled flight without the use of the ground effect or any additional propellers. The 2,200 pounds craft had a much simpler design than previous quadcopters due to the fact that control was obtained by varying the thrust between the individual rotors eliminating the need for complex cyclic-pitch-control systems and additional rotors on the sides of the fuselage. This design first flew in March of 1956 with great success. The design, in particular its control system, was a precursor of a majority of the current vertical takeoff aircraft designs that incorporate tandem wings.

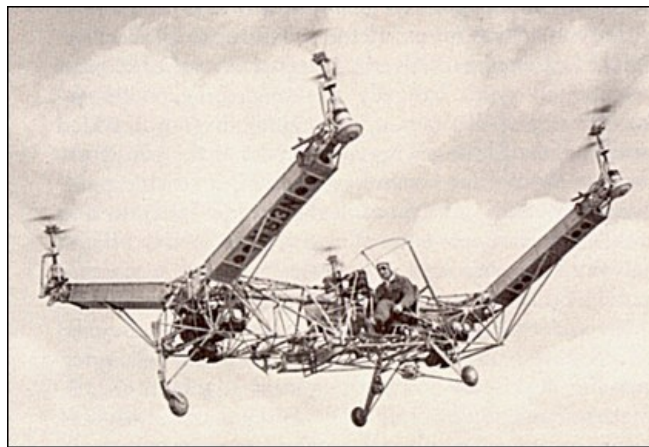


Figure 2-4: Convertawings, Model A

2.1.2 History of Tilt Rotor Vertical Takeoff Vehicles

Tilt Rotors combined the properties of a helicopter which included Vertical Take Off and Landing (VTOL), hovering, and vertical, forward, and lateral flight, with the desirable properties of a fixed-wing aircraft including long range flight, low power consumption and the ability to carry heavier payloads. The first design that resembled a modern tilt rotor device was patented in May of 1930 by George Lehberger (Figure (2-5))⁵.

⁴<https://en.wikipedia.org/wiki/De-Bothezat-helicopter>

⁵<http://history.nasa.gov/monograph17.pdf>

SEPT. 16, 1930 G. LEHBERGER 1,775,961
FLYING MACHINE
FILED MAY 26, 1930

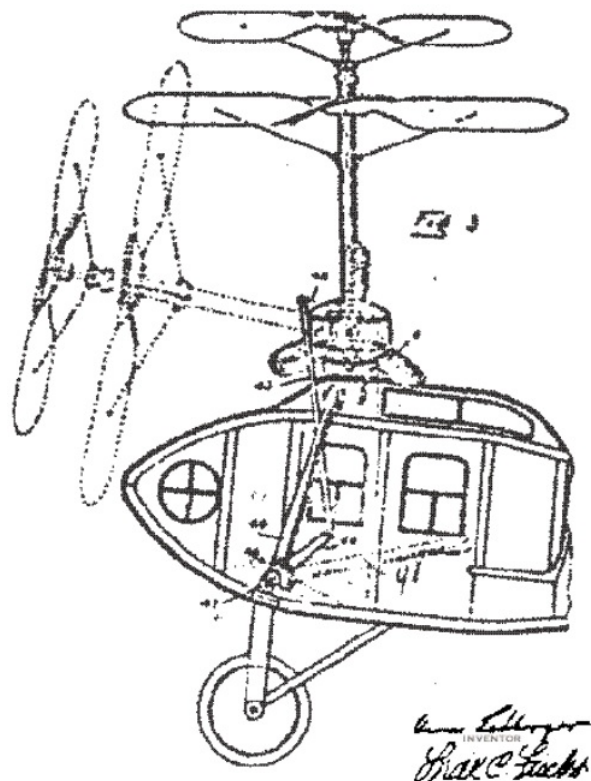


Figure 2-5: George Lehbergers 1930 tilting propeller vertical take-off “flying machine”.

Though this design never amounted to a prototype, it was the first step in making a functional VTOL capable tiltrotor vehicle and inspired the design of the Focke-Achgelis FA-269 (Figure (2-6)⁶) trail-rotor convertiplane project in Germany during World War II[43].

⁶<http://history.nasa.gov/monograph17.pdf>

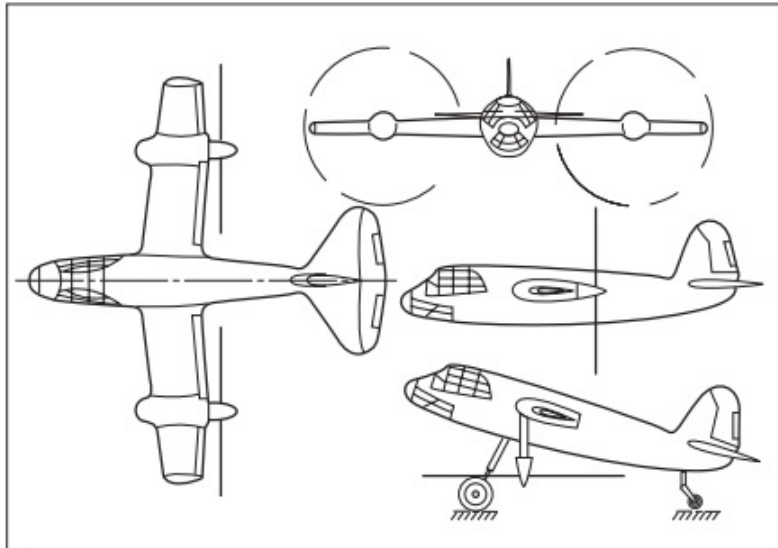


Figure 2-6: Three-view drawing of the Focke-Achgelis FA-269 convertiplane

A prototype of this aircraft was built in 1943 and consisted of two pusher propellers that tilted below the two wings for takeoff and landing. However, the project was discontinued after the allies destroyed a full scale mock-up of this design and much of the research during a bombing in 1944. A few years later, variants of this tilt rotor configuration surfaced again in the design studies at Bell and McDonnell Douglas.

The Bell XV-3 (Figure (2-7)⁷) was a tiltrotor aircraft designed by Bell in the 1950s[15]. Its first successful flight was in August 1955. It was the first aircraft to successfully transition between helicopter and fixed wing for normal flight. The XV-3 was powered by a single 450hp radial engine that propelled the aircraft at a maximum speed of 296 km/h. The craft had a maximum altitude of 4600 meters. This aircraft was a proof of concept and made over 100 successful transitions before it was severely damaged in a wind tunnel accident and the design was scraped.

⁷<http://ntrs.nasa.gov/archive/nasa/casi.ntrs.nasa.gov/20040087005.pdf>



Figure 2-7: The Bell XV-3, during flight testing.

The data and experience collected during this trial were key to the development of the Bell-XV15 (Figure (2-8) ⁸) and the V-22 Osprey (Figure (2-9) ⁹)[57, 43].



Figure 2-8: XV-15 taking off

⁸<https://en.wikipedia.org/wiki/Bell-XV-3>

⁹<https://en.wikipedia.org/wiki/Bell-Boeing-V-22-Osprey>



Figure 2-9: The V-22 Osprey, during transition flight

Both these designs followed the same principles as the Bell XV-3 and had many successful flights over their life.

2.1.3 History of Tilt Rotor Quadcopter

In respect to quadcopter tilting machines, there have been two early designs that stand out, the Curtiss X-19 and the Bell X-22. The Curtiss X-19 (Figure (2-10)¹⁰) built in 1960s was a passenger plane that consisted of two sets of thin wings each with a 3 bladed rotor that could rotate 90 degrees [30]. With its massive 2,200 hp engines, it could carry up to 550kg of cargo or 4 passengers along with the two crew members. Two turboshaft engines were housed in the rear fuselage and powered the four rotors. The aircraft's first flight was in 1963 and was capable of flying up to 523 Km and reached a maximum speed of 650 Km/h. Two prototypes of the X-19 were built but the project was canceled after the first prototype crashed during its second flight.

¹⁰<https://en.wikipedia.org/wiki/Curtiss-Wright-X-19>



Figure 2-10: X-19 in hovering flight

The Bell X-22 was built a couple years after the Curtiss X-19 and is considered to be one of the most versatile and longest lived of the many VTOL aircrafts that have been developed[30]. It is similar to the X-19 in that it has four wings each with their own 3 bladed propeller each able to rotate 90 degrees but instead of having 2 motors, the Bell X-22 had four 1250 hp motors each powering their own rotor. The design was able to carry up to six passengers and two pilots and reached a maximum speed of 507 km/hour with a range of up to 716km. The two prototypes of the Bell X-22 were used for many years by both NASA and the US Navy for V/STOL and performed very well. One is still on display at the Niagara Falls Aerospace Museum in New York (Figure (2-11)¹¹). More modules of quadcopters are currently being developed for the US Army Corps Including the Bell Boeing Quad Tiltrotor (QTR). It is currently under study and was first designed in 1999. The Bell Boeing Quad Tiltrotor is predicted to be able to carry up to 80 passengers with a cruise speed of 520 km/hour.



Figure 2-11: Bell X-22A

¹¹<https://en.wikipedia.org/wiki/Bell-X-22>

2.2 Current Quadcopters

Quadcopters are one of the most popular designs for miniature aerial vehicles (MAVs) due to their vertical take-off and landing capability, simplicity of construction, maneuverability, and ability to negotiate tight spaces making it possible for their use in cluttered indoor areas. Due to these capabilities, quadcopters have recently been considered for a variety of applications both in military and civilian domains. In particular, quadcopter MAVs have been explored for applications such as surveillance and exploration of disasters (such as fire, earthquake, and flood), search and rescue operations, monitoring of hazmat spills, and mobile sensor networks[37] [64][14]. Blimps, fixed-wing planes, single rotor helicopters, bird-like prototypes, coaxial dual rotor helicopters, quad-rotors, tilting rotor quadcopters are examples of different configurations and propulsion mechanisms that have been developed to allow 3D movements in aerial platforms [39] [5] [90] [50] . Each of these designs have advantages as well as drawbacks. This work focuses on quadcopters or quad-rotors which consist of four rotors in total, with two pairs of counter-rotating, fixed-pitch blades located at the four corners of the aircraft. This kind of design has two main advantages over the comparable vertical takeoff and landing (VTOL) Unmanned Aerial Vehicles (UAVs) such as single rotor helicopters. Firstly, quad-rotors do not require complicated mechanical linkage for rotor actuation. Quad-rotors utilize four fixed pitch rotors the variations of whose speeds form the basis of the control. It results in simplified design and maintenance of the quad-rotors. Secondly, the use of four individual rotors results in their smaller diameters as compared to the similar single rotor of a helicopter. Smaller rotors imply less stored kinetic energy associated with each rotor. This diminishes the risk posed by the rotors if it comes in contact with any external object. Furthermore, by securing the rotors inside a frame, the protection of rotors during collisions is achieved. This configuration allows indoor flights in obstacle-dense environments with lower risk of quad-rotor damage, and higher operator and surrounding safety. These benefits have resulted in safe test flights by inexperienced pilots in indoor environments and lesser recovery time in case of collisions [25]. In particular, stable, vertical, low speed and stationary flights are well-known characteristics of a quad-rotor. Structurally, quad-rotors can be designed in a small size, with simple mechanics and control. The quadcopters have been found to be an attractive choice in particular for surveillance, for

imaging dangerous environments, and for outdoor navigation and mapping [59] , [22]. The major drawback, however, is high energy consumption due to the use of four rotors.

Conventionally, the quad-rotor attitude is controlled by changing the rotational speed of each motor. The front rotor and back rotor pair rotates in a clockwise direction, while the right rotor and left rotor pair rotates in a counter-clockwise direction. This configuration is devised in order to balance the moment created by each of the spinning rotor pairs. There are basically four maneuvers that can be accomplished by changing the speeds of the four rotors. By changing the relative speed of the right and left rotors, the roll angle of the quad-rotor is controlled. Similarly, the pitch angle is controlled by varying the relative speeds of the front and back rotors, and the yaw angle by varying the speeds of clockwise rotating pair and counter-clockwise rotating pair. Increasing or decreasing the speeds of all four rotors simultaneously controls the collective thrust generated by the robot [9].

One of the basic limitations of the classical quad-rotor design is that by having only 4 independent control inputs, i.e., the 4 propeller spinning velocities, the independent control of the six-dimensional position and orientation of the quad-rotor is not possible. For instance, a quad-rotor can hover in place only and if only while being horizontal to the ground plane or it needs to tilt along the desired direction of motion to be able to move. Tilting rotor quadcopter design has been developed to solve these basic limitations of a quad-rotor. In next section, there are several examples of recent development about tilting concept.

Recently, there has been a renewed interest in quadcopters from hobbyists, universities, and corporations across the globe. The renewed interest is due to the many significant technological advances in sensors and micro-controllers over the past decade that have allowed these once large machines to be miniaturized to fit in the palm of a hand and be autonomously controlled. A significant number of quadcopters have been introduced for both military and civilian use as a result of partnerships between companies and universities that have enabled this quadcopter UAV revolution. Many companies such as AeroQuad, ArduCopter, DJI, and Parrot AR.Drone have sparked the interest of hobbyist; Coupled with the DIY (Do It Yourself) and open source movement, Quadcopter UAVs are more popular and progress in the sector is advancing faster than ever before.

2.2.1 Quadcopters with Tilting Mechanism

Quadcopters with tilting propellers are divided into two categories. Quadcopters which have the capability of flying both as a conventional quadcopter as well as a fixed wing aerial vehicle by tilting all propellers in the same direction by the same amount of angle and the one which is capable of making a tilt in any individual propellers independently. In the first type of tilting quadcopter(Convertible Quad Tilt Rotor (CQTR)), all propellers are changing their orientation simultaneously with the same amount of angle. However, variety of platform, mechanism and control methods have been used by different researchers and universities. Since all propellers tilt with the same angle, the dynamic equation of the aircraft does not change a lot and the complexity of the equation is not the most critical obstacle that needs to be tackled for the designers. The ability of transition between vertical take off and hover flight to horizontal flight is one the most difficulties the needs to be consider for CQTR. With this ability, aircraft will be able not only to take off and land at any inappropriate area, but also by taking an advantage of aerodynamic shape of the wing, it will be able of flying horizontally in long distances. The flight mode that makes the transition between vertical and horizontal flight has been gaining remarkable interest among researchers. Numerous innovative CQTR platform have been studied in very last few years. Papachristos et al [62] from university of Patras, Greece, have focused on hybrid model predictive flight mode conversion control of CQTR. Their aircraft platform (shown in Figure (2-12)¹²)

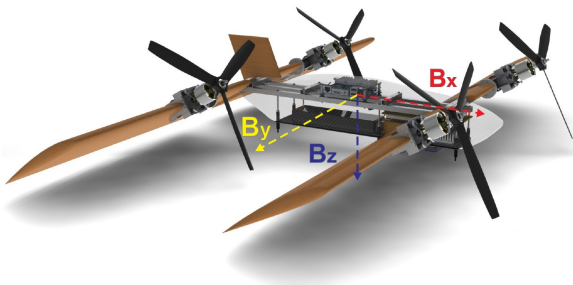


Figure 2-12: The Quad-TiltRotor concept, University of Patras.

capable of flying both as a quadcopter as well as fix wing aircraft. They have developed an innovative control scheme based on hybrid systems theory. An approximation of complete

¹²<http://www.nt.ntnu.no/users/skoge/prost/proceedings/ecc-2013/data/papers/1271.pdf>

nonlinear dynamics has been derived and used as a model for control during autonomous mid-flight conversion. Although they have not flown the aircraft, but by using simulation studies its been shown that their proposed strategy exceeds the functionality of the flight-modes conversion. The standard NACA2411 airfoil has been selected for the design. The wings with total span of 1 meter are mounted on the tilting mechanism. The wings are capable of rotating 90 degrees angle.

Another research group has focused on design and control of gas-electric hybrid CQTR with morphing wing in order to extend the hovering flight up to 3 hours or up to 10 hours of horizontal flight [13]. They have minimized the mechanical morphing wings and aerodynamic cost for both high speed and low speed flights. A variety of novel features have been used in their concept Figure (2-13)¹³.

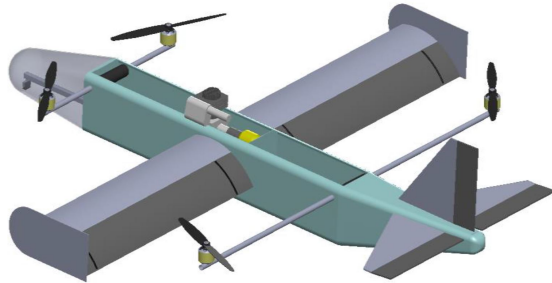


Figure 2-13: CAD design of the CQTR, Istanbul Commerce University.

A gas engine-battery hybrid propulsion is used due to capability of carrying heavy payload and very long flight duration, plus a carbon composite wings not only to reduce the weight but also for handling both high speed and low speed flight. The V-type structure of the aircraft allows to extension of the rear rotors from the center of the mass which ensure the full coverage of the wing area by the rotor for preventing stalls as well as minimum required speed for horizontal flight. For the transition, two servo motors have been located next to shaft of rear and front rotors. The vehicle's take off weight is 20 kg and the wing-span including the larger winglets is 2.5 meters. Numerical simulation has been used to validate and understand the flight behavior and performance of the aircraft. By placing four rotors in two axes with almost the same level, rotor's thrust will not cover the most, even if like the previous work, the rotors

¹³<http://ieeexplore.ieee.org/stamp/stamp.jsp?arnumber=7152278>

of one the axis extend from the center. The researchers in Beihang University, China, [65] have proposed a prototype concept of CQTR that place the rotors of the front and rear axis of the horizontal mode in two different levels. In their concept, for change in configuration, the two front rotors tilt down to -90 degree, while the two rear rotor tilt up to 90 degree. After the transition is done, all rotors will be facing front with exactly the same angle but in two different levels. Figure (2-14)¹⁴ shows the configuration of the CQTR in both quadcopter and flying wing mode.

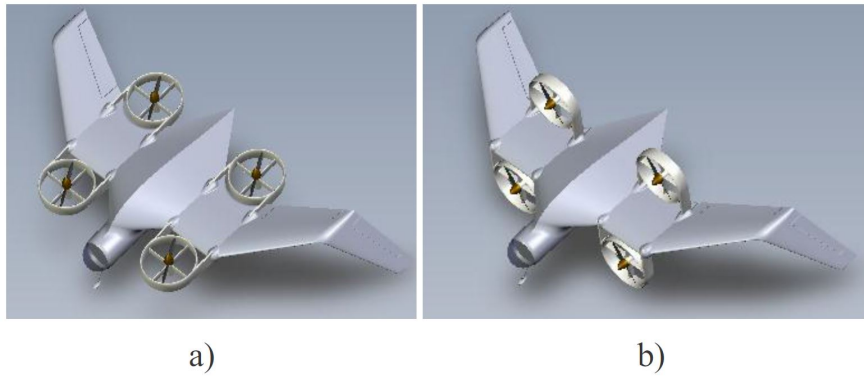


Figure 2-14: The Configuration of the QTR UAV under research a) Quadcopter mode b) Flying wing mode, Beihang University.

They have focused on the trajectory tracking control for hovering and acceleration flight of CQTR by using dynamic inversion. Their scenario is based on 4 strategies as follows: take-off and reach a certain altitude, find an optimal transition trajectory to not only minimize the transition time but also not to lose altitude, the next scenario is to keep flying in fixed wing mode and the ability to change the altitude. During the cruise flight, the rotor speed and the forces allocated between the rotors and the wings maintain the needed thrust to control altitude and attitude. Attitude Command Attitude Hold (ACAH) method is being used for attitude control strategy. The last scenario is to lower the speed and keep tilting back the rotors to their original angle during the takeoff. Although they have built a prototype version of the vehicle with dimension of 1.8 meter for the wing span and gross weight of 5.2kg, but numerical simulation is used to evaluate their proposed control system.

Several researches have introduced many interesting prototype of CQTR, but there are few

¹⁴<http://comb.buaa.edu.cn/PUBLICATIONS/PATEERS/2014/48.html>

groups that validate their control systems by experimental results. Hancer et al [23] presented a prototype CQTR equipped with robust position controller to track desired trajectory under aerodynamic and external wind disturbances, as shown in Figure (2-15)¹⁵¹⁶.

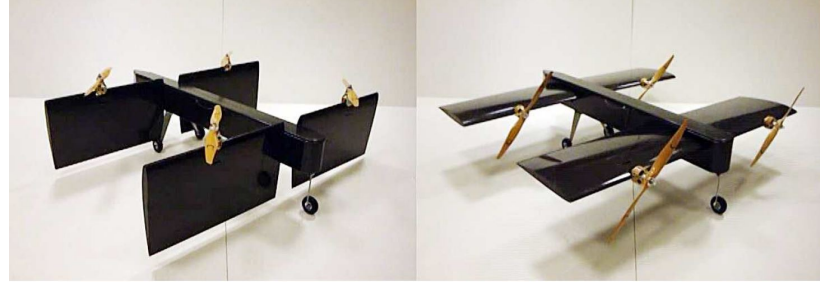


Figure 2-15: CQTR with integrated actuators in different flight configurations.

Dryden model has been used to model wind effects which is included in dynamic model. These disturbances are being estimated by using disturbance observer which is commonly used in motion control systems. Parametric uncertainties and nonlinear term are also added to external disturbances as a total disturbance. Performance of the hovering flight is verified with the experimental results. The transition from hovering flight to horizontal cruise flight which is the most critical part of the experiment is not tested in real world, but trajectory tracking performance is confirmed with numerical simulations.

Mikami and Uchiyama [47] from Nihon University have validated their concept by numerical simulation as well as experimental results. Due to strong nonlinearities of dynamical behavior, a linearization method without any approximation has been applied to their control strategy. This proposed control strategy is being used in both translational and rotational controllers. Figure (2-16)¹⁷ shows an overview of developed CQTR

¹⁵<http://research.sabanciuniv.edu/15316/1/cdc10.pdf>

¹⁶<http://people.sabanciuniv.edu/munel/Publications/JournalPapers/Mechatronics-2012.pdf>

¹⁷<http://ieeexplore.ieee.org/stamp/stamp.jsp?arnumber=7152364>



Figure 2-16: Overview of developed CQTR, Nihon University.

Overall weight of the prototype is 0.48 kg with the length and wing span of 0.8 and 0.7 meter, respectively. Although, due to weight limitation and small size of the battery, the endurance of the vehicle is not longer than 15 minutes, but the experimental results verified the validity of flight control strategy. The vehicle is equipped with micro-computer, flow sensor, radio module, IMU and ultra-sonic sensor. The experimental results show that the transition from hover flight to horizontal cruise flight has been accomplished.

Even-though above mentioned air-crafts are using a tilting mechanism for the propellers, but the under actuation problem of the robot still remains, and in addition to that, these additional dynamic of convertible quad tilt rotor is not making the big problem for the control systems. Also by changing the angle of all propellers simultaneously, translational motion can not be achieved independently without tilting the aircraft. If the aircraft's arm had the capability of independently tilting about their own axis, the dependency of translation and orientation problem, could be solved and the system would not be called an under actuated robot. There have been some attempts to carryout this problem by several groups. Ryll et al. [76] from Max Plank Institute, Germany, proposed a tilting quadcopter with 8 independent control inputs that allows the aircraft for independent attitude and position control. They have added four additional servo motors to allow the propellers to tilt about their axes¹⁸.

¹⁸<https://www.semanticscholar.org/paper/Modeling-and-control-of-a-quadrotor-UAV-with-Ryll-BC3BClthoff/3508f3f9497425a4cbc4bc2d2c2d30df3fc6be77>

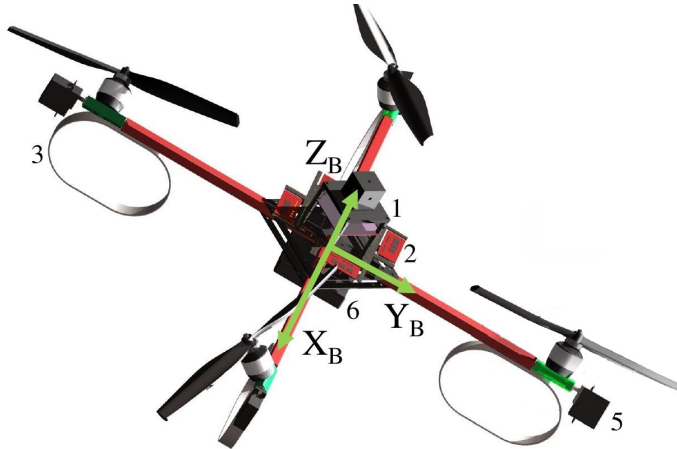


Figure 2-17: CAD model of the quadcopter with tilting propellers, Max Planck Institute.

The linearized compensation control based on the quadcopter's dynamic has been used to achieve 6 DOF of motion control. The tracking of an arbitrary trajectory was the main focus of the group. They have simplified the dynamic model in order to have a suited model for control design. Since 8 independent inputs are available, their proposed control design is over actuated. As in many output tracking control techniques, an appropriate way they solved the problem was to place the output feedback linearization method. Numerical simulation was the way they applied the controller presented in [76]. The tracking performance of the controller was validated and the capability of the proposed method to avoid the singularities was guaranteed. Another paper has been published from the same authors [77] to validate the proposed strategies. Although the prototype which is called "omnicopter" has been tested on a testing gimbals, but their results show the full controllability over 6 DOF body pose in space. Another group [81] has tested their prototype on the ball joint rig. Ball joint rig is a device that can be attached to the underneath of the quadcopter and it can let the quadcopter to orient around and follow the desired orientation without an actual flight¹⁹.

¹⁹<https://www.semanticscholar.org/paper/A-Novel-Actuation-Concept-for-a-Multi-Rotor-UAV-Segui-Gasco-Al-Rihani/28bdc9144a153c132b37382be32e94d83b1abfed/pdf>

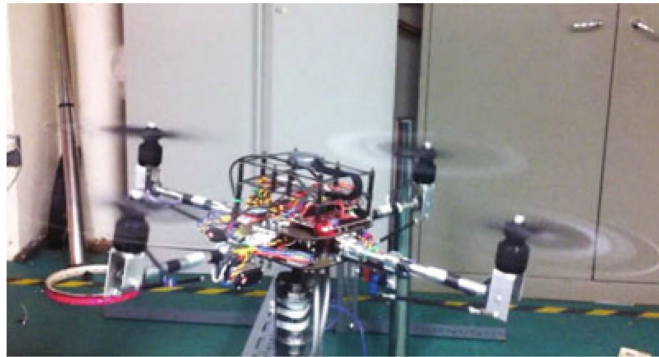


Figure 2-18: Vehicle prototype on the ball joint rig flight test, Cranfield University.

The main proposal of the prototype was to improve the performance and fault tolerance of quadcopter vehicles. They have proposed dual axis tilting propellers which enables gyroscope torque, differential thrusting and thrust vectoring. Not only the mathematical representation of the model was modeled and verified by the experimental results, but also a control system was developed based on PD controller and validated through test on a ball joint rig flight test.

Tilt-design makes the dynamics of the quadcopter more complex, and introduces additional challenges in the control design. However, tilting rotor quadcopter, designed by using additional four servo motors that allow the rotors to tilt, is an over-actuated system that potentially can track an arbitrary trajectory over time. It gives the full controllability over the quad-rotor position and orientation providing possibility of hovering in a tilted configuration. This work presents a mathematical dynamic modeling of the tilting rotor quadcopter which provides a description of the dynamical behavior of the quadcopter as a function of the rotational speeds of each of the four rotors and their respective tilt-angles. The developed mathematical representation of the tilting rotor quadcopter can be used to obtain the position and orientation of the quad-rotor. The same model can further be used to develop a linear and nonlinear control strategy via which the speeds of the individual motors and the respective tilt-angles can be manipulated to achieve the desired motion and configuration.

Chapter 3

Dynamic Modeling

Unlike traditional quad-rotor models, which have only four rotatory propellers as the vehicle's inputs, in tilting rotor quadcopters, there are four more servo motors attached to the each arm that adds one degree of freedom to each of the propellers, resulting in the tilting motion along their axes. In this chapter, first the dynamic model of a traditional quad-rotor is described, then, the equations of motion of a tilting rotor quadcopter are presented.

3.1 Traditional Quad-rotor

Figure (3-1) schematically shows the coordinate system and forces acting on a traditional quad-rotor. In the 3 dimensional space, the world-frame (E) denotes the fixed reference frame with respect to which all motions can be referred to and the body-frame (B) is a frame attached to the center of mass of the vehicle. The rotation of each rotor causes an aerodynamic force or thrust that acts perpendicular to the plane of rotation of the rotor. In addition to the forces, each rotor produces a moment perpendicular to the plane of propeller rotation. The moment produced by a propeller on the vehicle is directed opposite to the direction of rotation of the propeller, and therefore to cancel out rotation along the Z -axis, the moments for rotor 1 and 3 are set in clockwise ($-Z_B$) direction and for rotor 2 and 4 are set in counter clockwise (Z_B) direction.

Based on NASA Standard Airplane [35], Euler angle transformations are defined by ψ , θ and ϕ which respectively represents the heading, attitude and bank angles also referred to as yaw, pitch and roll angles. Combined transformation matrix from body coordinate to the

world coordinate is obtained by three successive rotations. The first rotation is about X axis, followed by another rotation about Y axis and the last rotation is about Z axis. For each rotation, transformation matrix can be written as:

$$R_x = \begin{bmatrix} 1 & 0 & 0 \\ 0 & \cos\phi & -\sin\phi \\ 0 & \sin\phi & \cos\phi \end{bmatrix}$$

$$R_y = \begin{bmatrix} \cos\theta & 0 & \sin\theta \\ 0 & 1 & 0 \\ -\sin\theta & 0 & \cos\theta \end{bmatrix}$$

$$R_z = \begin{bmatrix} \cos\psi & -\sin\psi & 0 \\ \sin\psi & \cos\psi & 0 \\ 0 & 0 & 1 \end{bmatrix}$$

Resultant transformation matrix will be given by:

$$R_{EB} = \begin{bmatrix} c\psi c\theta & c\psi s\theta s\phi - s\psi c\phi & c\psi s\theta c\phi + s\psi s\phi \\ s\psi c\theta & s\psi s\theta s\phi + c\psi c\phi & s\psi s\theta c\phi - c\psi s\phi \\ -s\theta & c\theta s\phi & c\theta c\phi \end{bmatrix} \quad (3.1)$$

where $c\psi$ and $s\psi$ denote $\cos(\psi)$ and $\sin(\psi)$ respectively, and similarly for other angles.

By obtaining vehicle's vertical forces in the world frame and writing the equations of motion based on the Newton second law along the X , Y and Z axes, we can write:

$$\begin{aligned} m\ddot{x} &= \sum F_i(s\psi s\phi + c\psi s\theta c\phi) - C_1\dot{x} \\ m\ddot{y} &= \sum F_i(s\psi s\theta c\phi - c\psi s\phi) - C_2\dot{y} \\ m\ddot{z} &= \sum F_i(c\theta c\phi) - mg - C_3\dot{z} \end{aligned} \quad (3.2)$$

where m is the total mass of quad-rotor, g is the acceleration due to gravity, x , y and z are quadcopter position in world frame coordinate, C_1 , C_2 and C_3 are drag coefficients. Note that

the drag forces are negligible at the low speed. F_i , ($i = 1, 2, 3, 4$) are forces produced by the four rotors as given by the following equation:

$$F_i = K_f \omega_i^2 \quad (3.3)$$

where ω_i is the angular velocity of i^{th} rotor and K_f is a constant. In addition, Euler equations are written in order to obtain angular accelerations of the vehicle given by:

$$\begin{aligned} I_x \ddot{\phi} &= l(F_3 - F_1 - C'_1 \dot{\phi}) \\ I_y \ddot{\theta} &= l(F_4 - F_2 - C'_2 \dot{\theta}) \\ I_z \ddot{\psi} &= M_1 - M_2 + M_3 - M_4 - C'_3 \dot{\psi} \end{aligned} \quad (3.4)$$

where l is distance of each rotor from the vehicle's center of mass. I_x , I_y and I_z are moment of inertia along x , y and z directions respectively. C'_1 , C'_2 and C'_3 are rotational drag coefficients. M_i , ($i = 1, 2, 3, 4$) are rotors moment produced by angular velocity of rotors and given by:

$$M_i = K_m \omega_i^2 \quad (3.5)$$

where ω_i is the angular velocity of i^{th} rotor and K_m is a constant.

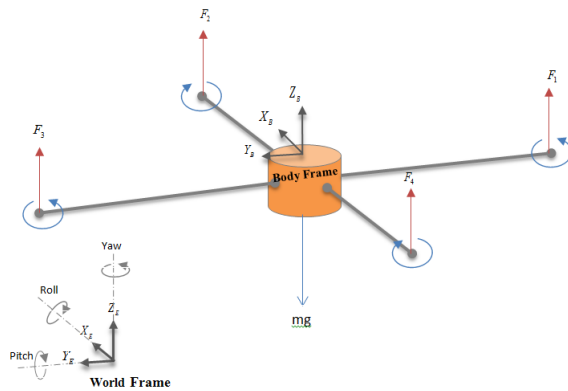


Figure 3-1: Schematic diagram showing the coordinate systems and forces acting on the quad-rotor

During a hovering flight, the quad-rotor not only has zero acceleration and velocity but also

needs to have zero pitch and roll angles, i.e. $r = r_0, \theta = \phi = 0, \psi = \psi_0, \dot{r} = 0, \dot{\theta} = \dot{\phi} = \dot{\psi} = 0$.

At this nominal hover state, the produced force from each propellers must satisfy:

$$F_i = \frac{1}{4}(mg) \quad (3.6)$$

and hence motor speeds are given by:

$$\omega_i = \omega_h = \sqrt{\frac{mg}{4k_f}} \quad (3.7)$$

3.2 Tilting Rotor Quadcopters

For a tilting rotor quadcopter, four other variables are added representing the angles of the quad-rotor arms. Adjustment of these angles results into improved vehicle maneuverability and capability for hovering at a tilted angle.

To illustrate the motion of the tilting rotors quadcopter, a schematic diagram showing the forces/momenta acting and coordinate frames used in the modeling is provided in Figure (3-2). As it can be seen from this figure, the propellers are free to tilt along their axes. The planes shown with dashed lines are the original planes of rotation with zero tilt angles for the respective propellers. Similarly, the planes shown with the rigid lines are the tilted planes of rotation for the respective propellers. θ_i , ($i = 1, 2, 3, 4$) is the tilted angle of the corresponding propellers. It may be noted that the forces generated by the propellers are perpendicular to these respective planes of rotations.

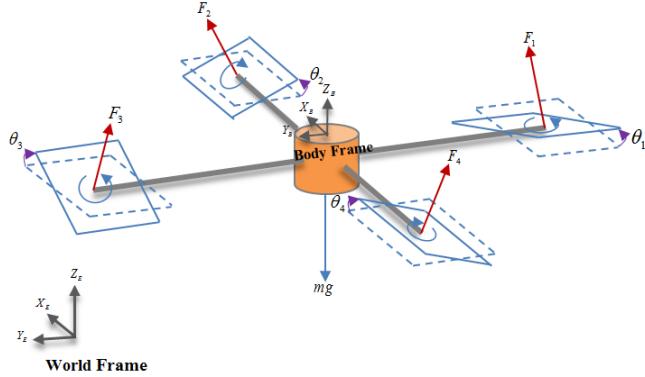


Figure 3-2: Coordinate Frames and Free body diagram of Tilting Quadcopter

The equation governing the acceleration of the center of mass is:

$$m \begin{bmatrix} \ddot{x} \\ \ddot{y} \\ \ddot{z} \end{bmatrix} = \begin{bmatrix} 0 \\ 0 \\ -mg \end{bmatrix} - R_{EB} \begin{bmatrix} F_1 s\theta_1 - F_3 s\theta_3 \\ F_2 s\theta_1 - F_4 s\theta_3 \\ F_1 c\theta_1 + F_2 c\theta_2 + F_3 c\theta_3 + F_4 c\theta_4 \end{bmatrix} - \begin{bmatrix} C_1 \dot{x} \\ C_2 \dot{y} \\ C_3 \dot{z} \end{bmatrix}$$

Using the rotational matrix in (1), equations of motion in world-frame can be rewritten as:

$$\begin{aligned} m\ddot{x} &= F_1 s\theta_1 c\psi c\theta - F_3 s\theta_3 c\psi c\theta - F_4 s\theta_4 c\psi s\theta s\phi \\ &\quad + F_2 s\theta_2 c\psi s\theta s\phi + F_4 s\theta_4 s\psi c\phi - F_2 s\theta_2 s\psi c\phi \\ &\quad + F_1 c\theta_1 c\psi s\theta c\phi + F_2 c\theta_2 c\psi s\theta c\phi \\ &\quad + F_3 c\theta_3 c\psi s\theta c\phi + F_4 c\theta_4 c\psi s\theta c\phi + F_1 c\theta_1 s\psi s\phi \\ &\quad + F_2 c\theta_2 s\psi s\phi + F_3 c\theta_3 s\psi s\phi + F_4 c\theta_4 s\psi s\phi - C_1 \dot{x} \\ m\ddot{y} &= F_1 s\theta_1 s\psi c\theta - F_3 s\theta_3 s\psi c\theta - F_4 s\theta_4 s\psi s\theta s\phi \\ &\quad + F_2 s\theta_2 s\psi s\theta s\phi - F_4 s\theta_4 c\psi c\phi + F_2 s\theta_2 c\psi c\phi \\ &\quad + F_1 c\theta_1 s\psi s\theta c\phi + F_2 c\theta_2 s\psi s\theta c\phi \\ &\quad + F_3 c\theta_3 s\psi s\theta c\phi + F_4 c\theta_4 s\psi s\theta c\phi - F_1 c\theta_1 c\psi s\phi \\ &\quad - F_2 c\theta_2 c\psi s\phi - F_3 c\theta_3 c\psi s\phi - F_4 c\theta_4 c\psi s\phi - C_2 \dot{y} \end{aligned}$$

$$\begin{aligned}
m\ddot{z} &= -F_1 s\theta_1 s\theta + F_3 s\theta_3 s\theta - F_4 s\theta_4 c\theta s\phi \\
&+ F_2 s\theta_2 c\theta s\phi + F_1 c\theta_1 c\theta c\phi + F_2 c\theta_2 c\theta c\phi \\
&+ F_3 c\theta_3 c\theta c\phi + F_4 c\theta_4 c\theta c\phi - mg - C_3 \dot{z}
\end{aligned} \tag{3.8}$$

Similarly, the angular accelerations are determined by Euler equations:

$$\begin{aligned}
I_x \ddot{\phi} &= l(F_3 c\theta_3 - F_1 c\theta_1 - C'_1 \dot{\phi}) \\
&+ (M_1 s\theta_1 - M_3 s\theta_3) + (M_2' + M_4') \\
I_y \ddot{\theta} &= l(F_4 c\theta_4 - F_2 c\theta_2 - C'_2 \dot{\theta}) \\
&+ (M_4 s\theta_4 - M_2 s\theta_2) + (M_1' + M_3') \\
I_z \ddot{\psi} &= l(F_1 s\theta_1 + F_2 s\theta_2 + F_3 s\theta_3 + F_4 s\theta_4 - C'_3 \dot{\psi}) \\
&+ (M_1 c\theta_1 - M_2 c\theta_2 + M_3 c\theta_3 - M_4 c\theta_4)
\end{aligned} \tag{3.9}$$

where $M'_i, (i = 1, 2, 3, 4)$ are the tilting moments created by the four servo motors attached to the end of each arm to enable their tilting motion. It may be noted that these moments are negligible because the moments produced by the servo motors are used to tilt the arms which are connected to the main body via mechanical bearings. Neglecting bearing friction, the moments transmitted to the main body of the quadrotor are negligible. Based on the dynamic model presented above, we propose the following two Theorems. Note that without loss of generality, yaw angle is assumed to be zero in following theorems.

Theorem 1: *Considering the dynamics of the tilting rotor quadcopter given by Equations (3.8) and (3.9), and assuming the relationship between the tilting angles of the four rotors $\theta_1 = -\theta_3$ and $\theta_2 = -\theta_4$ and all rotors having equal rotational speeds, the quadcopter, at an equilibrium hovering state, achieves a roll angle ϕ given by $\phi = \theta_1/2$ when the pitch angle is zero, and a pitch angle θ given by $\theta = \theta_2/2$ when the roll angle is zero.*

Proof: In tilt-hovering, the arm angles of the first and third propellers are tilted by θ_1 and $\theta_3 = -\theta_1$, respectively. This produces a roll angle ϕ of the vehicle, and, the equations for linear

motion of the quadcopter is given by:

$$\begin{bmatrix} m\ddot{x} \\ m\ddot{y} \\ m\ddot{z} \end{bmatrix} = \begin{bmatrix} F_1 s(\theta_1 - \phi) + F_3 s(-\theta_3 - \phi) - F_2 s\phi - F_4 s\phi \\ 0 \\ F_1 c(\theta_1 - \phi) + F_2 c\phi + F_3 c(-\theta_3 - \phi) + F_4 c\phi \end{bmatrix} + \begin{bmatrix} 0 \\ 0 \\ -mg \end{bmatrix} \quad (3.10)$$

For hovering, the accelerations \ddot{x} , \ddot{y} , and \ddot{z} should all be equal to zero. Using the equation corresponding to the acceleration in X direction, and noting that $F_1 = F_2 = F_3 = F_4$ since rotational speeds of all rotors are the same, the angle ϕ can be obtained as:

$$\phi = \frac{\theta_1}{2} \quad (3.11)$$

Similarly to the equation (3.10), if the second and fourth arms are tilted, the equations of motion can be written as:

$$\begin{bmatrix} m\ddot{x} \\ m\ddot{y} \\ m\ddot{z} \end{bmatrix} = \begin{bmatrix} 0 \\ -F_1 s\theta - F_3 s\theta_3 + F_2 s(\theta_2 - \theta) + F_4 s(-\theta_4 - \theta) \\ F_1 c\theta + F_2 c(\theta_2 - \theta) + F_3 c\theta + F_4 c(-\theta_4 - \theta) \end{bmatrix} + \begin{bmatrix} 0 \\ 0 \\ -mg \end{bmatrix} \quad (3.12)$$

Similar to above, the angle θ resulted from tilting of the second and forth arms, is given by:

$$\theta = \frac{\theta_2}{2} \quad (3.13)$$

Theorem 2: Considering the dynamics of the tilting rotor quadcopter given by Equations (3.8) and (3.9), and assuming the relationship between the tilting angles of the four rotors $\theta_1 = -\theta_3$ and $\theta_2 = -\theta_4$, the motor speed needed for vehicle for hovering with a tilt angle is given by:

$$\omega_i = \omega_h = \sqrt{\frac{mg}{4k_f c \frac{\theta_1}{2}}} \quad \text{when } \theta = 0$$

and

$$\omega_i = \omega_h = \sqrt{\frac{mg}{4k_f c \frac{\theta_2}{2}}} \quad \text{when } \phi = 0 \quad (3.14)$$

Proof: In hovering with roll angle and zero pitch angle, the acceleration along z axis is zero, $\ddot{z} = 0$. Therefore, using the third row of Equation (3.10), we get:

$$\cos\left(\frac{\theta_1}{2}\right) \sum F_i = mg \quad (3.15)$$

Based on Equation (3.3), and noting that each rotor's angular speed is the same (i.e., $F_1 = F_2 = F_3 = F_4$), the angular speed is given by:

$$\omega_i = \omega_h = \sqrt{\frac{mg}{4k_f c \frac{\theta_1}{2}}} \quad (3.16)$$

Similarly, considering hovering with pitch angle and zero roll angle, the Equation (3.12) gives:

$$\cos\left(\frac{\theta_2}{2}\right) \sum F_i = mg \quad (3.17)$$

Now similar to above, the angular speeds of the rotors is given by:

$$\omega_i = \omega_h = \sqrt{\frac{mg}{4k_f c \frac{\theta_2}{2}}} \quad (3.18)$$

Chapter 4

Control System

4.1 Linear Controller Design

In this chapter, the control strategy of the tilting rotor quadcopter is presented. The aim of the control strategy is not only control the position of the vehicle to follow an arbitrary trajectory in 3 dimensions, but also to have control over the orientation of the vehicle in hovering as well as during trajectory tracking.

4.1.1 Proportional Derivative Control

The controller inputs are four independent speeds of propellers and their rotations about the axes of quadcopter arms. Referring to Figure (3-2) and the two Theorems, it is assumed that $\theta_1 = -\theta_3$ and $\theta_2 = -\theta_4$. It may be noted that these constraints, in fact, make the over-actuated system into fully actuated system (two inputs to tilt the rotors another four inputs for their rotational speeds make the total number of independent control inputs to be six). For 6 DoF quadcopter, this results into complete control over its position and orientation. The dynamic model of the tilting rotor quadcopter, described in (3.8) and (3.9), is used to design the PD controllers for orientation adjustment and trajectory tracking. Figure (4-1) shows the block diagram of the control algorithm for orientation and position control during the flight.

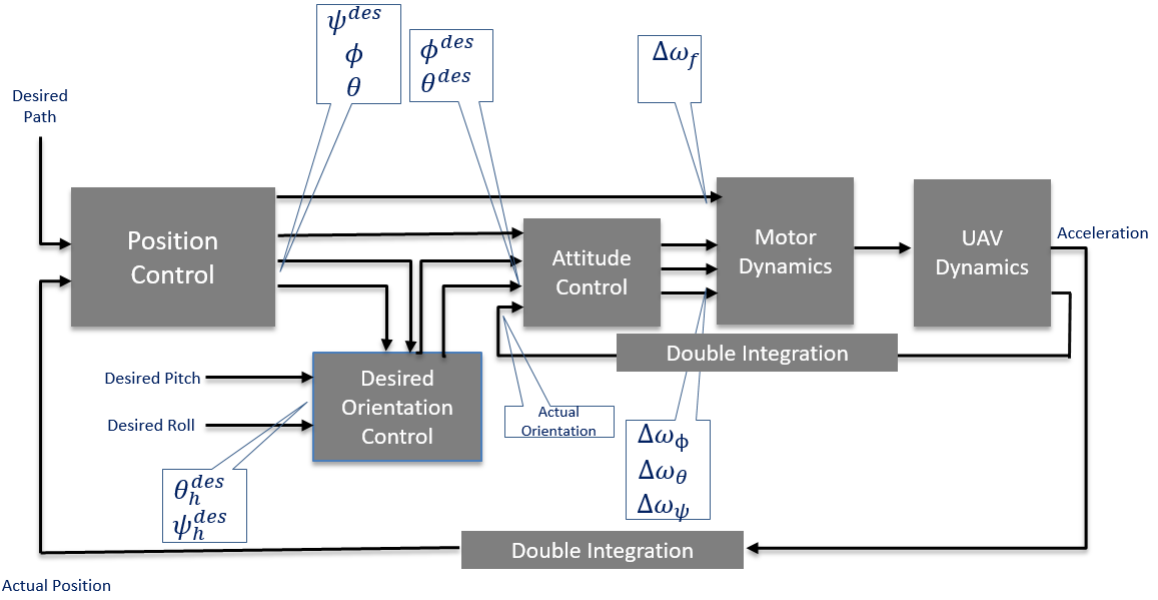


Figure 4-1: The block diagram of position and orientation control algorithm

To start tracking a specific trajectory, first, hovering from the initial starting point is necessary. Then, the orientation of the vehicle to a specific pitch or roll angle is obtained. In [46], the relationship between the rotational speeds of the motors and the deviation of the orientations from nominal vectors for hovering and navigation is described in detail for conventional quadcopter. Similar to that approach for the tilting rotor quadcopter, the rotational speeds are observed as:

$$\begin{bmatrix} \omega_1^{des} \\ \omega_2^{des} \\ \omega_3^{des} \\ \omega_4^{des} \end{bmatrix} = \begin{bmatrix} 1 & 0 & -1 & 1 \\ 1 & 1 & 0 & -1 \\ 1 & 0 & 1 & 1 \\ 1 & -1 & 0 & -1 \end{bmatrix} \begin{bmatrix} \omega_h + \Delta\omega_f \\ \Delta\omega_\phi \\ \Delta\omega_\theta \\ \Delta\omega_\psi \end{bmatrix} \quad (4.1)$$

where ω_i^{des} , ($i = 1, 2, 3, 4$) are the desired angular velocities of the respective rotors. The hovering speed, ω_h , is calculated from Theorem II. The proportional- derivative laws are used to control $\Delta\omega_\phi$, $\Delta\omega_\theta$, $\Delta\omega_\psi$ and $\Delta\omega_f$ which are deviations that result into forces/moment causing

roll, pitch, yaw, and a net force along the z_B axis, respectively, which are calculated as:

$$\begin{aligned}\Delta\omega_\phi &= k_{p,\phi}(\phi^{des} - \phi) + k_{d,\phi}(p^{des} - p) \\ \Delta\omega_\theta &= k_{p,\theta}(\theta^{des} - \theta) + k_{d,\theta}(q^{des} - q) \\ \Delta\omega_\psi &= k_{p,\psi}(\psi^{des} - \psi) + k_{d,\psi}(t^{des} - t)\end{aligned}\quad (4.2)$$

where p, q and t are the component of angular velocities of the vehicle in the body frame. The relationship between these components and derivatives of the roll, pitch and yaw angles are provided below [34].

$$\begin{bmatrix} \dot{\phi} \\ \dot{\theta} \\ \dot{\psi} \end{bmatrix} = T \begin{bmatrix} p \\ q \\ t \end{bmatrix}$$

$$T = \begin{bmatrix} 1 & \tan\theta \cdot \sin\phi & \tan\theta \cdot \cos\phi \\ 0 & \cos\phi & -\sin\phi \\ 0 & \sec\theta \cdot \sin\phi & \sec\theta \cdot \cos\phi \end{bmatrix}$$

The relationship between the tilt angles of individual rotors, given by $\theta_i^{des}, i = 1, 2..4$, and the reference pitch and roll angles is given by :

$$\begin{bmatrix} \theta_1^{des} \\ \theta_2^{des} \\ \theta_3^{des} \\ \theta_4^{des} \end{bmatrix} = \begin{bmatrix} 1 & 0 & 1 & 0 \\ 0 & 1 & 0 & 1 \\ 1 & 0 & 1 & 0 \\ 0 & 1 & 0 & 1 \end{bmatrix} \begin{bmatrix} 2\phi_h^{des} \\ 2\theta_h^{des} \\ \Delta\phi_h \\ \Delta\theta_h \end{bmatrix} \quad (4.3)$$

where ϕ_h^{des} and θ_h^{des} are reference roll and pitch angles and $\Delta\phi_h$ and $\Delta\theta_h$ are orientation deviations. Figure (4-2) shows the orientation of the vehicle with respect to the tilted propellers. A proportional-derivative controller is used to control the orientation deviation using the reference

orientation values as:

$$\begin{aligned}\Delta\phi_h &= k_{p,\phi_h}(\phi_h^{des} - \phi) + k_{d,\phi_h}(\dot{\phi}_h^{des} - p) \\ \Delta\theta_h &= k_{p,\theta_h}(\theta_h^{des} - \theta) + k_{d,\theta_h}(\dot{\theta}_h^{des} - q)\end{aligned}\quad (4.4)$$

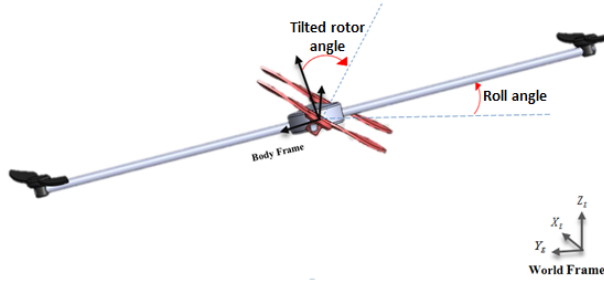


Figure 4-2: Hovering with tilted arms

The mathematical model of DC servo motor is obtained by the following first order transfer function that relates the motor angular velocity (rad/s) to input voltage (V) as:

$$\frac{\Omega(s)}{V(s)} = \frac{K}{\tau s + 1} \quad (4.5)$$

where τ represents the time constant of the system, and K represents the steady state gain value. The angular position of the servo motor can be obtained by integrating the motor angular velocity. The transfer function relating the angular position (rad) and input voltage (V) can be obtained as:

$$\frac{\Theta(s)}{V(s)} = \frac{K}{s(\tau s + 1)} = \frac{K}{\tau s^2 + s} \quad (4.6)$$

The above equation represents a second order transfer function. So, this system is identical to a second order actuation system. Such systems exhibit a transient response when they are subjected to external inputs or environmental disturbances. It should be noted that, the transient response characteristics are one of the most important factors in system design. In general,

transfer function of a 2nd order system with input, $u(t)$ and output, $y(t)$ can be expressed as:

$$\frac{y(s)}{u(s)} = \frac{k\omega^2}{s^2 + 2\zeta\omega + \omega^2} \quad (4.7)$$

The TGY-210DMH servo motor used in tilt rotor quadrotor system is similar to an actuator system with damping ratio (ζ) = 0.7, and it has an angular speed of 8 rad/s when operated at 6V and 6.98 rad/s when operating at 4.8V . The natural frequency for mathematical model is considered to be as 16 rad/s by considering a factor of safety equal to 2, the DC gain has been considered as unity.

In order to have the quad-rotor track a desired trajectory $r_{i,T}$, the command acceleration, \ddot{r}_i^{des} is calculated from proportional-derivative controller based on position error, as [46]:

$$(\ddot{r}_{i,T} - \ddot{r}_i^{des}) + k_{d,i}(\dot{r}_{i,T} - \dot{r}_i) + k_{p,i}(r_{i,T} - r_i) = 0 \quad (4.8)$$

where r_i and $r_{i,T}$ ($i = 1, 2, 3$) are the 3-dimensional position of the quad-rotor and desired trajectory respectively. It may be noted that $\dot{r}_{i,T} = \ddot{r}_{i,T} = 0$ for hover.

During the flight of a tilting quadcopter, the orientation of the vehicle needs to be set at specific pitch or roll. This can be obtained by linearizing the equation of motion that correspond to the nominal hover states. The nominal hover state ($\phi = \phi_h^{des} = \theta_1/2, \theta = \theta_h^{des} = \theta_2/2, \psi = \psi_T, \dot{\theta} = \dot{\psi} = \dot{\phi} = 0$) corresponds to equilibrium hovering configuration with the reference pitch or roll angles. The change of the pitch or roll angles are supposed to be small during flight. By linearizing Equation (3.8) about these nominal hovering states, desired pitch and roll angles to cause the motion can be derived as given by the following equations :

$$\begin{aligned} \ddot{r}_1^{des} &= 2g(A\tilde{\theta}^{des} + B\tilde{\phi}^{des} + C) \\ \ddot{r}_2^{des} &= 2g(D\tilde{\theta}^{des} + E\tilde{\phi}^{des} + F) \\ \ddot{r}_2^{des} &= \frac{8k_f\omega_h}{mG}\Delta\omega_F \end{aligned} \quad (4.9)$$

where

$$\begin{aligned}
A &= -s(2\phi_h^{des})c(\psi_T)s(\theta_h^{des}) + s(2\theta_h^{des})c(\psi_T)s(\phi_h^{des})c\theta_h^{des} \\
&\quad + c(\phi_h^{des})c(\psi_T)c\theta_h^{des}c\phi_h^{des} + c(2\theta_h^{des})c(\psi_T)c(\theta_h^{des})c(\phi_h^{des}) \\
B &= s(2\theta_h^{des})c(\psi_T)s(\theta_h^{des})s(\phi_h^{des}) + s(2\theta_h^{des})s(\psi_T)s(\phi_h^{des}) \\
&\quad - c(2\phi_h^{des})c(\psi_T)s(\theta_h^{des})s(\phi_h^{des}) \\
&\quad - c(2\theta_h^{des})c(\psi_T)s(\theta_h^{des})s(2\phi_h^{des}) + c(2\phi_h^{des})s(\psi_T)c(\phi_h^{des}) \\
&\quad + c(2\theta_h^{des})s(\psi_T)c(\phi_h^{des}) \\
C &= s(2\phi_h^{des})c(\psi_T)c(\theta_h^{des}) + s(2\theta_h^{des})c(\psi_T)s(\theta_h^{des})s(\phi_h^{des}) \\
&\quad - s(2\theta_h^{des})s(\psi_T)c(\phi_h^{des}) + c(2\phi_h^{des})c(\psi_T)s(\theta_h^{des})c(\phi_h^{des}) \\
&\quad + c(2\theta_h^{des})c(\psi_T)s(\theta_h^{des})s(\phi_h^{des}) + c(2\phi_h^{des})s(\psi_T)s(\phi_h^{des}) \\
&\quad + c(2\theta_h^{des})s(\psi_T)s(\phi_h^{des}) \\
D &= -(2\phi_h^{des})c(\psi_T)s(\theta_h^{des}) + s(2\theta_h^{des})s(\psi_T) \\
&\quad + c(2\theta_h^{des})s(\psi_T)c(\theta_h^{des})s(\phi_h^{des}) \\
&\quad + c(2\phi_h^{des})s(\psi_T)c(\theta_h^{des})s(\phi_h^{des}) \\
E &= s(2\theta_h^{des})s(\psi_T)s(\theta_h^{des})c(\phi_h^{des}) - (2\phi_h^{des})s(\psi_T) \\
&\quad + (2\phi_h^{des})s(\psi_T)s(\theta_h^{des})c(\phi_h^{des}) \\
&\quad + (2\theta_h^{des})s(\psi_T)s(\theta_h^{des})c(\phi_h^{des}) - c(2\phi_h^{des})c(\psi_T)c(\phi_h^{des}) \\
&\quad - c(2\theta_h^{des})c(\psi_T)c(\phi_h^{des}) \\
F &= s(\phi_h^{des})c(\psi_T)c(\theta_h^{des}) + s(2\theta_h^{des})s(\psi_T)s(\theta_h^{des})s(\phi_h^{des}) \\
&\quad + s(\theta_h^{des})c(\psi_T)c(\phi_h^{des}) + c(2\phi_h^{des})s(\psi_T)s(\theta_h^{des})s(\phi_h^{des}) \\
&\quad + c(2\theta_h^{des})s(\psi_T)s(\theta_h^{des})s(\phi_h^{des}) - c(\phi_h^{des})c(\psi_T)c(\phi_h^{des}) \\
&\quad - c(\theta_h^{des})c(\psi_T)c(\phi_h^{des}) \\
G &= c\left(\frac{\theta_1}{2}\right)c\left(\frac{\theta_2}{2}\right)
\end{aligned}$$

where $\tilde{\phi}^{des}$ and $\tilde{\theta}^{des}$ are respectively the desired deviation in roll and pitch angles from the nominal hovering values (ϕ_h^{des} and θ_h^{des} respectively) that are needed for position control when

the orientation is set to be given by the nominal hovering values. Equation (5.14) represents a pair of two coupled linear equations which are to be solved to obtain the $\tilde{\phi}^{des}$ and $\tilde{\theta}^{des}$. The final desired pitch or roll angles are calculated by:

$$\begin{aligned}\phi^{des} &= \tilde{\phi}^{des} + \phi_h^{des} \\ \theta^{des} &= \tilde{\theta}^{des} + \theta_h^{des}\end{aligned}\quad (4.10)$$

The desired speeds of the individual rotors are calculated by Equation (5.12). Equation (5.12) is obtained after determination of Equations (5.13) to (4.10).

4.2 Nonlinear Control

The four rotational velocities of the rotors are the inputs of the vehicle, but in order to simplify the equations of motion which are described in (3.8) and (3.9), new artificial input variables are defined as the following. It may be noted that we assume that the tilting happens only along the roll direction.

$$\begin{aligned}u_1 &= (F_1 + F_2 + F_3 + F_4)/m \\ u_2 &= l(F_3 - F_1)/I_x \\ u_3 &= l(F_4 - F_2)/I_y \\ u_4 &= k(F_1\cos\theta_1 - F_2\cos\theta_2 + F_3\cos\theta_3 - F_4\cos\theta_4)/I_z\end{aligned}\quad (4.11)$$

where k is force/moment scaling factor.

The equations of motion of the vehicle, considering small angle assumption and tilting

along only roll direction (hence, $\theta_1 = -\theta_3$ and $\theta_2 = \theta_4 = 0$), can be obtained as:

$$\begin{aligned}
\ddot{x} &= \frac{1}{2} \sin\theta_1 \cos\theta + u_1 \cos\theta_1 \cos\phi^h \cos\phi \sin\theta \\
\ddot{y} &= -u_1 \cos\theta_1 \sin\phi^h \cos\phi - u_1 \cos\theta_1 \cos\phi^h \sin\phi \\
\ddot{z} &= -mg - \frac{1}{2} u_1 \sin\theta_1 \sin\theta + u_1 \cos\theta_1 \cos\phi^h \cos\phi \cos\theta \\
&\quad - u_1 \cos\theta_1 \sin\phi^h \sin\phi \cos\theta \\
\ddot{\phi} &= (\cos\theta_1 + k \sin\theta_1) u_2 \\
\ddot{\theta} &= u_3 \\
\ddot{\psi} &= ku_4
\end{aligned} \tag{4.12}$$

where ϕ^h is the the desired roll angle that the quadcopter is supposed to tilt during the flight.

4.2.1 Feedback Linearization

A brief review of nonlinear control using feedback linearization method [86, 94, 80, 79] is presented here. Among the two fundamental design techniques for feedback linearization, i.e., Input-Output linearization and Input-State linearization, we utilize the Input-Output linearization technique in which we differentiate the output of the systems as many as times as needed so that the input of the system appears in the last derivative[32, 1]. This technique is a systematic way to linearize globally part of, or all, the dynamics of system [29]. The following paragraphs explains how the new/synthetic input v is chosen in order to yield the following transfer function from the synthetic input to the output y [36]:

$$\frac{Y(s)}{V(s)} = \frac{1}{s^\gamma}$$

where γ , the relative degree, is the last derivative of output so that the physical input appears in the equation. If this order is less than the system order (n), then there will be internal dynamics in the feedback linearized system. In cases when internal dynamics appears, the stability of these dynamics should be also be considered. Here we consider a nonlinear system in the

following form:

$$\begin{aligned}\dot{\mathbf{x}} &= f(\mathbf{x}) + g(\mathbf{x})u \\ \mathbf{y} &= h(\mathbf{x})\end{aligned}\tag{4.13}$$

where $\mathbf{x}(\in R^n)$ is the state vector, $u(\in R^m)$ represents the control inputs, and $\mathbf{y}(\in R^p)$ stands for the outputs, f and g are smooth vector fields, and h is a smooth scalar function. A smooth function is defined as an infinitely differentiable function. The control design process is to find an integer γ and a state feedback control law,

$$u = \alpha(\mathbf{x}) + \beta(\mathbf{x})v\tag{4.14}$$

where α and β are smooth functions. This control law exactly linearizes the map between the transformed input v and the output y and yields a linear system (linear from the synthetic input v to the output \mathbf{y}). The above idea can be implemented by successively differentiating the output as:

$$\mathbf{y}^{(\gamma)} = L_f^\gamma h(\mathbf{x}) + L_g L_f^{\gamma-1} h(\mathbf{x})u\tag{4.15}$$

where $\mathbf{y}^{(\gamma)}$ represents the γ^{th} derivative of \mathbf{y} , $L_f^k h(\mathbf{x})$ is called the *Lie derivative* of $L_f^{k-1} h(\mathbf{x})$ with respect to field f . Here, if $L_g L_f^{\gamma-1} h(\mathbf{x})$ is bounded away from zero for all \mathbf{x} , the control law is given by

$$u = \frac{1}{L_g L_f^{\gamma-1} h} (-L_f^\gamma h + v)\tag{4.16}$$

The functions $\alpha(\mathbf{x})$ and $\beta(\mathbf{x})$ in (4.14) can be obtained as:

$$\begin{aligned}\alpha(\mathbf{x}) &= \frac{-L_f^\gamma h(\mathbf{x})}{L_g L_f^{\gamma-1} h(\mathbf{x})} \\ \beta(\mathbf{x}) &= \frac{1}{L_g L_f^{\gamma-1} h(\mathbf{x})}\end{aligned}\tag{4.17}$$

In order to facilitate the design block, assuming

$$\begin{aligned} F(\mathbf{x}) &= L_f^\gamma h(\mathbf{x}) \\ G(\mathbf{x})^{-1} &= \frac{1}{L_g L_f^{\gamma-1} h(\mathbf{x})} \end{aligned} \quad (4.18)$$

Eq. (4.16) can then be written as:

$$u = G^{-1}(\mathbf{x})(v - F(\mathbf{x})) \quad (4.19)$$

We see that the above inversion-based control law has the capability to shape the output response by simply designing the new control v to get the closed-loop linear system which finally yields the desired output.

$$\mathbf{y}^{(\gamma)} = v \quad (4.20)$$

Once linearization has been achieved, any further control objective such as pole placement may be easily met using the linear controls theory.

For the nonlinear quadcopter system under consideration in this section, in order to make the system feedback linearizable, one may consider choosing x, y and z as the output variables. It can easily be seen that u_2 and u_3 in (4.11), which are the control inputs representing the pitch and roll angular accelerations of the vehicle, do not appear in the equation of the outputs. By successively differentiating of equations of motion till the input terms appear, we can generate the new control input of the system. It can be seen the new input terms appear in the fourth derivatives of the outputs as obtained from (4.12):

$$\begin{aligned} x^{(4)} &= f(x)_x + \begin{bmatrix} g(x)_{x1} & g(x)_{x2} & g(x)_{x3} \end{bmatrix} u \\ y^{(4)} &= f(x)_y + \begin{bmatrix} g(x)_{y1} & g(x)_{y2} & g(x)_{y3} \end{bmatrix} u \\ z^{(4)} &= f(x)_z + \begin{bmatrix} g(x)_{z1} & g(x)_{z2} & g(x)_{z3} \end{bmatrix} u \end{aligned} \quad (4.21)$$

where

$$\begin{aligned}
f(x)_x &= -\dot{u}_1 \dot{\theta} \sin \theta_1 \sin \theta + \dot{u}_1 \dot{\theta} \cos \theta_1 \cos \phi^h \cos \phi \cos \theta \\
&\quad - \dot{u}_1 \dot{\phi} \cos \theta_1 \cos \phi^h \sin \phi \sin \theta \\
&\quad - \dot{u}_1 \dot{\phi} \dot{\theta} \cos \theta_1 \cos \phi^h \sin \phi \cos \theta) \\
g(x)_{x1} &= \frac{1}{2} \sin \theta_1 \cos \theta + \cos \theta_1 \cos \phi^h \cos \phi \sin \theta \\
g(x)_{x2} &= -\frac{1}{2} u_1 \sin \theta_1 \cos \theta - u_1 \cos \theta_1 \cos \phi^h \cos \phi \sin \theta \\
g(x)_{x3} &= -u_1 \cos \theta_1 \cos \phi^h \cos \phi \sin \theta \\
f(x)_y &= 2 \dot{u}_1 \dot{\phi} \cos \theta_1 \sin \phi^h \sin \phi - 2 \dot{u}_1 \dot{\phi} \cos \theta_1 \cos \phi^h \cos \phi \\
g(x)_{y1} &= -\cos \theta_1 \sin \phi^h \cos \phi - \cos \theta_1 \sin \phi^h \sin \phi \\
g(x)_{y2} &= 0 \\
g(x)_{y3} &= u_1 \cos \theta_1 \sin \phi^h \cos \phi + u_1 \cos \theta_1 \sin \phi^h \sin \phi \\
f(x)_z &= 2 - \dot{u}_1 \dot{\theta} \sin \theta_1 \cos \theta - 2 \dot{u}_1 \dot{\theta} \cos \theta_1 \cos \phi^h \cos \phi \sin \theta \\
&\quad - 2 \dot{u}_1 \dot{\phi} \cos \theta_1 \cos \phi^h \sin \phi \cos \theta \\
&\quad + 2 u_1 \dot{\theta} \dot{\phi} \cos \theta_1 \cos \phi^h \sin \phi \sin \theta \\
&\quad + 2 \dot{u}_1 \dot{\theta} \cos \theta_1 \sin \phi^h \sin \phi \sin \theta \\
&\quad - 2 \dot{u}_1 \dot{\phi} \cos \theta_1 \sin \phi^h \cos \phi \cos \theta \\
&\quad + 2 u_1 \dot{\theta} \dot{\phi} \cos \theta_1 \sin \phi^h \cos \phi \sin \theta \\
g(x)_{z1} &= -\frac{1}{2} \sin \theta_1 \sin \theta + \cos \theta_1 \cos \phi^h \cos \phi \cos \theta \\
&\quad + \cos \theta_1 \sin \phi^h \sin \phi \cos \theta \\
g(x)_{z2} &= \frac{1}{2} u_1 \sin \theta_1 \sin \theta - u_1 \cos \theta_1 \cos \phi^h \cos \phi \cos \theta \\
&\quad + u_1 \cos \theta_1 \sin \phi^h \sin \phi \cos \theta \\
g(x)_{z3} &= -u_1 \cos \theta_1 \cos \phi^h \cos \phi \cos \theta + u_1 \cos \theta_1 \sin \phi^h \sin \phi \cos \theta \\
u &= \begin{bmatrix} \ddot{u}_1 & u_2 & u_3 \end{bmatrix}^T
\end{aligned}$$

where u is the control inputs which control the x, y and z . We choose u as:

$$u = \begin{bmatrix} g(x)_{x1} & g(x)_{x2} & g(x)_{x3} \\ g(x)_{y1} & g(x)_{y2} & g(x)_{y3} \\ g(x)_{z1} & g(x)_{z2} & g(x)_{z3} \end{bmatrix}^{-1} \cdot \begin{bmatrix} -f(x)_x + v_1 \\ -f(x)_y + v_2 \\ -f(x)_z + v_3 \end{bmatrix} \quad (4.22)$$

The output equation is now given by:

$$\begin{bmatrix} x^{(4)} \\ y^{(4)} \\ z^{(4)} \end{bmatrix} = \begin{bmatrix} v_1 \\ v_2 \\ v_3 \end{bmatrix} \quad (4.23)$$

We set pseudo inputs terms as:

$$\begin{bmatrix} v_1 \\ v_2 \\ v_3 \end{bmatrix} = \begin{bmatrix} x_d^{(4)} - k_{x1}e_x^{(3)} - k_{x2}e_x^{(2)} - k_{x3}\dot{e}_x - k_{x4}e_x \\ y_d^{(4)} - k_{y1}e_y^{(3)} - k_{y2}e_y^{(2)} - k_{y3}\dot{e}_y - k_{y4}e_y \\ z_d^{(4)} - k_{z1}e_z^{(3)} - k_{z2}e_z^{(2)} - k_{z3}\dot{e}_z - k_{z4}e_x \end{bmatrix} \quad (4.24)$$

where e_x, e_y and e_z are errors defined as: $e_x = x - x_d, e_y = y - y_d$ and $e_z = z - z_d$, $[k_{x1}, \dots, k_{x4}]$, $[k_{y1}, \dots, k_{y4}]$ and $[k_{z1}, \dots, k_{z4}]$ are gains, x_d, y_d and z_d are desired outputs. From (4.24), the error dynamics are given by:

$$\begin{aligned} e_x^{(4)} - k_{x1}e_x^{(3)} - k_{x2}e_x^{(2)} - k_{x3}\dot{e}_x - k_{x4}e_x &= 0 \\ e_y^{(4)} - k_{y1}e_y^{(3)} - k_{y2}e_y^{(2)} - k_{y3}\dot{e}_y - k_{y4}e_y &= 0 \\ e_z^{(4)} - k_{z1}e_z^{(3)} - k_{z2}e_z^{(2)} - k_{z3}\dot{e}_z - k_{z4}e_x &= 0 \end{aligned} \quad (4.25)$$

A PD controller is also design to control the yaw motion, and is given by:

$$u_4 = \ddot{\psi}_d = k_{\psi 1}(\dot{\psi}_d - \dot{\psi}) + k_{\psi 2}(\psi_d - \psi) \quad (4.26)$$

where $k_{\psi 1}$ and $k_{\psi 2}$ are derivative and proportional gains respectively.

4.2.2 PD Based Tilting Angle Controller

Tilting rotor quadcopter is designed by using additional four servo motors attached to the end of each arm that allow the rotors to tilt. This capability turns the vehicle into an over-actuated system that potentially can track an arbitrary trajectory over time. During the flight, as the non-linear control based on the proposed feedback linearization method provides the amount of pitch and roll required to track an arbitrary trajectory, a PD controller is also designed to allow the vehicle to either fly or hover with desired orientation or tilting. The relationship between the tilt angles of the individual rotors, given by θ_i^{des} , $i = 1, 2..4$, and the reference pitch and roll angles is given by [51] :

$$\begin{bmatrix} \theta_1 \\ \theta_2 \\ \theta_3 \\ \theta_4 \end{bmatrix} = \begin{bmatrix} 1 & 0 & 1 & 0 \\ 0 & 1 & 0 & 1 \\ 1 & 0 & 1 & 0 \\ 0 & 1 & 0 & 1 \end{bmatrix} \begin{bmatrix} 2\phi^h \\ 2\theta^h \\ \Delta\phi_h \\ \Delta\theta_h \end{bmatrix} \quad (4.27)$$

where ϕ^h and θ^h are reference roll and pitch angles and $\Delta\phi_h$ and $\Delta\theta_h$ are orientation deviations. A proportional-derivative controller is used to control the orientation deviation using the reference orientation values as:

$$\begin{aligned} \Delta\phi_h &= k_{p,\phi_h}(\phi^h - \phi) - k_{d,\phi_h}p \\ \Delta\theta_h &= k_{p,\theta_h}(\theta^h - \theta) - k_{d,\theta_h}q \end{aligned} \quad (4.28)$$

where p, q (and t in the Equation below) are the components of angular velocities of the vehicle in the body frame. The relationship between these components and derivatives of the roll, pitch and yaw angles are provided in [74].

It may be noted that this PD controller is designed to desirably control both pitch and roll angles. However, in this section, for design of feedback linearization method, we assumed the quadcopter to be tilted just in roll direction. Hence, for the simulation studies carried out at chapter 7, we set the reference pitch angle to be zero for this controller.

4.3 Stability Analysis

The inherently unstable tilting quadcopter dynamics described in (3.8) and (3.9) can be written in state-space form: $\dot{\mathbf{X}}(t) = f(\mathbf{X}(t), \mathbf{U}(t))$ where $\mathbf{U}(t)$ and $\mathbf{X}(t)$ are input and state vectors.

$$\begin{aligned} x_1 &= x \\ x_2 &= \dot{x}_1 = \dot{x} \\ x_3 &= y \\ x_4 &= \dot{x}_3 = \dot{y} \\ x_5 &= z \\ x_6 &= \dot{x}_5 = \dot{z} \\ x_7 &= \phi \\ x_8 &= \dot{x}_7 = \dot{\phi} \\ x_9 &= \theta \\ x_{10} &= \dot{x}_9 = \dot{\theta} \\ x_{11} &= \psi \\ x_{12} &= \dot{x}_{11} = \dot{\psi} \end{aligned}$$

$$\mathbf{X} = \begin{bmatrix} x & \dot{x} & y & \dot{y} & z & \dot{z} & \phi & \dot{\phi} & \theta & \dot{\theta} & \psi & \dot{\psi} \end{bmatrix}^T$$

$$\mathbf{U} = \begin{bmatrix} F_1 & F_2 & F_3 & F_4 & \theta_1 & \theta_2 \end{bmatrix}^T$$

The state space model $\dot{\mathbf{X}}(t) = f(\mathbf{X}(t), \mathbf{U}(t))$ is not only non-linear but also highly complicated due to tight coupling between different terms. In order to reduce the number of complicated derivative terms involved in further dynamics, the small angle assumption has been applied to differentiation described in (3.8) and (3.9). We have linearized the system about an operating hovering point while tilting along pitch or roll direction. The operating hovering point \mathbf{X}^e is achieved with the input (\mathbf{U}^e) such that $f(\mathbf{X}^e(t), \mathbf{U}^e(t))=0$. The linearized system is given by:

$$\dot{\mathbf{X}}(t) = A\mathbf{X}(t) + B\mathbf{U}(t)$$

The linearization is carried out via calculating the Jacobian matrices as: $A = \frac{\partial f}{\partial \mathbf{X}}$ and $B = \frac{\partial f}{\partial \mathbf{U}}$ calculated at operating point: $\mathbf{X}^e, \mathbf{U}^e$. This yields:

$$A = \begin{bmatrix} 0 & 1 & 0 & 0 & 0 & 0 & 0 & 0 & 0 & 0 & 0 & 0 & 0 \\ 0 & 0 & 0 & 0 & 0 & 0 & K_1 & 0 & K_2 & 0 & 0 & 0 & 0 \\ 0 & 0 & 0 & 1 & 0 & 0 & 0 & 0 & 0 & 0 & 0 & 0 & 0 \\ 0 & 0 & 0 & 0 & 0 & 0 & L_1 & 0 & 0 & 0 & 0 & 0 & 0 \\ 0 & 0 & 0 & 0 & 0 & 0 & 1 & 0 & 0 & 0 & 0 & 0 & 0 \\ 0 & 0 & 0 & 0 & 0 & 0 & M_1 & 0 & M_2 & 0 & 0 & 0 & 0 \\ 0 & 0 & 0 & 0 & 0 & 0 & 0 & 1 & 0 & 0 & 0 & 0 & 0 \\ 0 & 0 & 0 & 0 & 0 & 0 & 0 & 0 & 0 & 0 & 0 & 0 & 0 \\ 0 & 0 & 0 & 0 & 0 & 0 & 0 & 0 & 0 & 0 & 1 & 0 & 0 \\ 0 & 0 & 0 & 0 & 0 & 0 & 0 & 0 & 0 & 0 & 0 & 0 & 0 \\ 0 & 0 & 0 & 0 & 0 & 0 & 0 & 0 & 0 & 0 & 0 & 0 & 1 \\ 0 & 0 & 0 & 0 & 0 & 0 & 0 & 0 & 0 & 0 & 0 & 0 & 0 \end{bmatrix},$$

$$B = \begin{bmatrix} 0 & 0 & 0 & 0 & 0 & 0 \\ A_1 & A_2 & A_3 & A_4 & A_5 & A_6 \\ 0 & 0 & 0 & 0 & 0 & 0 \\ B_1 & B_2 & B_3 & B_4 & B_5 & B_6 \\ 0 & 0 & 0 & 0 & 0 & 0 \\ C_1 & C_2 & C_3 & C_4 & C_5 & C_6 \\ 0 & 0 & 0 & 0 & 0 & 0 \\ D_1 & 0 & D_3 & 0 & D_5 & 0 \\ 0 & 0 & 0 & 0 & 0 & 0 \\ 0 & E_2 & 0 & E_4 & 0 & E_6 \\ 0 & 0 & 0 & 0 & 0 & 0 \\ F_1 & F_2 & F_3 & F_4 & F_5 & F_6 \end{bmatrix} \quad (4.29)$$

where:

$$\begin{aligned}
K_1 &= \frac{1}{m}(-F_4 \sin \theta_4 \sin \theta \cos \phi + F_2 \sin \theta_2 \sin \theta \cos \phi - F_1 \cos \theta_1 \sin \theta \sin \phi \\
&\quad - F_2 \cos \theta_2 \sin \theta \sin \phi - F_3 \cos \theta_2 \sin \theta \sin \phi - F_4 \cos \theta_2 \sin \theta \sin \phi) \\
K_2 &= \frac{1}{m}(-F_1 \sin \theta_1 \sin \theta - F_3 \sin \theta_1 \sin \theta + F_4 \sin \theta_2 \cos \theta \sin \phi \\
&\quad + F_2 \sin \theta_2 \cos \theta \sin \phi + F_1 \cos \theta_1 \cos \theta \cos \phi + F_2 \cos \theta_2 \cos \theta \cos \phi \\
&\quad + F_3 \cos \theta_1 \cos \theta \cos \phi + F_4 \cos \theta_2 \cos \theta \cos \phi) \\
L_1 &= \frac{1}{m}(-F_4 \sin \theta_2 \sin \phi - F_2 \sin \theta_2 \sin \phi - F_1 \cos \theta_1 \cos \phi \\
&\quad - F_2 \cos \theta_2 \cos \phi - F_3 \cos \theta_1 \cos \phi - F_4 \cos \theta_2 \cos \phi) \\
M_1 &= F_4 \sin \theta_2 \cos \theta \cos \phi + F_2 \sin \theta_2 \cos \theta \cos \phi - F_1 \cos \theta_1 \cos \theta \sin \phi \\
&\quad - F_2 \cos \theta_2 \cos \theta \sin \phi - F_3 \cos \theta_1 \cos \theta \sin \phi - F_4 \cos \theta_2 \cos \theta \sin \phi) \\
M_2 &= -F_1 \sin \theta_1 \cos \theta - F_3 \sin \theta_1 \cos \theta \cos \phi - F_4 \sin \theta_2 \sin \theta \cos \phi \\
&\quad - F_2 \sin \theta_2 \sin \theta \sin \phi - F_1 \cos \theta_1 \sin \theta \cos \phi - F_2 \cos \theta_2 \sin \theta \cos \phi \\
&\quad - F_3 \cos \theta_1 \sin \theta \cos \phi - F_4 \cos \theta_2 \sin \theta \cos \phi
\end{aligned}$$

$$\begin{aligned}
A_1 &= \sin\theta_1 + \cos\theta_1 \sin\theta, A_2 = \cos\theta_2 \sin\theta, A_3 = \sin\theta_1 + \cos\theta_1 \sin\theta \\
A_4 &= \cos\theta_2 \sin\theta, A_5 = F_1 \cos\theta_1 + F_3 \cos\theta_1 - F_1 \sin\theta_1 \sin\theta + F_3 \sin\theta_1 \sin\theta \\
A_6 &= -F_2 \sin\theta_2 \sin\theta - F_4 \sin\theta_2 \sin\theta \\
B_1 &= -\cos\theta_1 \sin\phi, B_2 = \sin\theta_2 - \cos\theta_2 \sin\phi, B_3 = -\cos\theta_1 \sin\phi \\
B_4 &= \sin\theta_2 - \cos\theta_2 \sin\phi, B_5 = F_1 \sin\theta_1 \sin\phi + F_3 \sin\theta_1 \sin\phi \\
B_6 &= F_4 \cos\theta_2 + F_2 \cos\theta_2 + F_2 \sin\theta_2 \sin\phi + F_4 \sin\theta_2 \sin\phi \\
C_1 &= -\sin\theta_1 \sin\theta + \cos\theta_1, C_2 = \sin\theta_2 \sin\phi + \cos\theta_2 \\
C_3 &= -\sin\theta_1 \sin\theta + \cos\theta_1, C_4 = \sin\theta_2 \sin\phi + \cos\theta_2 \\
C_5 &= -F_1 \cos\theta_1 \sin\theta - F_3 \cos\theta_1 \sin\theta - F_1 \sin\theta_1 - F_3 \sin\theta_1 \\
C_6 &= F_4 \cos\theta_2 \sin\phi + F_2 \cos\theta_2 \sin\phi - F_2 \sin\theta_2 - F_4 \sin\theta_2 \\
D_1 &= -l \cos\theta_1 + k \sin\theta_1, D_3 = l \cos\theta_1 - k \sin\theta_1 \\
D_5 &= -l F_3 \sin\theta_1 + l F_1 \sin\theta_1 + k F_1 \cos\theta_1 - k F_3 \cos\theta_1 \\
E_2 &= -l \cos\theta_2 - k \sin\theta_2, E_4 = l \cos\theta_2 + k \sin\theta_2 \\
E_6 &= -l F_4 \sin\theta_2 + l F_2 \sin\theta_2 + k F_4 \cos\theta_2 - k F_2 \cos\theta_2 \\
F_1 &= l \sin\theta_1 + k \cos\theta_1, F_2 = l \sin\theta_2 - k \cos\theta_2, F_3 = l \sin\theta_1 + k \cos\theta_1 \\
F_4 &= l \sin\theta_2 - k \cos\theta_2, F_5 = l F_1 \cos\theta_1 + l F_3 \cos\theta_1 - k F_1 \sin\theta_1 - k F_3 \sin\theta_1 \\
F_6 &= l F_2 \cos\theta_2 + l F_4 \cos\theta_2 - k F_2 \sin\theta_2 - k F_4 \sin\theta_2
\end{aligned}$$

Once the system is linearized, the controllability of the system in the vicinity of equilibrium points can be analyzed using tools of linear system theory. We analyzed the system's controllability for ranges of values on tilting angles along pitch or roll directions. As an example, we provide results for one particular hovering point when $F_1 = F_2 = F_3 = F_4 = \frac{mg}{4}$, $\phi_h^{des} = 0$, and $\theta_h^{des} = 20^0$.

$$A = \begin{bmatrix} 0 & 1 & 0 & 0 & 0 & 0 & 0 & 0 & 0 & 0 & 0 & 0 \\ 0 & 0 & 0 & 0 & 0 & 0 & 0.011 & 0 & 21.342 & 0 & 0 & 0 \\ 0 & 0 & 0 & 1 & 0 & 0 & 0 & 0 & 0 & 0 & 0 & 0 \\ 0 & 0 & 0 & 0 & 0 & 0 & -10.340 & 0 & 0 & 0 & 0 & 0 \\ 0 & 0 & 0 & 0 & 0 & 1 & 0 & 0 & 0 & 0 & 0 & 0 \\ 0 & 0 & 0 & 0 & 0 & 0 & 3.762 & 0 & -0.078 & 0 & 0 & 0 \\ 0 & 0 & 0 & 0 & 0 & 0 & 0 & 1 & 0 & 0 & 0 & 0 \\ 0 & 0 & 0 & 0 & 0 & 0 & 0 & 0 & 0 & 0 & 0 & 0 \\ 0 & 0 & 0 & 0 & 0 & 0 & 0 & 0 & 0 & 1 & 0 & 0 \\ 0 & 0 & 0 & 0 & 0 & 0 & 0 & 0 & 0 & 0 & 0 & 0 \\ 0 & 0 & 0 & 0 & 0 & 0 & 0 & 0 & 0 & 0 & 0 & 1 \\ 0 & 0 & 0 & 0 & 0 & 0 & 0 & 0 & 0 & 0 & 0 & 0 \end{bmatrix},$$

$$C = \begin{bmatrix} 1 & 0 & 0 & 0 & 0 & 0 & 0 & 0 & 0 & 0 & 0 & 0 \\ 0 & 0 & 1 & 0 & 0 & 0 & 0 & 0 & 0 & 0 & 0 & 0 \\ 0 & 0 & 0 & 0 & 1 & 0 & 0 & 0 & 0 & 0 & 0 & 0 \\ 0 & 0 & 0 & 0 & 0 & 0 & 1 & 0 & 0 & 0 & 0 & 0 \\ 0 & 0 & 0 & 0 & 0 & 0 & 0 & 0 & 1 & 0 & 0 & 0 \\ 0 & 0 & 0 & 0 & 0 & 0 & 0 & 0 & 0 & 0 & 1 & 0 \end{bmatrix}$$

$$B = \begin{bmatrix} 0 & 0 & 0 & 0 & 0 & 0 \\ 0.0314 & 0.0028 & 0.0314 & 0.0028 & 11.8610 & -0.0114 \\ 0 & 0 & 0 & 0 & 0 & 0 \\ 0 & 0.3421 & 0 & 0.3421 & 0 & 10.2456 \\ 0 & 0 & 0 & 0 & 0 & 0 \\ 1.0000 & 0.9397 & 1.0000 & 0.9397 & -0.0335 & 0 \\ 0 & 0 & 0 & 0 & 0 & 0 \\ -0.2500 & 0 & 0.2500 & 0 & -0.0400 & 0 \\ 0 & 0 & 0 & 0 & 0 & 0 \\ 0 & -0.2281 & 0 & 0.2281 & 0 & -0.9028 \\ 0 & 0 & 0 & 0 & 0 & 0 \\ 0.0250 & 0.0667 & 0.0250 & 0.0667 & 0.5000 & 0.4562 \end{bmatrix}$$

The matrices A and B were used to determine the controllability of the system and was found to be controllable. This means that a feedback control law $\mathbf{U}(t) = -K_{fd}\mathbf{X}(t)$ can be designed to stabilize and control the system via pole placement method where K_{fd} is a 6×12 feedback control gain matrix.

Chapter 5

Fault Tolerant Flight

5.1 Introduction

In this chapter, stability and control of tilting-rotor quadcopter is presented upon failure of one propeller during flight. The tilting rotor quadcopter provides advantage in terms of additional stable configurations. On failure of one propeller, the quadcopter has a tendency of spinning about the primary axis fixed to the vehicle as an outcome of the asymmetry about the yaw axis. The tilting-rotor configuration is an over-actuated form of a traditional quadcopter and it is capable of handling a propeller failure, thus making it a fault tolerant system. In this chapter, a dynamic model of tilting-rotor quadcopter with one propeller failure is derived and a controller is designed to achieve hovering and navigation capability. The simulation results of translational and hovering motion are presented.

Multicopters with six or more propellers are also popular as the vehicle is able to maintain normal flight if one of the propellers fails [48]. But multicopters are costly as compared to the quadcopters while applications are the same. VTOL UAVs are finding more and more applications in civilian domain and this changing scenario demands new rules and regulations in future[63, 89]. System failures are inevitable during flight of UAVs. Propeller or motor failure is one of the most common failure in case of quadcopters[6]. Currently, the commercial solution available to deal with propeller failure is emergency parachute which assists in emergency landing of quadcopters [75].

The operational scenario of quadcopters requires the design of controllers capable of fault detection, isolation, and diagnosis [3]. Once the failure occurs, the system must be capable of

maintaining the stability of the system and complete the mission without much compromise in system performance. In passive fault tolerant control system (PFTCS) the control algorithm is designed to achieve a given objective in healthy or faulty situation without changing its control law [93], whereas In active fault tolerant control system (AFTCS), to preserve the ability of system to achieve the objective, the control law is changed according to fault situation [8, 42]. The fault diagnosis and identification (FDI) block, also termed as diagnosis unit, consists residual generator and residual evaluation sub-units. A residual is generated by comparing the process output and the model output, if the residual differs from zero. The residual evaluation compares it to a threshold to decide and indicate fault. Based on the diagnosis result the reconfiguration block has to adapt the controller in such a way that the new controller is able to cope with the faulty process.

Fault Detection and Isolation (FDI) system for actuator faults for an hexacopter vehicle has been presented in [20] . A diagnostic Thau observer is applied to the hexacopter nonlinear model to generate residual signals. In the fault-free case, residuals are close to zero, while in case of a faulty actuator, the value of residuals and fault is detected. Further, Fault isolation is realized by exploiting the mathematical model of the hexacopter. By quickly detecting the fault, the control law can be modified to satisfy the closed-loop requirements of the system and thus making it an active fault tolerant control.

In [48] the control strategy is presented using periodic solutions for a quadcopter experiencing one, two opposite, or three complete rotor failures. The strategy employed is to define an axis, fixed with respect to the vehicle body, and have the vehicle rotate freely about this axis. By tilting this axis, and varying the total amount of thrust produced, the vehicles position can be controlled.

Emergency landing procedure of quadcopter has been presented in [38, 41, 24] by using PID and Backstepping control approach respectively. The strategy is to switch off the propeller aligned on the same quadcopter axis of the failed propeller. This action converts the quadcopter configuration into a birotor aerial vehicle. The UAV becomes free to spin in yaw axis while controlling the remaining attitudes of the UAV and then emergency landing procedure is exercised.

The tilting-rotor quadcopter is an over-actuated [51, 52, 82] form of a traditional quadcopter and it is capable of handling a propeller failure, thus making it a fault tolerant system. A robust, fault tolerant control law and redundant mechanical design of the quadcopter can ensure safe handling of the quadcopter even after the propeller failure. In this chapter, the tilt rotor mechanism and PD control of the quadcopter have been used to stabilize the quadcopter after the propeller failure and thus control all states of the UAV.

5.2 Fault Detection

Fault Detection and Isolation (FDI) system for motor failure is a very important aspect of fault tolerant control for quadcopters. Quadcopters belong to the class of very fragile aircraft and if a motor failure occurs, it leads to highly unstable system dynamics. On failure of one propeller, the quadcopter has a tendency of spinning about the primary axis fixed to the vehicle as an outcome of the asymmetry about the yaw axis. The second major asymmetry is created in the roll or pitch plane depending on the corresponding motor failure. If any one of motor 1 or 3 fails, the asymmetry will be in pitch and yaw plane whereas if motor 2 or 4 fails there would be a roll and yaw asymmetry. A robust Fault Detection and Isolation (FDI) system can minimize the reaction time for control system reconfiguration and improve the efficiency of fault tolerant control significantly. As such, this mechanism plays a key role in FTC. FDI can be implemented with a current sensor that can be used to monitor the amount of current supplied to each quadcopter motor. The signal from this sensor can be used to take identify the fault and take further decision for control system reconfiguration. These current sensors fall in category of arduino energy monitors and are very easily available.

5.3 Dynamic Modeling

Unlike traditional quadcopter models, which have only four rotary propellers as the vehicle's inputs, in tilting rotor quadcopters, there are four more servo motors attached to the each arm that adds one degree of freedom to each of the propellers, resulting in the tilting motions along their axes. The equation of motion of a tilting rotor quadcopter has been discussed in

previous sections. In this section, the equations of motion of a tilting rotor quadcopter with one propeller failure is presented.

5.3.1 Tilting Rotor Quadcopters with One Propeller Failure

When all the propellers of the tilt-rotor quadcopter are working then it yields a stable configuration as a result of symmetry of forces and moments. Assuming that one propeller/motor fails during hovering flight of quadcopter which is located in the pitch plane. Then, the quadcopter would possess three working propellers and one failed propeller. Once the failure occurs, the UAV will experience asymmetry about the yaw axis because of M_1, M_3, M_4 moments of working propellers while $M_2 = 0$. Another asymmetry would occur in pitch plane as $F_2 = 0$ and F_4 would still have some magnitude. The equations of motion can be modified by putting F_2 and M_2 equal to zero.

Once again by using rotational matrix in (3.1), equations of motion in world-frame can be written as:

$$\begin{aligned}
 m\ddot{x} &= F_1 s\theta_1 c\psi c\theta - F_3 s\theta_3 c\psi c\theta - F_4 s\theta_4 c\psi s\theta s\phi \\
 &\quad + F_4 s\theta_4 s\psi c\phi + F_1 c\theta_1 c\psi s\theta c\phi + F_3 c\theta_3 c\psi s\theta c\phi \\
 &\quad + F_4 c\theta_4 c\psi s\theta c\phi + F_1 c\theta_1 s\psi s\phi + F_3 c\theta_3 s\psi s\phi \\
 &\quad + F_4 c\theta_4 s\psi s\phi - C_1 \dot{x} \\
 m\ddot{y} &= F_1 s\theta_1 s\psi c\theta - F_3 s\theta_3 s\psi c\theta - F_4 s\theta_4 s\psi s\theta s\phi \\
 &\quad - F_4 s\theta_4 c\psi c\phi + F_1 c\theta_1 s\psi s\theta c\phi + F_3 c\theta_3 s\psi s\theta c\phi \\
 &\quad + F_4 c\theta_4 s\psi s\theta c\phi - F_1 c\theta_1 c\psi s\phi - F_3 c\theta_3 c\psi c\phi \\
 &\quad - F_4 c\theta_4 c\psi s\phi - C_2 \dot{y} \\
 m\ddot{z} &= -F_1 s\theta_1 s\theta + F_3 s\theta_3 s\theta - F_4 s\theta_4 c\theta s\phi \\
 &\quad + F_1 c\theta_1 c\theta c\phi + F_3 c\theta_3 c\theta c\phi + F_4 c\theta_4 c\theta c\phi \\
 &\quad - mg - C_3 \dot{z}
 \end{aligned} \tag{5.1}$$

It should be noted that F_2 terms have vanished from the equations which will result in asym-

metry because of one propeller failure.

Similarly, the angular accelerations are determined by Euler equations:

$$\begin{aligned}
 I_x \ddot{\phi} &= l(F_3 c \theta_3 - F_1 c \theta_1 - C'_1 \dot{\phi}) + (M_1 s \theta_1 - M_3 s \theta_3) \\
 &\quad + M_4' \\
 I_y \ddot{\theta} &= l(F_4 c \theta_4 - C'_2 \dot{\theta}) + M_4 s \theta_4 \\
 &\quad + (M_1' + M_3') \\
 I_z \ddot{\psi} &= l(F_1 s \theta_1 + F_3 s \theta_3 + F_4 s \theta_4 - C'_3 \dot{\psi}) \\
 &\quad + (M_1 c \theta_1 + M_3 c \theta_3 - M_4 c \theta_4)
 \end{aligned} \tag{5.2}$$

where $M'_i, (i = 1, 2, 3, 4)$ are the same tilting moments which are created by the four servo motors attached to the end of each arm to cause a tilt angle. The absence of F_2, M_2 should be noted in pitch and yaw acceleration equations. The components of rotor moment M_1, M_3, M_4 would not produce a symmetrical outcome which represent unstable dynamics of quadcopter upon propeller failure. The available inputs to stabilize and control this system are angular speed $\omega_1, \omega_3, \omega_4$ of three working rotors and tilt angle $\theta_i, (i = 1, 2, 3, 4)$ of all rotors.

Theorem-III: Considering the dynamics of tilt-rotor quadcopter upon propeller failure given by Equations (5.1) and (5.2), the quadcopter can be stabilized in yaw and pitch plane if fourth rotor is tilted by an angle θ_4 such that $\theta_4 = c^{-1}[\omega_4^2/(\omega_1^2 c \theta_1 + \omega_3^2 c \theta_3)]$.

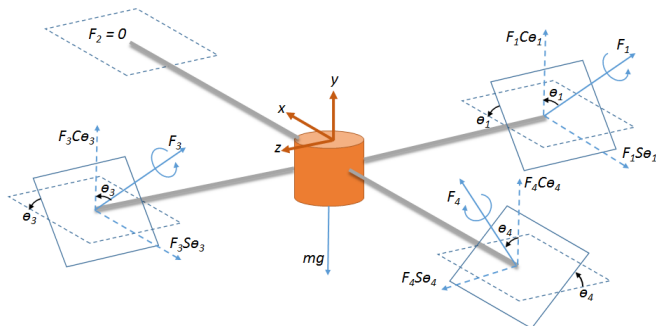


Figure 5-1: Free body diagram of tilt-rotor quadcopter upon propeller failure

Proof: When propeller failure occurs the dynamics of the quadcopter are highly non-linear.

Thus, we ignore the drag forces and moments generated because of rotor tilt for simplification. This assumption simplifies the angular acceleration equations and the equations for pitch and yaw acceleration are given by:

$$\begin{aligned} I_y \ddot{\theta} &= lF_4 c\theta_4 + M_4 s\theta_4 \\ I_z \ddot{\psi} &= lF_4 s\theta_4 + M_1 c\theta_1 + M_3 c\theta_3 - M_4 c\theta_4 \end{aligned} \quad (5.3)$$

If the quadcopter has to be stabilized in pitch and yaw plane, $\ddot{\theta}, \ddot{\psi}$ should be zero. Thus, equation (5.3) can be equated to zero to solve for θ_4 .

$$\begin{aligned} lF_4 c\theta_4 &= -M_4 s\theta_4 \\ lF_4 &= -M_4(s\theta_4/c\theta_4) \\ lF_4 s\theta_4 - M_4 c\theta_4 &= -M_1 c\theta_1 - M_3 c\theta_3 \end{aligned} \quad (5.4)$$

Substituting the value lF_4 in equation (5.4) and rearranging the equation:

$$\begin{aligned} -M_4(s\theta_4 s\theta_4/c\theta_4) - M_4 c\theta_4 &= -M_1 c\theta_1 - M_3 c\theta_3 \\ -M_4(s^2\theta_4 + c^2\theta_4)/(c\theta_4) &= -M_1 c\theta_1 - M_3 c\theta_3 \end{aligned} \quad (5.5)$$

Since, $s^2\theta_4 + c^2\theta_4 = 1$ the above equation reduces to the following form:

$$\begin{aligned} c\theta_4 &= M_4/(M_1 c\theta_1 + M_3 c\theta_3) \\ \theta_4 &= c^{-1}[M_4/(M_1 c\theta_1 + M_3 c\theta_3)] \end{aligned} \quad (5.6)$$

The above expression can be re-written in terms of angular velocity by using equation (3.3) :

$$\theta_4 = c^{-1}[\omega_4^2/(\omega_1^2 c\theta_1 + \omega_3^2 c\theta_3)] \quad (5.7)$$

This condition should hold for attaining a stable configuration after one propeller failure in the tilt-rotor quadcopter. Otherwise, the system can not be stabilized or controlled. In fact, once

the system is stabilized minor deviation in angular speeds of propellers and rotor tilt angle can be utilized to maneuver the quadcopter

Theorem-IV: Once propeller failure occurs, the quadcopter can hold a certain altitude if the angular speed of remaining propellers is increased by:

$$\begin{aligned}\omega'_1 &= \omega_1 + \omega_2/3 \\ \omega'_3 &= \omega_3 + \omega_2/3 \\ \omega'_4 &= \omega_4 + \omega_2/3\end{aligned}\tag{5.8}$$

which means:

$$\omega_h^{new} = \omega_h + \omega_2/3\tag{5.9}$$

Proof: ω_2 represents the angular speed of the second propeller at the instant of failure, this will result in the loss of altitude but the angular speed of three remaining propellers can be increased by a factor of $\omega_2/3$ in order to compensate for the loss. On the other hand, an extra compensation component $\omega_4/c\theta_4$ should come in the equation of fourth rotor to overcome the tilt effect of the rotor. Thus, angular speed of fourth rotor will be higher as compared to angular speed of first and third rotor. $\omega'_1, \omega'_3, \omega'_4$ are the increased angular speeds of the propellers in order to hold the altitude.

Future, the new angular speeds must satisfy equation (5.7) in order to yield a stable configuration. We can conclude this statement in the form of equation (5.8):

$$\theta_4 = c^{-1}[\omega_4'^2 / (\omega_1'^2 c\theta_1 + \omega_3'^2 c\theta_3)]\tag{5.10}$$

5.4 Controller Design

In this section, the control strategy of the tilting rotor quadcopter in a case of motor failure during the flight is presented. Two PD controllers are used due to compensate the unbalance moments created by an odd number of propellers, and also to stabilize vehicle's orientation and make it functional to continue its mission without crash. The vehicle originally has eight independent inputs which includes four speed of propellers and four tilted angle of each motor about its axis. In the case of motor failure, two inputs are automatically out of equations. To make the vehicle compensate the moments of the vehicle, not only the speed of the remaining propellers needs to be controlled individually, but also the tilted mechanism needs to be set in a way that compensates the moment from the breakdown motor. In this work, it's assumed that motor two is the one that stopped working during the flight. It should be noted that the measurement sensor needs to report the failure immediately. Referring to the theorems, the tilting angle of motor 1 and motor 3 needs to be set at the same orientation and the tilted angle of the remaining motors can be immediately set according to Theorem *III*.

To start compensating the unbalanced moment situation after the failure, first, getting back to hovering is necessary. Then, the orientation of the vehicle to a specific pitch or roll angle is obtained. In [46], the relationship between the rotational speeds of the motors and the deviation of the orientations from nominal vectors for hovering and navigation is described in detail for conventional quadcopter. Based on the new dynamics equation of the vehicle with three propellers and one tilted servo motor (motors 1 and 3 are assumed to be level), the following equations are obtained:

$$\begin{bmatrix} M_x^B \\ M_y^B \\ M_z^B \end{bmatrix} = \begin{bmatrix} Lk_f\omega_1' & -Lk_f\omega_3' & 0 & 0 \\ 0 & 0 & Lk_f\omega_4' & 0 \\ 0 & 0 & 0 & 1 \end{bmatrix} \begin{bmatrix} \omega_1' \\ \omega_3' \\ \omega_4' \\ \theta_4 \end{bmatrix} \quad (5.11)$$

where M_x^B , M_y^B and M_z^B are torque components separated in body frame. It needs to be mentioned that these equations are obtained from linearization of equation (5.2) around its nominal

hover states while first and third servo motors are assumed not to be tilted. The rotational speed on each individual motor and the tilted angle of the rear motor are calculated as:

$$\begin{bmatrix} \omega_1^{des} \\ \omega_3^{des} \\ \omega_4^{des} \\ \theta_4^{des} \end{bmatrix} = \begin{bmatrix} 1 & -1 & 0 & 0 \\ 1 & 1 & 0 & 0 \\ 1 & 0 & 1 & 0 \\ 0 & 0 & 0 & 1 \end{bmatrix} \begin{bmatrix} \omega_h^{new} + \Delta\omega_f \\ \Delta\omega_\phi \\ \Delta\omega_\theta \\ \theta_4 + \Delta\theta_4 \end{bmatrix} \quad (5.12)$$

where ω_i^{des} , ($i = 1, 3, 4$) are the desired angular velocities of the respective rotors. θ_4 is the tilted angle that needs to be hold for motor 4 to attaining a stable configuration and is calculated in Theorem III. The hovering speed, ω_h^{new} , is calculated from Theorem IV. The proportional-derivative laws are used to control $\Delta\omega_\phi$, $\Delta\omega_\theta$, $\Delta\theta_4$ and $\Delta\omega_f$ which are deviations that result into forces/moment causing roll, pitch, yaw, and a net force along the z_B axis, respectively, which are calculated as:

$$\begin{aligned} \Delta\omega_\phi &= k_{p,\phi}(\phi^{des} - \phi) + k_{d,\phi}(p^{des} - p) \\ \Delta\omega_\theta &= k_{p,\theta}(\theta^{des} - \theta) + k_{d,\theta}(q^{des} - q) \\ \Delta\theta_4 &= k_{p,\psi}(\psi^{des} - \psi) + k_{d,\psi}(t^{des} - t) \end{aligned} \quad (5.13)$$

where p, q and t are the component of angular velocities of the vehicle in the body frame.

During the flight of a tilting quadcopter, the orientation of the vehicle needs to be set level. This can be obtained by linearizing the equation of motion that correspond to the nominal hover states. The nominal hover state ($\phi = \theta = 0, \psi = \psi_T, \dot{\theta} = \dot{\psi} = \dot{\phi} = 0$) corresponds to equilibrium hovering configuration with the reference pitch or roll angles. The change of the pitch or roll angles are supposed to be small during flight. By linearizing Equation (3.8) about these nominal hovering states, desired pitch and roll angles to cause the motion can be derived as given by the following equations :

$$\begin{aligned} \ddot{r}_1^{des} &= g(c\psi\theta^{des} + s\psi\phi^{des}) - s\psi F_4 s\theta_4 \\ \ddot{r}_2^{des} &= g(s\psi\theta^{des} - c\psi\phi^{des}) + c\psi F_4 s\theta_4 \end{aligned} \quad (5.14)$$

where θ^{des} and ϕ^{des} are the desired pitch and roll to be added to the nominal hover states to move the vehicle to desired trajectory $r_{i,T}$, the command acceleration, \ddot{r}_i^{des} is calculated from proportional-derivative controller based on position error, as [46]:

$$(\ddot{r}_{i,T} - \ddot{r}_i^{des}) + k_{d,i}(\dot{r}_{i,T} - \dot{r}_i) + k_{p,i}(r_{i,T} - r_i) = 0 \quad (5.15)$$

where r_i and $r_{i,T}$ ($i = 1, 2, 3$) are the 3-dimensional position of the quad-rotor and desired trajectory respectively. It may be noted that $\dot{r}_{i,T} = \ddot{r}_{i,T} = 0$ for hover.

5.5 Linearization and Stability Analysis

The dynamic model of the vehicle with one motor failure can be described with the differential equations (5.1) and (5.2). This inherently unstable tilting quadcopter dynamics can be written in state-space form: $\dot{\mathbf{X}}(t) = f(\mathbf{X}(t), \mathbf{U}(t))$ where $\mathbf{U}(t)$ and $\mathbf{X}(t)$ are input and state vectors [10].

$$\begin{aligned} x_1 &= x \\ x_2 &= \dot{x}_1 = \dot{x} \\ x_3 &= y \\ x_4 &= \dot{x}_3 = \dot{y} \\ x_5 &= z \\ x_6 &= \dot{x}_5 = \dot{z} \\ x_7 &= \phi \\ x_8 &= \dot{x}_7 = \dot{\phi} \\ x_9 &= \theta \\ x_{10} &= \dot{x}_9 = \dot{\theta} \\ x_{11} &= \psi \\ x_{12} &= \dot{x}_{11} = \dot{\psi} \end{aligned}$$

$$\begin{aligned}\mathbf{X} &= \begin{bmatrix} x & \dot{x} & y & \dot{y} & z & \dot{z} & \phi & \dot{\phi} & \theta & \dot{\theta} & \psi & \dot{\psi} \end{bmatrix}^T \\ \mathbf{U} &= \begin{bmatrix} F_1 & F_3 & F_4 & \theta_4 \end{bmatrix}^T\end{aligned}$$

Since the quadcopter will not be used for acrobatic maneuvers after the motor failure, the highly nonlinear and also complicated dynamics, can be simplified with the small angle assumption [87] to cover hovering and moving around with small deviation in orientation. In order to reduce the number of complicated derivative terms involved in further dynamics, the small angle assumption has been applied to differentiation described in (5.1) and (5.2). We have linearized the system about an operating hovering state ($\phi = \theta = 0, \psi = \psi_T, \dot{\theta} = \dot{\psi} = \dot{\phi} = 0$). These operating hovering point \mathbf{X}^e is achieved with the input (\mathbf{U}^e) such that

$$f(\mathbf{X}^e(t), \mathbf{U}^e(t)) = 0 \quad (5.16)$$

The linearization of the dynamics will result in A and B matrices,

$$\dot{\mathbf{X}}(t) = A\mathbf{X}(t) + B\mathbf{U}(t)$$

where:

$$\begin{aligned}a_{i,j} &= \frac{\partial f_i(X_0, U_0)}{\partial X_j} \\ b_{i,j} &= \frac{\partial f_i(X_0, U_0)}{\partial U_j}\end{aligned}$$

The linearization is carried out via calculating the Jacobian matrices [40] yields:

$$A = \begin{bmatrix} 0 & 1 & 0 & 0 & 0 & 0 & 0 & 0 & 0 & 0 & 0 & 0 \\ 0 & 0 & 0 & 0 & 0 & 0 & A_{2,7} & 0 & A_{2,9} & 0 & 0 & 0 \\ 0 & 0 & 0 & 1 & 0 & 0 & 0 & 0 & 0 & 0 & 0 & 0 \\ 0 & 0 & 0 & 0 & 0 & 0 & A_{4,7} & 0 & 0 & 0 & 0 & 0 \\ 0 & 0 & 0 & 0 & 0 & 1 & 0 & 0 & 0 & 0 & 0 & 0 \\ 0 & 0 & 0 & 0 & 0 & 0 & 0 & A_{6,7} & 0 & A_{6,9} & 0 & 0 \\ 0 & 0 & 0 & 0 & 0 & 0 & 0 & 0 & 1 & 0 & 0 & 0 \\ 0 & 0 & 0 & 0 & 0 & 0 & 0 & 0 & 0 & 0 & 0 & 0 \\ 0 & 0 & 0 & 0 & 0 & 0 & 0 & 0 & 0 & 0 & 1 & 0 \\ 0 & 0 & 0 & 0 & 0 & 0 & 0 & 0 & 0 & 0 & 0 & 0 \\ 0 & 0 & 0 & 0 & 0 & 0 & 0 & 0 & 0 & 0 & 0 & 1 \\ 0 & 0 & 0 & 0 & 0 & 0 & 0 & 0 & 0 & 0 & 0 & 0 \end{bmatrix},$$

$$B = \begin{bmatrix} 0 & 0 & 0 & 0 \\ A_{2,1} & A_{2,2} & A_{2,3} & A_{2,4} \\ 0 & 0 & 0 & 0 \\ A_{4,1} & A_{4,2} & A_{4,3} & A_{4,4} \\ 0 & 0 & 0 & 0 \\ A_{6,1} & A_{6,2} & A_{6,3} & A_{6,4} \\ 0 & 0 & 0 & 0 \\ A_{8,1} & A_{8,2} & 0 & 0 \\ 0 & 0 & 0 & 0 \\ 0 & 0 & A_{10,3} & A_{10,4} \\ 0 & 0 & 0 & 0 \\ A_{12,1} & A_{12,2} & A_{12,3} & A_{12,4} \end{bmatrix} \quad (5.17)$$

where:

$$\begin{aligned}
A_{2,7} &= \frac{1}{m}(-F_4 \sin \theta_4 \sin \theta \cos \phi - F_1 \cos \theta_1 \sin \theta \sin \phi - F_3 \cos \theta_3 \sin \theta \sin \phi \\
&\quad - F_4 \cos \theta_4 \sin \theta \sin \phi) \\
A_{2,9} &= \frac{1}{m}(-F_1 \sin \theta_1 \sin \theta + F_3 \sin \theta_3 \sin \theta - F_4 \sin \theta_4 \cos \theta \sin \phi \\
&\quad + F_1 \cos \theta_1 \cos \theta \cos \phi + F_3 \cos \theta_3 \cos \theta \cos \phi - F_4 \cos \theta_4 \cos \theta \cos \phi) \\
A_{4,7} &= \frac{1}{m}(F_4 \sin \theta_4 \sin \phi - F_1 \cos \theta_1 \cos \phi + F_3 \cos \theta_3 \cos \phi - F_4 \cos \theta_4 \cos \phi) \\
A_{6,7} &= F_4 \sin \theta_4 \cos \theta \cos \phi - F_1 \cos \theta_1 \cos \theta \sin \phi - F_3 \cos \theta_3 \cos \theta \sin \phi - F_4 \cos \theta_4 \cos \theta \sin \phi \\
A_{6,9} &= -F_1 \sin \theta_1 \cos \theta + F_3 \sin \theta_3 \cos \theta \cos \phi + F_4 \sin \theta_4 \sin \theta \cos \phi \\
&\quad - F_1 \cos \theta_1 \sin \theta \cos \phi - F_3 \cos \theta_3 \sin \theta \cos \phi - F_4 \cos \theta_4 \sin \theta \cos \phi \\
A_{2,1} &= \sin \theta_1 + \cos \theta_1 \sin \theta \cos \phi, A_{2,2} = -\sin \theta_3 + \cos \theta_3 \sin \theta \cos \phi \\
A_{2,3} &= \cos \theta_4 \sin \theta \cos \phi, A_{2,4} = F_4 \sin \theta_4 \sin \theta \cos \phi, \\
A_{4,1} &= -\cos \theta_1 \sin \phi, A_{4,2} = -\cos \theta_3 \cos \phi, A_{4,3} = -\sin \theta_4 \cos \phi - \cos \theta_4 \sin \phi \\
A_{4,4} &= -F_4 \cos \theta_4 \cos \phi + F_4 \sin \theta_4 \sin \phi \\
A_{6,1} &= -\sin \theta_1 \sin \theta + \cos \theta_1 \cos \theta \cos \phi, A_{6,2} = \sin \theta_3 \sin \theta + \cos \theta_3 \cos \theta \cos \phi \\
A_{6,3} &= -\sin \theta_4 \cos \theta \sin \phi + \cos \theta_4 \cos \theta \cos \phi, A_{6,4} = -F_4 \cos \theta_4 \cos \theta \sin \phi - F_4 \sin \theta_4 \cos \theta \cos \phi \\
A_{8,1} &= -l \cos \theta_1 + k \sin \theta_1, A_{8,2} = l \cos \theta_1 - k \sin \theta_1 \\
A_{10,3} &= l \cos \theta_4 + k \sin \theta_4 \\
A_{10,4} &= -l F_4 \sin \theta_4 + k F_4 \cos \theta_4 \\
A_{12,1} &= l \sin \theta_1 + k \cos \theta_1 \\
A_{12,2} &= l \sin \theta_3 + k \cos \theta_3 \\
A_{12,3} &= l \sin \theta_4 - k \cos \theta_4 \\
A_{12,4} &= l F_4 \cos \theta_4 + l F_4 \sin \theta_4
\end{aligned}$$

Once the system is linearized, the controllability of the system in the vicinity of equilibrium points can be analyzed using tools of linear system theory [92].

$$A = \begin{bmatrix} 0 & 1 & 0 & 0 & 0 & 0 & 0 & 0 & 0 & 0 & 0 & 0 \\ 0 & 0 & 0 & 0 & 0 & 0 & -4.1241 & 0 & 8.249 & 0 & 0 & 0 \\ 0 & 0 & 0 & 1 & 0 & 0 & 0 & 0 & 0 & 0 & 0 & 0 \\ 0 & 0 & 0 & 0 & 0 & 0 & -2.751 & 0 & 0 & 0 & 0 & 0 \\ 0 & 0 & 0 & 0 & 0 & 1 & 0 & 0 & 0 & 0 & 0 & 0 \\ 0 & 0 & 0 & 0 & 0 & 0 & 4.763 & 0 & 0 & 0 & 0 & 0 \\ 0 & 0 & 0 & 0 & 0 & 0 & 0 & 1 & 0 & 0 & 0 & 0 \\ 0 & 0 & 0 & 0 & 0 & 0 & 0 & 0 & 0 & 0 & 0 & 0 \\ 0 & 0 & 0 & 0 & 0 & 0 & 0 & 0 & 0 & 1 & 0 & 0 \\ 0 & 0 & 0 & 0 & 0 & 0 & 0 & 0 & 0 & 0 & 0 & 0 \\ 0 & 0 & 0 & 0 & 0 & 0 & 0 & 0 & 0 & 0 & 0 & 1 \\ 0 & 0 & 0 & 0 & 0 & 0 & 0 & 0 & 0 & 0 & 0 & 0 \end{bmatrix},$$

$$C = \begin{bmatrix} 1 & 0 & 0 & 0 & 0 & 0 & 0 & 0 & 0 & 0 & 0 & 0 \\ 0 & 0 & 1 & 0 & 0 & 0 & 0 & 0 & 0 & 0 & 0 & 0 \\ 0 & 0 & 0 & 0 & 1 & 0 & 0 & 0 & 0 & 0 & 0 & 0 \\ 0 & 0 & 0 & 0 & 0 & 0 & 0 & 0 & 0 & 0 & 0 & 0 \\ 0 & 0 & 0 & 0 & 0 & 0 & 0 & 0 & 0 & 0 & 0 & 0 \\ 0 & 0 & 0 & 0 & 0 & 0 & 0 & 0 & 0 & 0 & 0 & 0 \end{bmatrix}$$

$$B = \begin{bmatrix} 0 & 0 & 0 & 0 \\ 0 & 0 & 0 & 0 \\ 0 & 0 & 0 & 0 \\ 0 & -1.000 & -0.865 & -2.751 \\ 0 & 0 & 0 & 0 \\ 1.000 & 1.000 & 0.500 & -4.763 \\ 0 & 0 & 0 & 0 \\ -0.250 & 0.250 & 0 & 0 \\ 0 & 0 & 0 & 0 \\ 0 & 0 & 0.142 & -1.136 \\ 0 & 0 & 0 & 0 \\ 0.020 & 0.020 & 0.026 & 1.878 \end{bmatrix}$$

A feedback control law [58] $\mathbf{U}(t) = -K_{fd}\mathbf{X}(t)$ can be designed to stabilize and control the system via pole placement method where K_{fd} is a 4×12 feedback control gain matrix as below:

$$K_{fd} = \begin{bmatrix} 0.177 & -0.265 & 0.326 & 0.007 \\ 1.517 & -2.079 & 2.680 & 0.034 \\ -0.345 & 0.320 & -0.499 & -0.058 \\ -1.183 & 1.028 & -2.059 & -0.247 \\ -0.675 & 0.244 & -0.091 & -0.082 \\ -4.799 & 1.442 & -0.324 & -0.609 \\ -54.857 & 29.104 & -23.450 & -4.416 \\ -48.255 & 17.135 & -11.818 & -3.983 \\ 22.162 & -35.742 & 50.339 & -0.500 \\ 34.199 & -26.875 & 31.562 & 1.374 \\ 0.785 & -0.790 & 0.870 & 0.099 \\ 3.298 & -3.746 & 4.039 & 0.389 \end{bmatrix}^T$$

Figures (5-2) and (5-3) show how position and orientation of quadcopter with one failed motor remaining stable.

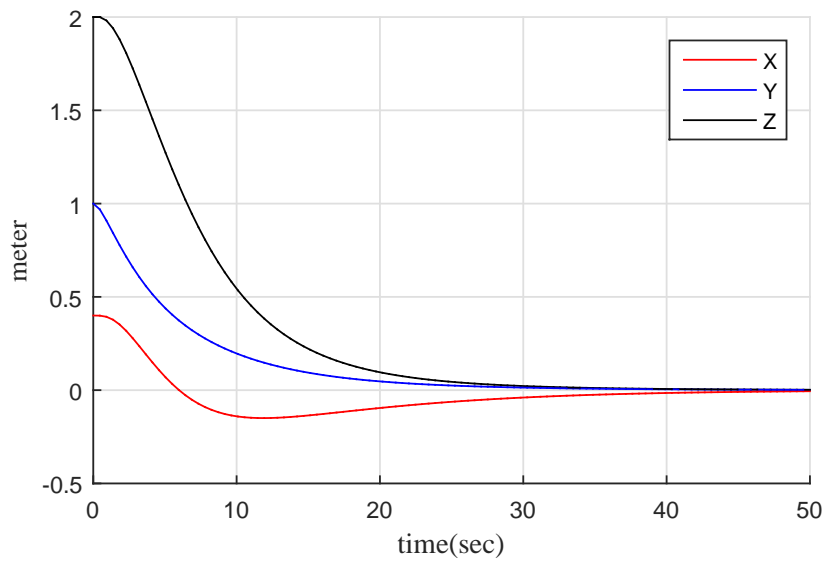


Figure 5-2: Vehicle's Position

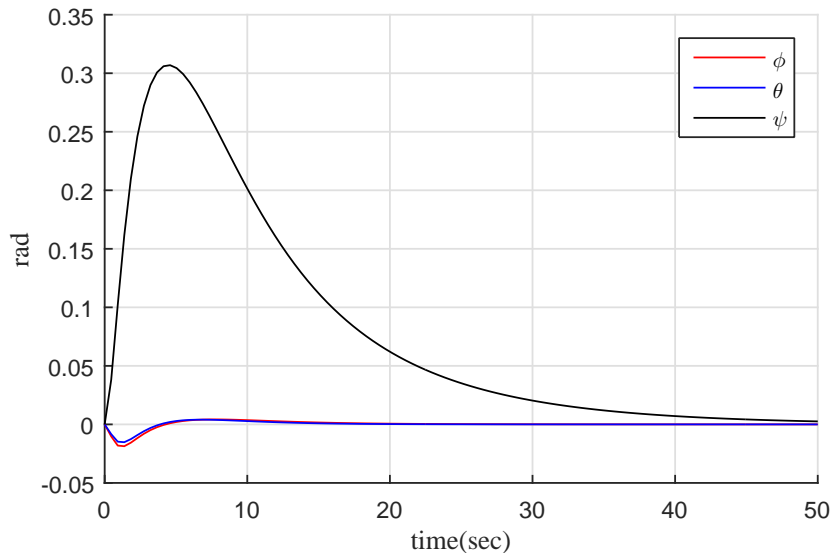


Figure 5-3: Vehicle's Orientation

Chapter 6

Hardware design

6.1 Description of the Prototype

The development of a proposed control techniques for tilting quadcopter requires the development of an adequate platform for the preliminary experiments. The primary consideration for the prototype design was to make the quadcopter small and lightweight so that it was able to carry an extra component required for the tilting mechanism during the flights. The initial configuration and concept of the tilting quadcopter are presented in Figure (6-1). As the fabricating process was a senior design project, the cost of the vehicle was kept as low as possible.

The structural design of the tilting quadcopter can be divided into two parts: the central body where all avionics and components are placed, and the tilting mechanism.



Figure 6-1: The CAD model of the tilting quadcopter

6.1.1 Central body

As the most important mechanical components of the tilting mechanism are located at the center area, this part not only needs to have enough space for all components, but also needs to maintain its symmetry requirement. The central body or core area needs to have space for essential component such as:

- Four Electronic Speed Controls (ESC) to control each motor
- Communication Hardware
- A power distribution board
- Autopilot
- Bearings, and
- Servo motors.

There are two prototypes which have been designed and fabricated. The core part in the first prototype is made using two sheets of flame-retardant Garolite which is connected by plastic bolts and spacer. The flame-retardant Garolite offers excellent strength, low water absorption and good electrical insulating quality in both humid and dry conditions with maximum temperature of $265^{\circ}F$. The material in flame-retardant Garolite is fiberglass-cloth with a flame retardant resin. The hardness also meets Rockwell M110-M115 which is standard hardness test. The reason to use two sheets is to have all bearings, servo motors and electronic parts in between. Four additional polycarbonate round tubes are also attached to the frame in order to make four arms for the quadcopter. Polycarbonate round tube is a cost effective material with outstanding mechanical, thermal, chemical, physical, and electrical properties. It is light in weight, has excellent impact strength, heat resistance to $250^{\circ}F$ and most importantly it comes in a round shape which provides the tilting mechanism with more degree of freedom to rotate.

6.1.2 Tilting Mechanism

The most important features of the tilting quadcopter is the fact that each arm can rotate about its axis independently. In order to have this independency, four additional inputs

are needed to rotate each arm to ensure the tilting mechanism. The servos (Figure (6-2)) are mounted on top of the lower sheet of the central core. Each arm is directly linked to the servo motor using gears. The gear is hooked around the tube in the middle by two bearings. All eight bearings (two for each arm) mount between upper and lower sheets. This unique design allows the arms to rotate separately with any desired angle without mechanical constraint. Figure (6-3) shows how servos, tubes, bearings and sheets are connected.



Figure 6-2: HS-5087MH HV Digital Micro Servo.

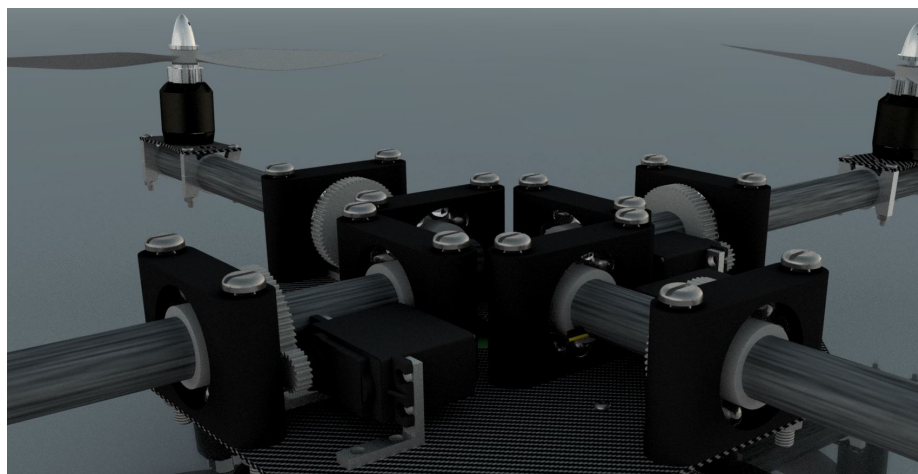


Figure 6-3: The CAD model of components of the tilting mechanism.

Table (6.1) and (6.2) summarize the specifications and the masses of the vehicle's components of the first prototype.

Table 6.1: Specifications of the Prototype

Dimensions	$65cm \times 65cm$
	without propellers
Gross weight	$2.4kg$
Motor Driver	ESC 30Amp
Battery	Lithium-polymer cells 4S
Propeller	11x47 APC propeller
Autopilot	Pixhawk
Motor	Motor 850Kv AC2830-358
Servo	HS-5087MH Digital servo
Communications	MAVLink, MAVROS and Wifi



Figure 6-4: The real model of the first model of tilting Quadcopter.

After ten test flights, due to weight of the vehicle, the motors were not strong enough to handle the tests and the experimental data was not acceptable. To reduce the weight and also make the tilt mechanism more agile, second prototype was designed in Autodesk Inventor and SolidWorks and fabricated by our group. For the second prototype, the 3D robotics framework was used as the body and four separate tilt mechanisms were designed and built by using a

3D printer. The printed 3D mechanism was mounted at the very end of each arm. The parts were made in a way that perfectly fit the arms to avoid any slinging. The electronics, power, propellers, motors and the auto pilot are same as the first prototype.

Table 6.2: Vehicle's component mass details.

Items	Weight (g)	Quantity	Subtotal (g)
Motors	80	4	320.0
Servos	45	4	180.0
Mechanical Gears	20	4	80.0
Prop adapters	8	4	32
Plastic Bolts	6	16	96
ESC	15	4	60
Battery	650	1	650
bearings	35	8	280
Landing gear	50	1	50
Center plates	85	2	170
Controller	38	1	38
Battery Holder	45	1	45
Arms	35	4	140
Wirings and Connectors	150	1	150
Total			2291

This vehicle also has eight control inputs which are used for rotating the four propellers and tilting mechanism for the arms. It weights 1kg less than the first prototype. The diameter also does not exceed 55cm. To tilt the motors around the arms, a tilting mechanism has been located at the end of each arms. Each tilting mechanism consist of three separate parts: i) the servo motor holder ii) the plate holder iii) and the motor plate which is mounted on the base via a tilting mechanism.

There are some similar mechanisms available in the market, but the main reason that makes

our design more reliable, is the way the servo is connected to the tilting part. In available versions of the tilting mechanism, the servo is screwed to the mechanism with the same screw which holds the tilting parts together. The problem comes when the screw is tightened enough to attach the servo to the tilting part to avoid any sliding. This also pushes the two separate mechanisms towards each other and makes it harder to tilt. While more force is needed to be able to make the pressed part to rotate, an extra force which comes from the servo motor, makes the cog loose. The looseness between the servo and the tilting part contributes to a delay when the command is received the motor starts tilting. This delay adds the nonlinear parts to the control system which is not easy to be taken into the equation.

The currently designed tilting mechanism has an extra screw which is placed between the tilting mechanism and the servo cog. By having this additional screw, the servo cog can be fastened to the tilting mechanism as much as needed, while the two tilting mechanisms are attached to each other with separate screw. With this design, not only there is no friction in tilting mechanism, the servo would never get loose. Figure (6-5) shows the transparent CAD model of the tilting mechanism. Figure (6-6) shows how the tilting mechanism is mounted at the end of quadcopter's arm and how the servo, tilting mechanism and the motor are connected. In Figure (6-7), both CAD and actual model are presented.

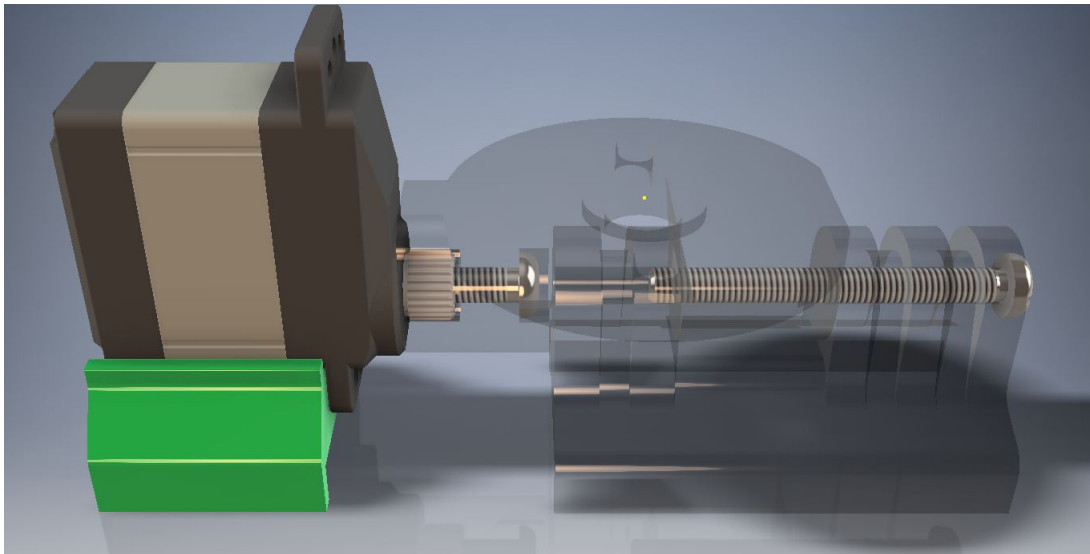


Figure 6-5: The CAD model of transparent tilting mechanism

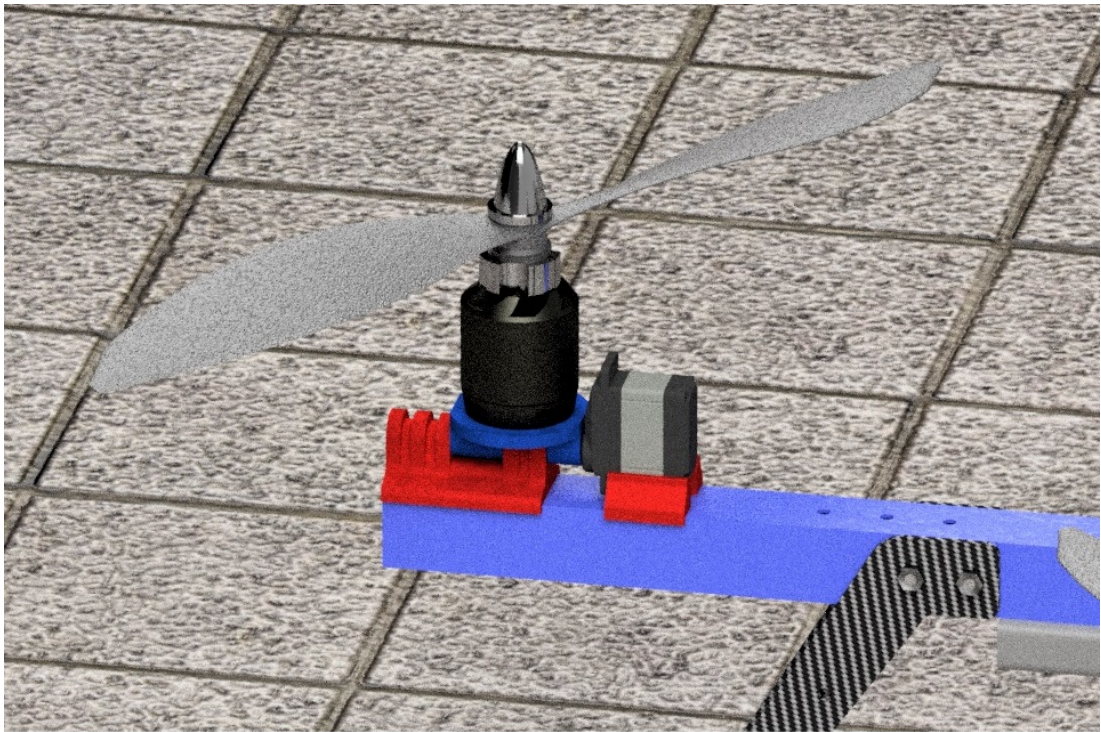


Figure 6-6: The CAD model of tilting mechanism mounted on the arm with the servo and the motor

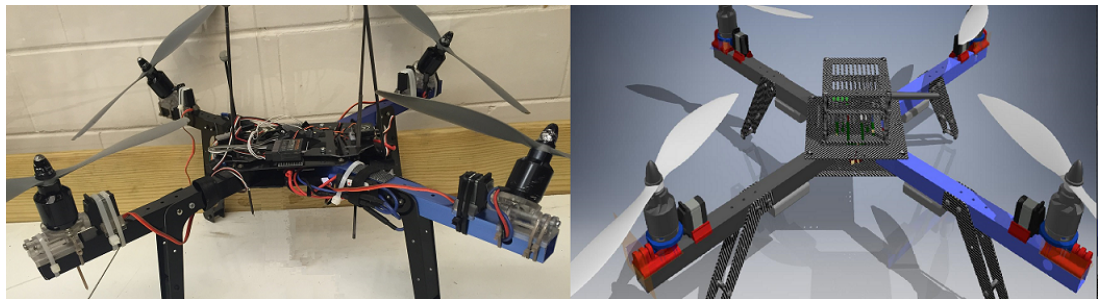


Figure 6-7: The CAD and the actual model of the prototype.

As the servo is directly connected to the tilting mechanism with no gears in between. The smaller and lighter servo which produces the lower torque compared to the previous design can also be used. This configuration not only eliminates external gears which were used before, but also reduces the weight of the servo by half. One of the drawback of this mechanism as compared to the previous one, is the freedom of tilting around the axis. In previous design there was not any mechanical limitation for the tilting mechanism. Although the previous design could rotate around the arms up to 360 degrees, it never was our concern. However, this

tilting mechanisms is limited to 60 degrees which meets the criteria of the experiments.

6.2 Drive System

6.2.1 Motors

A multi-rotor flying vehicle is more efficient when it is lighter. One of the important criteria to choose a suitable motor is to use the lightest possible motor which can provide at least twice as much thrust to lift the vehicle and has the best response for control system in difficult flight conditions. Brush-less DC motors afford better efficiency and power density compared to brushed DC motor [31]. Due to higher power density, controllability, minimum requirements for maintenance, compact size and light weight [60] they have become increasingly popular and most commonly used motors in MAV technology.

As a result of these advantages, the 850 KV Brush-less DC (BLDC) motor was selected for the tilting quadcopter. It is also used by most of the 3D Robotics multi-rotors vehicles. It delivers a very good level of the thrust compared to even bigger size of counterpart 850 KV motors.



Figure 6-8: 850 kv brushless DC motors

Most brush-less DC motors have three terminals as shown in Figure (6-8). While these three terminals are connected to stator, the permanent magnets are placed on the rotor such that the poles are facing the stator. An Electronic Speed Control (ESC) is used to send the command to control the rotation of the motor. The power output from ESC by using four cells LiPo and 10×47 Propeller are shown in Table (6.3).

Table 6.3: Power output from ESC, 4S LiPo, 10x47 Propeller.

	25%	50%	70%	100%
Amp (A)	1.83	5.16	8.9	15.9
Wattage (W)	27.7	79.1	133.4	232
Thrust(gr)	235	537	790	1440

6.2.2 Batteries

Lithium Polymer (LiPo) batteries are currently the preferred power sources for most light-weight, high-current, high-capacity power storage [7]. They offer high energy-storage/weight ratio and high discharge rate [88]. These batteries use normal lithium ion chemistry with the polymer separators to provide high discharge rates. It comes with different cell numbers. Each cell provide 3.7 Volts with internal resistance of approximately 0.03 Ohm [4].

6.3 Avionics

6.3.1 Control Board

A Control Board needs to be selected that would maintain list of requirements to be able to have control over position and orientation. As there is no control board for tilt mechanism in the market, in order to apply the proposed control strategy, it needs not only to be an open source, but also is required to be able to communicate with an out source computing devices. Furthermore three axis gyroscope and three axis accelerometers are also need to be included. Another criteria which was taken into the account to choose the control board was the reasonable price, the size and the weight. All these reasons led us to use PixHawk autopilot [44]. PixHawk is armed with advanced 32 bit ARM processor, micro SD card for logging, Integrated backup systems and 14 PWM servo outputs which are ideal for our vehicle to be connected to additional tilting servo motors [45]. Another specification that made us to use PixHawk was

the way it could communicate with Robot Operating System (ROS) which is the main coding environment to apply the control techniques [66]. ROS is a set of software frameworks for robot software development. ROS also provides low-level device control and message passing between processes which allows to share data across multiple and commonly specialized processes [16].

6.3.2 Communications

MAVLink (Micro Air Vehicle Link) is a very lightweight protocol for communicating with small unmanned vehicle. It is designed as a header-only message marshalling library [27]. It is mostly used for communication between ground station and small unmanned vehicles. It can be used to transmit all flight data including altitude, attitude, GPS position, air speed, battery status, way points etc[84, 85, 83]. The transmitted data has the packet structure. The payload from the packets are called as a MAVLink message which is identifiable by the ID for each message. The stream of bytes that can be encoded by the ground station can be sent via Telemetry or USB serial.

MAVROS is also the package in ROS environment that provides communication driver with MAVLink communication protocol for various autopilots including PixHawk. Not only all flight data is available in ROS, but also the new commands which are calculated through control systems can be sent back to the autopilot in real time.

Chapter 7

Numerical Simulations and Experimental Results

7.1 Numerical Simulations

7.1.1 Simulation set-up

To validate the presented dynamic model and the control method, numerical simulations of the tilting rotor quadcopter were carried out using the MATLAB. The discretized versions of the dynamic and the controller equations are solved by the Euler method. Here, we provide the results from one of the simulation scenarios studied. In this scenario, the vehicle's initial position was $(0.1, 0.8, 0)$. The final position was set to $(0.8, 0.3, 1.5)$. In this study the SI unit system is used. In this scenario, the desired pitch or roll angles were modified during the flight so that both of these angles were simultaneously controlled. Figure (7-1) shows the reference pitch and roll angle. It can be seen that for time $t = 0$ sec to $t = 1$ sec, the reference pitch and roll angles are zero. At $t = 1$ sec, the reference pitch angle increases from 0^0 and reaches the value of 18^0 at $t = 4$ sec and stays with the same until the end of trajectory. At $t = 4$ sec, the reference roll angle is also increased from 0^0 and reaches the value of 12^0 at $t = 7$ sec.

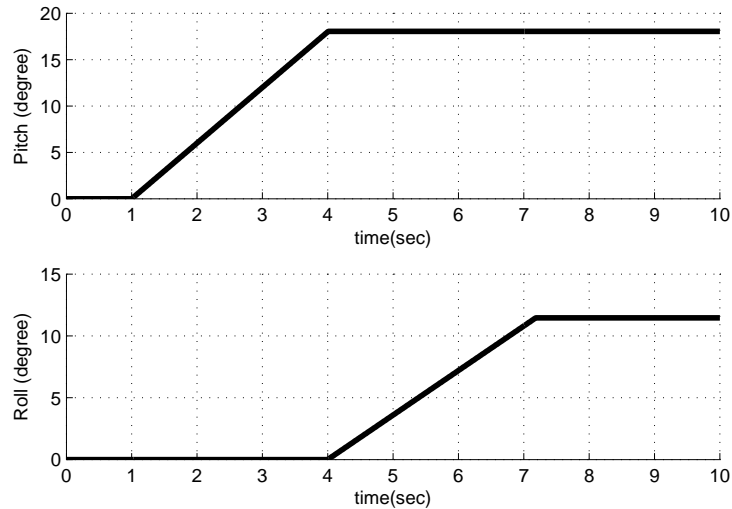


Figure 7-1: The reference (commanded) pitch and roll angle

7.1.2 Tilt-Rotor Quadcopter Simulation results

The procedure to accomplish the flight simulation is to have the vehicle take-off from an initial point vertically till the desired height, and then steer to the destination point with the horizontal flight. During flight, the orientation of the vehicle is supposed to change according to reference inputs without losing the height. The quadcopter trajectory in the three dimensional space from the initial point to the desired destination is shown in Figure (7-2).

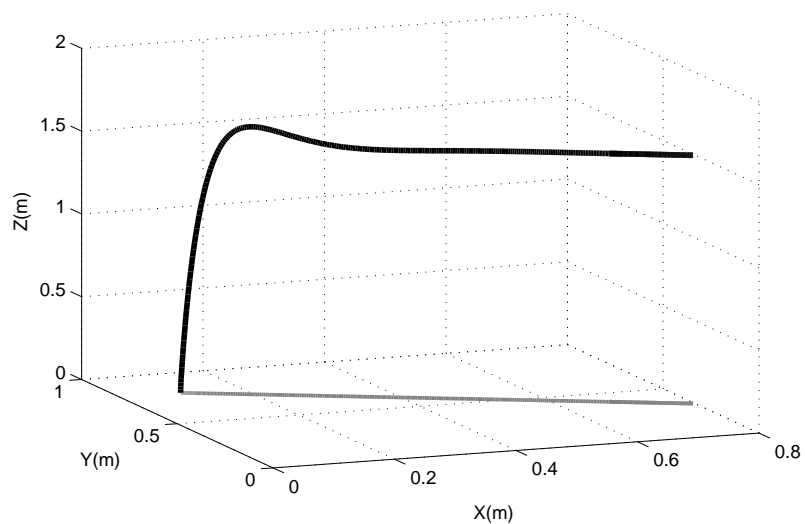


Figure 7-2: The actual trajectory followed by the UAV in 3-dimensions

Figure (7-3) shows the actual change in the pitch, roll, and yaw angles of the tilting rotor quadcopter during the flight. It can be seen that the change in the yaw angle is close to zero while the actual pitch and roll angles closely follow the reference values.

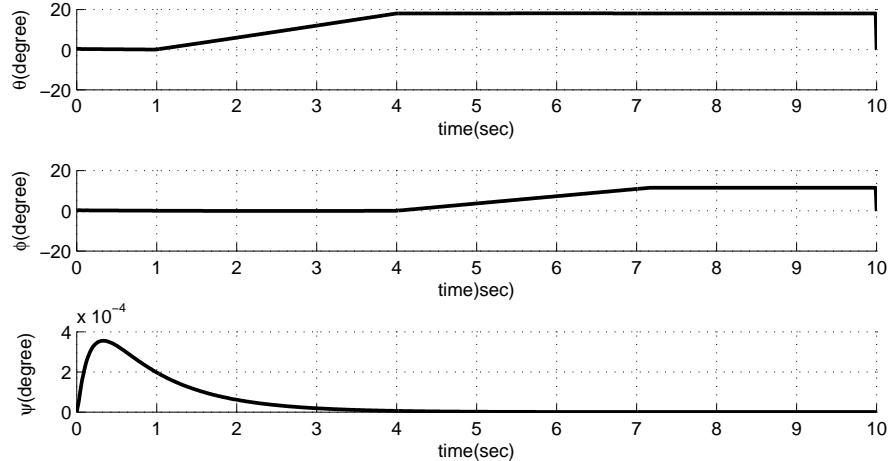


Figure 7-3: The actual orientation of the vehicle in 3 directions

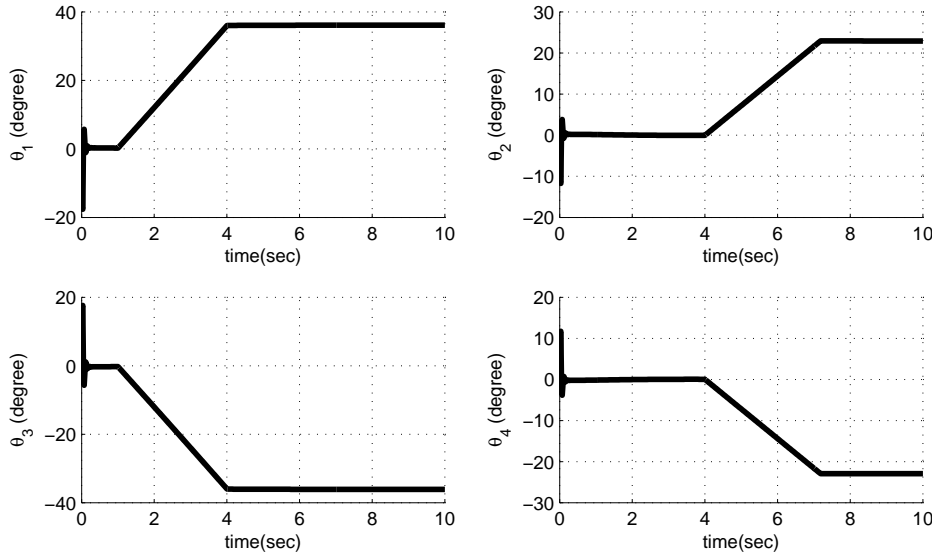


Figure 7-4: The angle of each arm during simulation

Figure (7-4) shows how four servomotors modulate the angle of each arm to follow the referenced orientation commands during the flight. Figure (7-5) shows how the speed of four motors changes during the flight to track the trajectory and maintain the height of the vehicle. Figure (7-6) shows the enlarged view of a portion of the Figure (7-6). It can be seen from Figure

(7-6) that the angular velocities of rotors stabilize close to $t = 1\text{ sec}$ (till when the reference tilts in pitch and roll are zero). At $t = 1\text{ sec}$, the reference pitch angle is commanded to gradually increase to reach a value of 18^0 at $t = 4\text{ sec}$. Corresponding to this, the individual rotor speeds can be seen to increase from $t = 1\text{ sec}$ to $t = 4\text{ sec}$. At $t = 4\text{ sec}$, the reference roll angle is commanded to gradually increase to reach a value of 12^0 at $t = 7\text{ sec}$. Consequently, there is further increase in the rotational speeds of the rotors. This increase in motor speed can be explained by Theorem 2. Comparing Equation (3.14) (for tilted configuration) to Equation (3.7) (for non-tilted configuration), the theory predicts the need of more rotor speed in tilted configuration so that the vertical component of force still balances the weight in the tilted configuration. The simulation results shown in Figure (7-6) just confirms the theory.

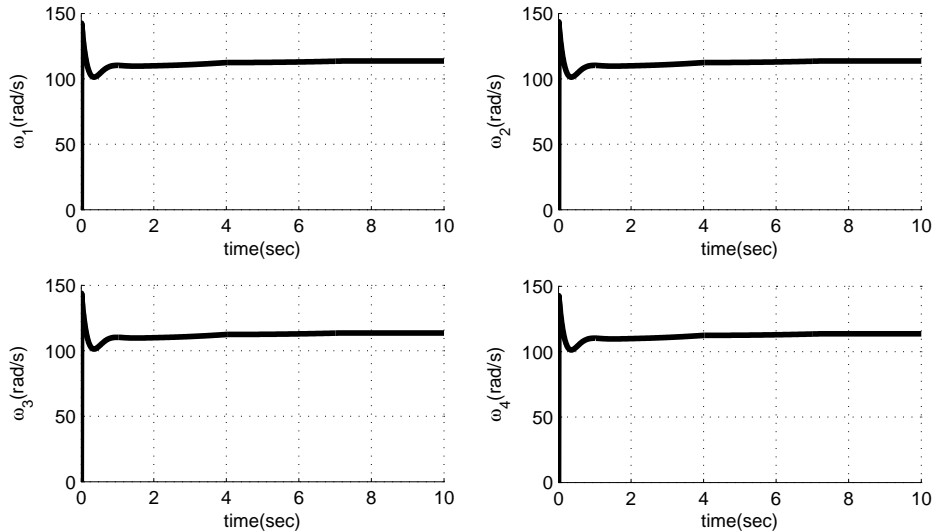


Figure 7-5: The speed of each rotor

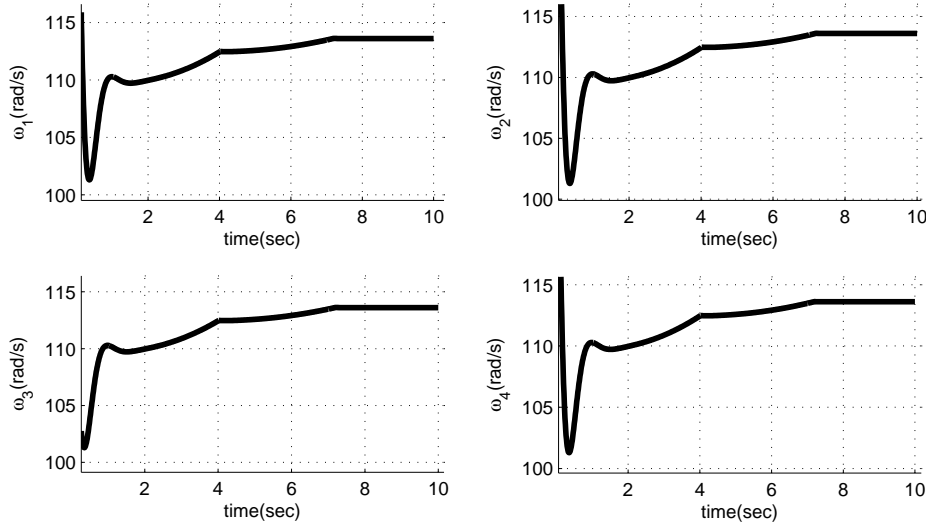


Figure 7-6: The enlarged view of the figure 8

7.1.3 Feedback Linearization Numerical Simulation

In order to verify the performance of the proposed feedback linearization based control method of the tilting-rotor quadcopter, numerous numerical simulations were carried out in MATLAB/Simulink environment. Here, we present the results from one of the simulations. The simulation comprises of the UAV taking off from the initial position located at (5.0 , 0.0 ,0.0) and reaching the desired destination located (4.5, 10.0, 10.0), via passing the waypoint located at (3.0, 4.0, 5.0). Also, during the flight, the orientation of the vehicle is supposed to change according to the reference input (in this case, the desired roll angle) without deviating from the desired trajectory. The reference roll angle is set as follows. During the flight, at $t = 5 \text{ sec}$, the reference roll angle is commanded to gradually increase from 0° to reach a value of 12° at $t = 10 \text{ sec}$. The quadcopter is then supposed to move towards the destination with the commanded roll angle (refer to the bottom plot of Figure (7-9)). The quadcopter trajectory obtained from the numerical simulation in the three-dimensional space from the initial point to the waypoint and then to the final position is shown in Figure (7-7).

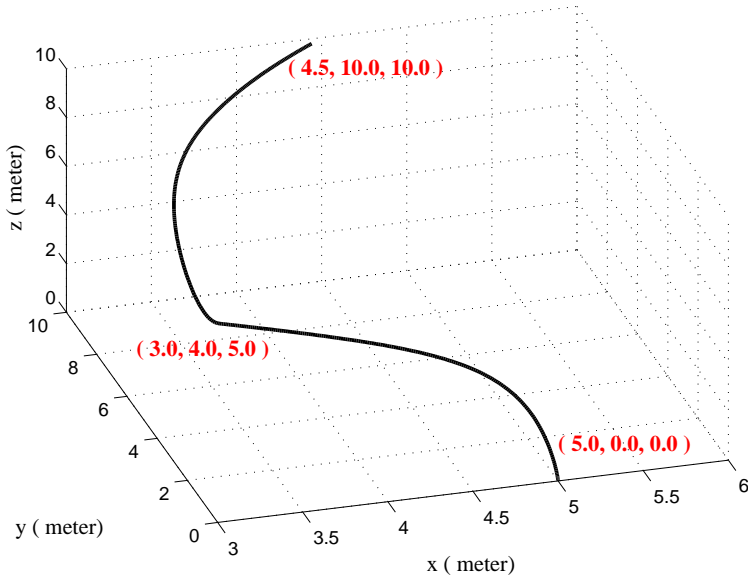


Figure 7-7: Quadcopter trajectory in three-dimensional space

Figure (7-8) shows the position and orientation of the vehicle during the flight. Figure (7-9) shows the comparison between the reference roll and the actual roll angle the the vehicle.

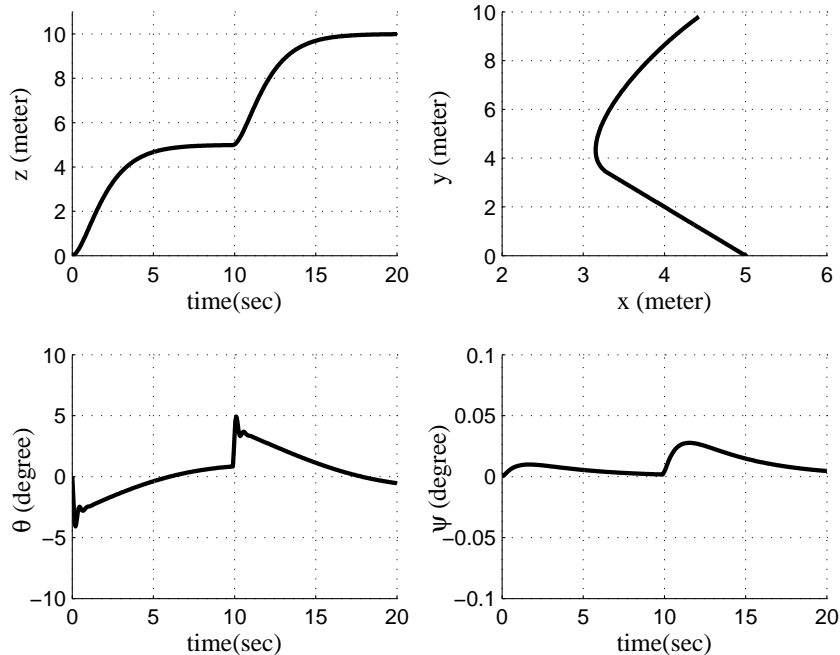


Figure 7-8: Position and orientation of the quadcopter: altitude vs. time (top left), x-position vs. y-position (top right), pitch vs. time (bottom left), and yaw vs. time (bottom right).

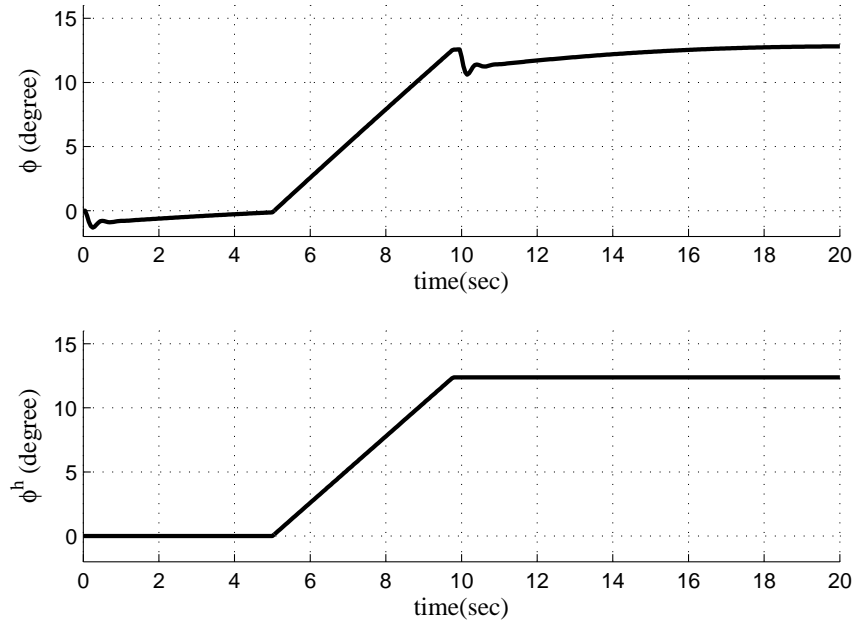


Figure 7-9: The reference roll (bottom) and actual roll angle (top) during the flight.

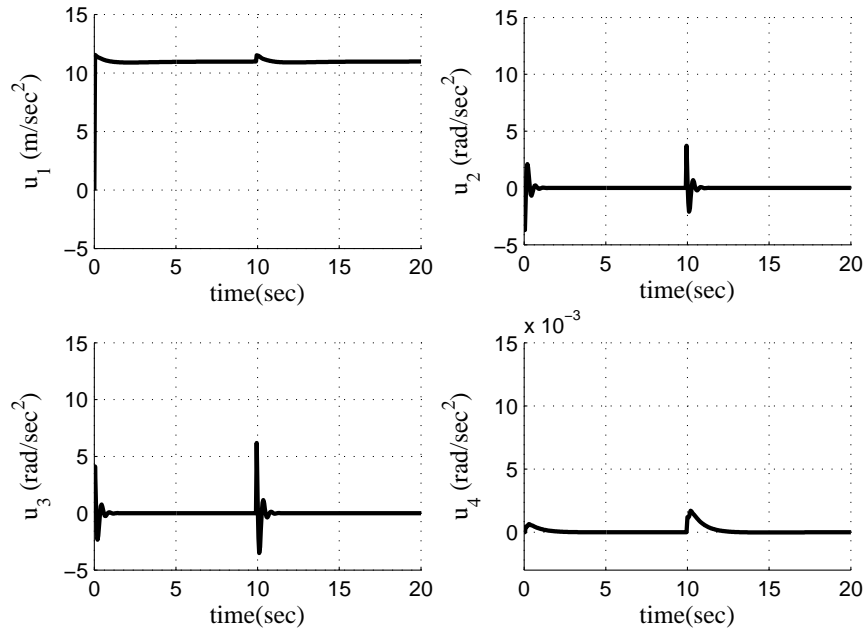


Figure 7-10: Inputs generated by the proposed feedback linearization method.

As we chose x , y , and z as the outputs of the feedback linearization method, and u_1, u_2, u_3 , and u_4 as the normalized total lift forces and control inputs for roll, pitch, and yaw respectively, Figure (7-10) shows that the zero dynamics of the controller are stable (as the relative degree

is smaller than the order of the system).

7.1.4 Fault Tolerant Numerical Simulation

To validate the presented dynamic model in the case of motor failure and the proposed control technique, numerical simulations of the tilting rotor quadcopter were carried out using the MATLAB. The discretized versions of the dynamic and the controller equations are solved by the Euler method. We have completed two different scenarios in order to evaluate the vehicle's response in the case of motor failure in following a trajectory as well as hover flight. In both scenarios, the altitude maintained its desired value.

7.1.4.1 Hover Flight

The first simulation is the hovering task in one spot with motor failure after stable hover flight. This scenario shows the performance of the controller and highlights the position control with motor failure. In the first scenario, mission was started by taking off and hovering in the fixed altitude and in one spot. The initial take off point is located at $(0.2, 0.0, 0.0)$. Figure (7-11) shows the 3 dimensional path of the flight. As it can be seen, the vehicle is flying in the neighborhood of the desired spot. The flight has the error in the range of 0.4 meters to hover around the spot after one of the motors failed.

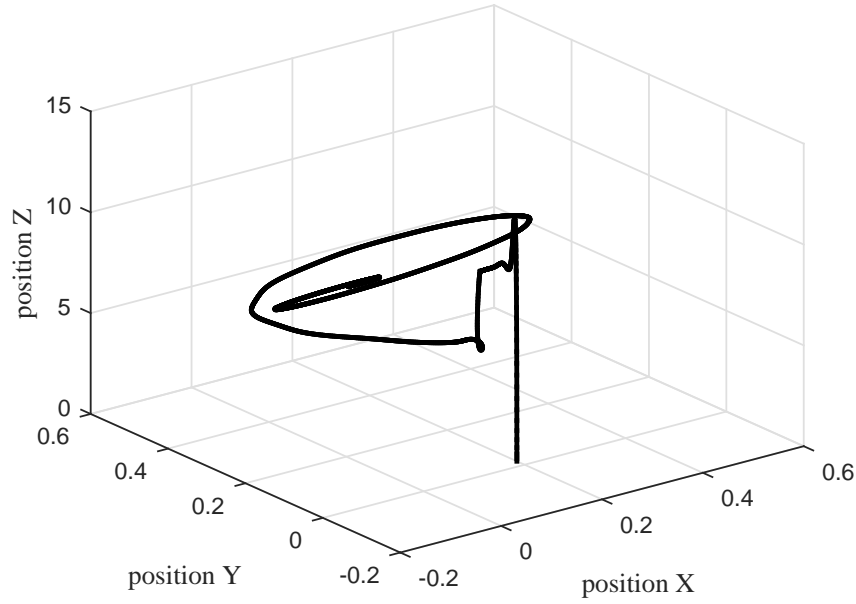


Figure 7-11: The actual trajectory followed by the UAV in 3- dimensions

In this scenario the vehicle flew for 200 seconds. Figure (7-12) shows the position of vehicle in each individual axis. At time $t = 20$ sec, when motor number 2 stops working, the altitude of the quadcopter drops and after very short time of adjusting, it maintained its altitude to the end of the flight. The vehicle also has small amount of movement along X and Y axis.

Figure (7-13) shows how the other motors increase the rotational speed in order to compensate the failed motor force to maintain the altitude. Although the rotational speed of the motors is increased, but the speed limitation of each motor, will not let the vehicle to maintain the exact previous altitude.

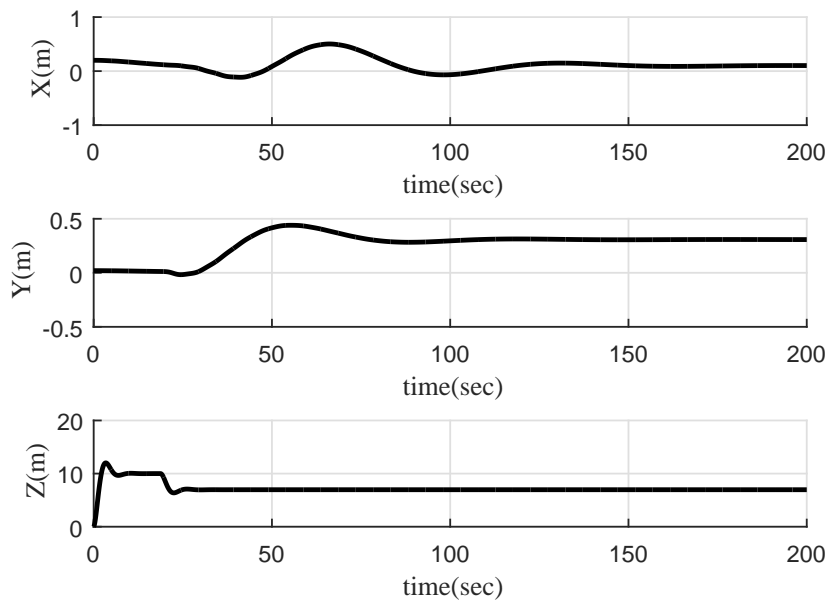


Figure 7-12: Vehicle's trajectory in X,Y and Z

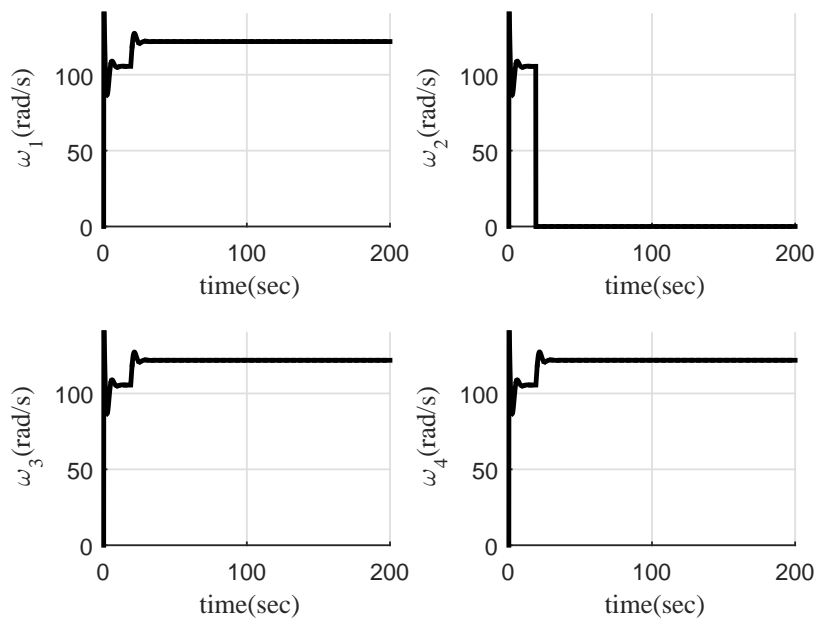


Figure 7-13: Vehicle's trajectory in X,Y and Z

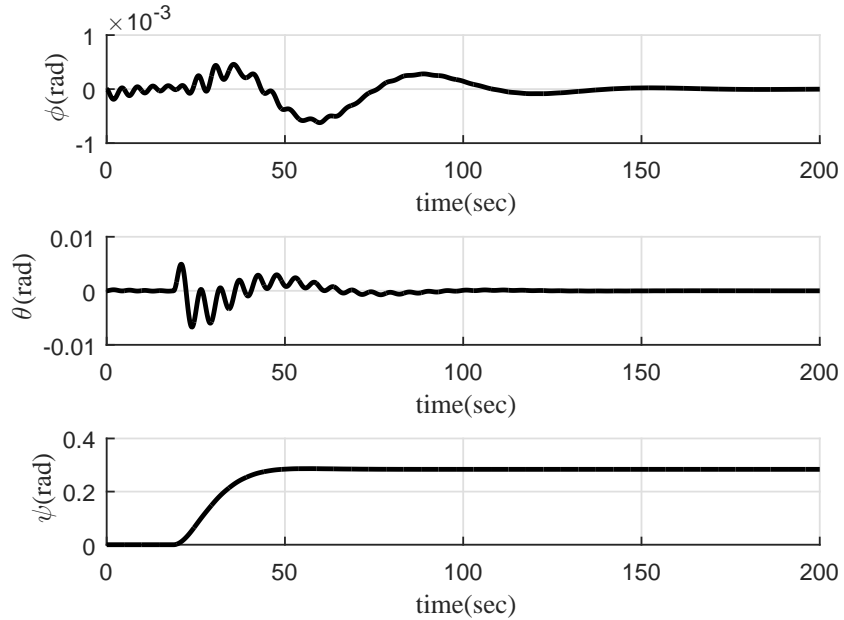


Figure 7-14: The actual orientation

Figure (7-14) shows how orientation of the vehicle change after the motor failure. As it can be seen from the Figure (7-14), the yaw angle changes right after the motor failure and remains in a constant angle. It can easily be notified that the vehicle is not spinning around Z axis after the motor failure.

7.1.4.2 Tracking a Trajectory

Here, we provide the results from the second simulation we studied. In this scenario, the vehicle's initial position was $(0.0, 0.0, 0.0)$. The final position was set to $(30.0, 10.0, 10.0)$. In this scenario, It can be seen that for time $t = 0$ sec to $t = 10$ sec, the quadcopter flew with all propellers working and it reached its designated altitude at 10 meters. at $t = 10$ sec, one the motors stopped working and the proposed control technique were applied immediately. During the simulation, it is assumed that right after the motor failure, the control system can take over and apply the control technique for new faulty system.

The quadcopter trajectory in the three dimensional space from the initial point to the desired destination is shown in Figure (7-15).

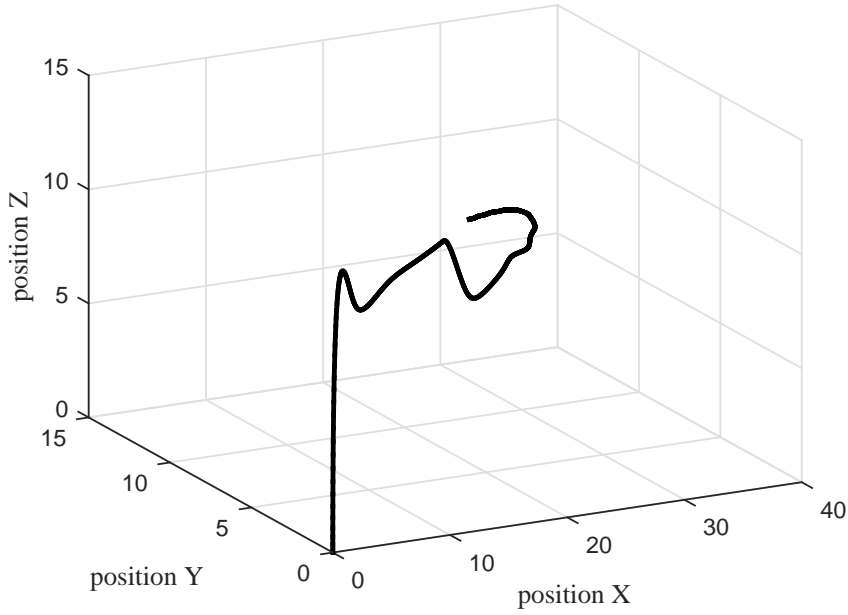


Figure 7-15: The actual trajectory followed by the UAV in 3- dimensions

Figure (7-16) shows the position of vehicle in each individual axis. At time $t = 10$ sec, when motor number 2 stops working, the altitude of the quadcopter drops by 3 meters and after very short time of adjusting, it maintained its altitude to the end of the flight.

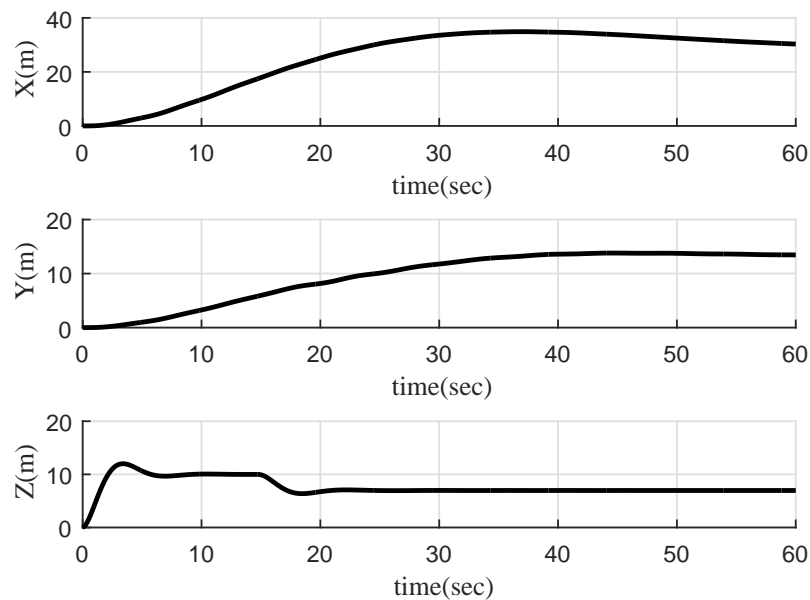


Figure 7-16: Vehicle's trajectory in X,Y and Z

Figure (7-17) shows how the other motors behaved after motor 2 failure. As it can be seen from the Figure (7-17), to compensate the lost force from motor 2, all working motors speed up. Although the rotational speed of the motors is increased, but still the altitude is decreased to 7 meters due to limitation of the amount of rotational speed each motor can provide.

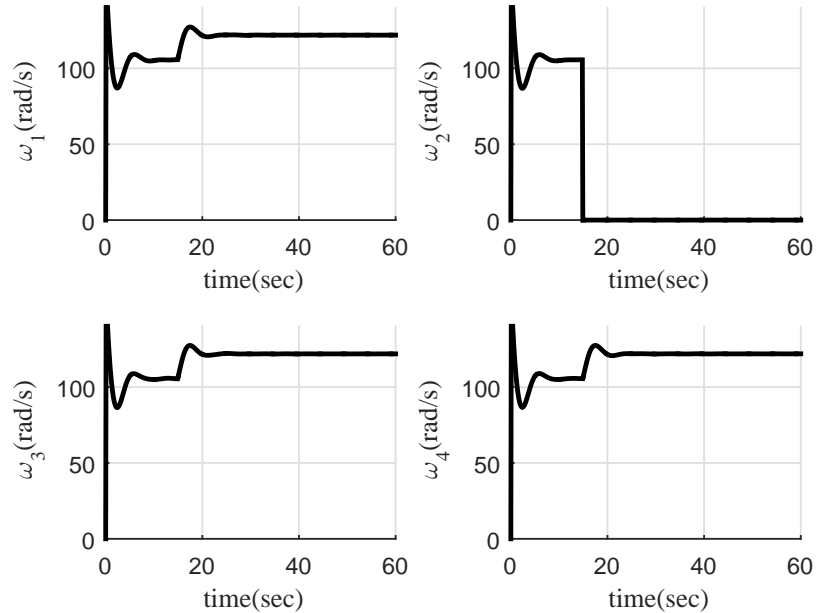


Figure 7-17: Vehicle's trajectory in X,Y and Z

Once the quadcopter started to adjust the stability after the motor failure, the unbalance moments caused most amount of change in yaw angle. As it can be seen, the yaw angle started to increase right after the motor failure.

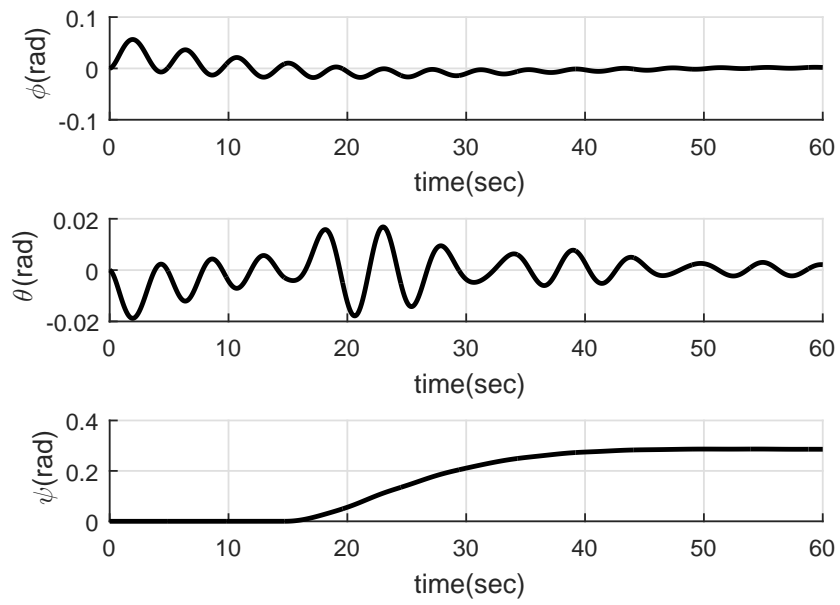


Figure 7-18: The actual orientation

Figure (7-18) shows the orientation of the vehicle before and after motor failure.

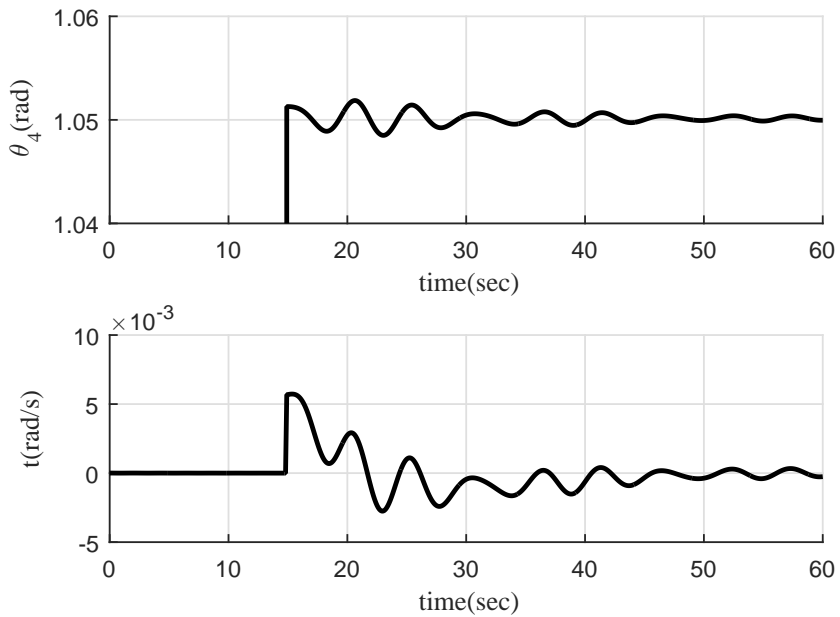


Figure 7-19: Angular velocity around Z axis

7.2 Preliminary Experimental Results

The tilting rotor quadcopter was tested to find out if it was correctly modeled and controlled. Extensive simulations were carried out to verify the validity of the dynamic model and control scheme. This section presents the experimental results obtained with the second prototype. The first experiment is the hovering task in one spot with tilted orientation. This scenario shows the performance of the controller and highlights the position control with tilted angle. The second experiment is intended to demonstrate the performance in tracking a simple trajectory while the orientation keeps the desired value during the flight. In both scenarios, the altitude maintained its desired value.

7.2.1 Hovering on the spot

In the first experiment, the scenario was started by taking off and hovering in the fixed altitude and in one spot while the quadcopter tilts by a desired angle. Figure (7-20) shows the snapshot of the hovering with the tilted angle.



Figure 7-20: Snapshot of the hovering with the tilted angle

The tilting starts at $t = 8s$ and continues till it reaches the desired angle at $t = 12s$. The vehicle hovers at the same spot with 0.4 rad tilt along the pitch direction till $t = 17s$ and starts to reduce the tilt to the horizontal flight. At $t = 25s$ it starts to tilt in the opposite direction along the pitch with the same angle and maintains the orientation till $t = 33s$ when it starts to tilt back to the original attitude again.

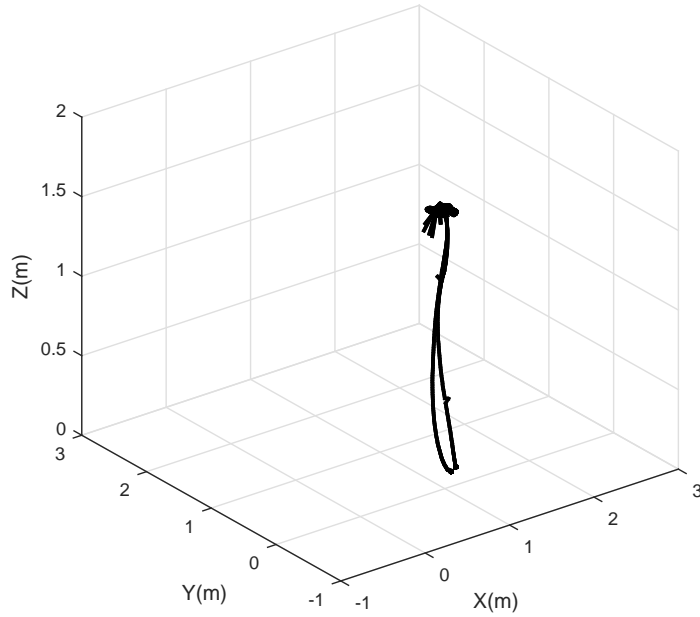


Figure 7-21: Vehicle's trajectory in 3-dimension

During the flight, the vehicle not only maintains the position at the same spot, but also keeps the roll and yaw close to zero. The altitude is also constant at 1.5m during the experiment.

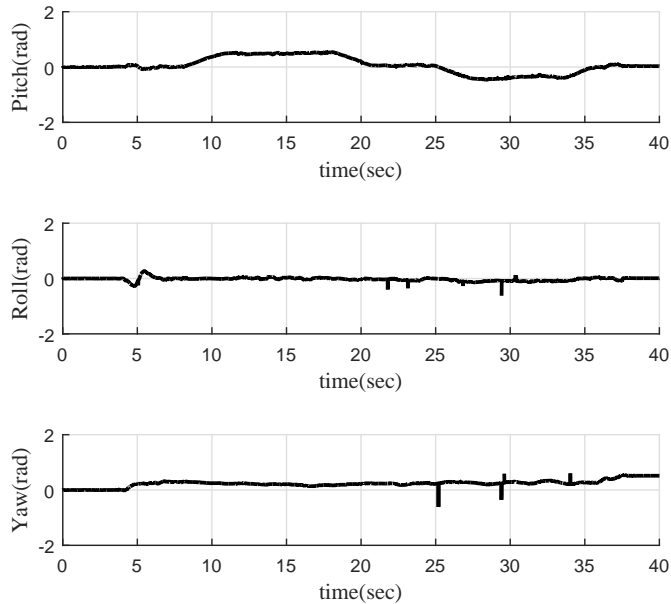


Figure 7-22: The actual orientation of the vehicle along the three directions

7.2.2 Trajectory

7.2.2.1 Line

Similarly, we carried out another experiment where the UAV performed the following operation: i) it took off and went vertically up till $t = 15s$ and altitude of $1.75m$; ii) then the vehicle tilted along the roll direction till $t = 17s$; iii) the vehicle was then commanded to move horizontally along with Y axes in the tilted position till $t = 32s$; iv) the vehicle was then commanded to come back to horizontally aligned orientation (i.e., no tilt) till $t = 35s$; and finally, v) the vehicle was commanded to land.

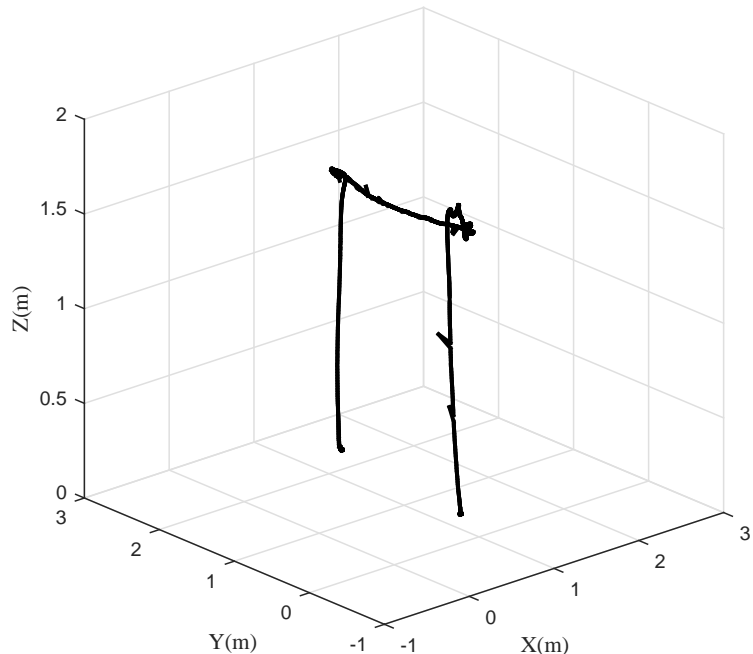


Figure 7-23: Vehicle's trajectory in 3-dimension

The UAV's trajectory is shown in Figure (7-23) and the plot of pitch, roll, and yaw angles versus time are shown in Figure (7-24). It should be noted that the spikes in the plots come from the noisy data by the Optitrack motion caption system.

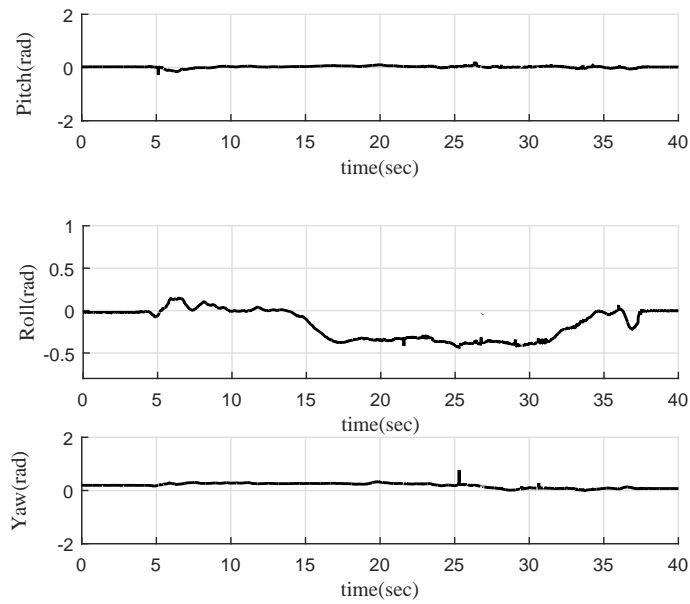


Figure 7-24: The actual orientation

Figure (7-24) shows that the vehicle maintained the desired roll angle while moving forward. During the flight, the pitch and the yaw angle were supposed to be around zero.

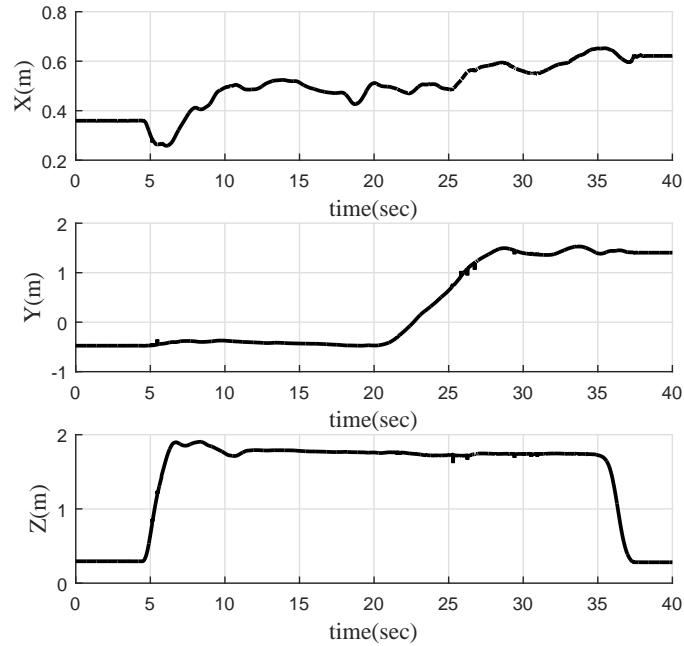


Figure 7-25: Vehicle's position versus time graph along the 3 directions

7.2.2.2 Box

Another trajectory were carried out to show that the vehicle can track with any desired orientation angle in the range of operation. The vehicle was supposed to move in a square shaped path. The vehicle was commanded to take off and hover in the height of $1.8m$ in $t = 8s$ and stay at the same altitude till $t = 55s$. The vehicle moved along X axis first. During the flight, the pitch angle was supposed to be maintained by $0.5rad$ from $t = 15s$ till $t = 50s$.

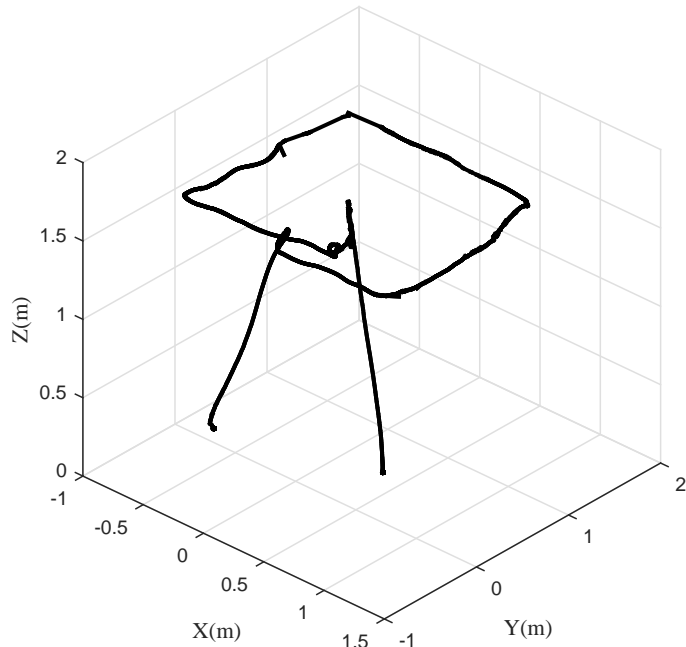


Figure 7-26: Vehicle's trajectory in 3-dimension

As it can be seen from (7-26), during the flight, the altitude is constant after short transient take-off period.

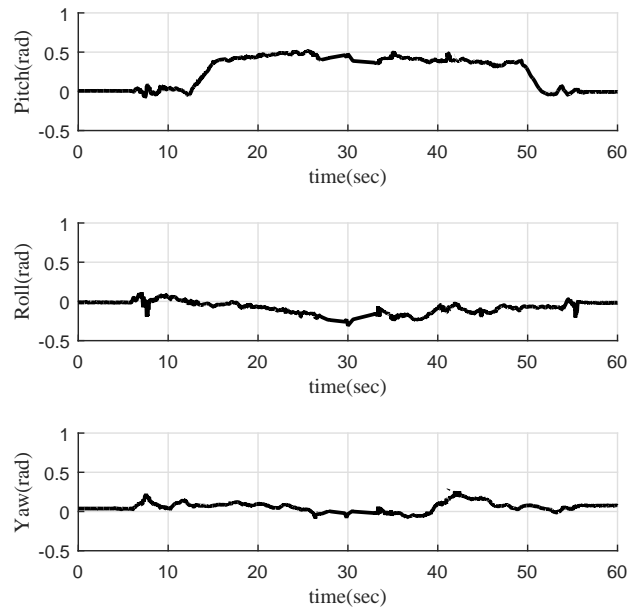


Figure 7-27: The actual orientation

Figure (7-27) shows the orientation of the vehicle during the flight. The vehicle was commanded to fly with a desired pitch angle from $t = 17$ sec to $t = 50$ sec.

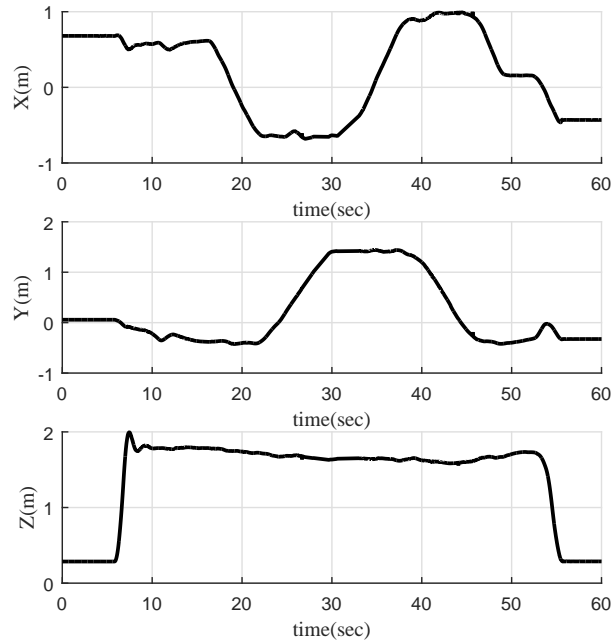


Figure 7-28: Vehicle's position versus time graph along the 3 directions

During this period of the time, regardless of direction of the vehicle along X or Y axis, the pitch was commanded to maintain at 0.5 rad. Figure (7-28) clearly shows the vehicle's movement along X , Y and Z versus time in three different plots.

Chapter 8

Conclusions and future work

8.1 Conclusions

In this work, the dynamic modeling and control of a tilting rotor quadcopter was presented. The tilting rotor design was accomplished by having the tilting capability for the four rotors achieved via four independent motors used to tilt the rotors along their respective tilting axes. The relationship between the tilting-rotor angles and the quadcopter orientation was derived using the dynamic model. However, due to added complexity arising from nonlinear relations with four additional inputs, and the correlation between these inputs and forces, the Newton-Euler equation of motions become highly nonlinear. The first two theorems were defined in order to derive simple relationships between the angular rotations along the tilt directions and the orientation of the vehicle and rotational speeds of the propellers for hovering. By definition of these theorems, it was shown that this design makes the quadcopter a fully-controlled system which can track any arbitrary trajectory.

Hovering with controlled pitch and roll angles, and motion with desired orientation are some of the features of the novel design of the quadcopter system.

This work, furthermore, suggests a PD based method to control the rotational speeds of the motors responsible for rotating as well as tilting the rotors in order to follow a desired trajectory.

An Input-Output feedback linearization technique has been applied to a tilting quadcopter to track a trajectory with a desired orientation during the flight. As the behavior of the tilting quadcopter, affected by the tilting forces and moments, is highly nonlinear, the linearization turns out to be a proper control technique to avoid complex behavior of the dynamics. How-

ever, in the presence of unmodeled dynamics or any other undefined disturbances, the system still remains nonlinear after feedback linearization loop. Theoretical results of this control technique have been supported by simulation results in MATLAB environment.

The dynamic modeling and control of a tilting rotor quadcopter in the case of one motor failure was also been presented. The relationship between the tilting-rotor angles and the quadcopter orientation was derived using the dynamic model. It was shown that the quadcopter can be stabilized if the rotor diagonally opposite to the failed rotor is tilted by an angle that has been calculated by the Euler equations. In order to maintain an altitude to the closest possible altitude after the failure, the rotational speed of each individual motor has also been calculated. The paper presents the dynamic model, and suggests a PD based control in order to avoid crashing of quadcopter and continue the mission. The model and the controller are verified with the help of numerical simulations.

Two different vehicles with tilting mechanism were designed and fabricated as a prototype of the concept. The proposed control scheme was implemented on the prototype during laboratory experiments which demonstrated the capability of the vehicle to hover and navigate with tilted orientation. Furthermore, such over-actuated systems promise to provide mechanisms to not only overcome wind disturbances more effectively but also provide tolerance to individual rotor failure.

8.2 Future Works

The work presented here addresses the dynamic modeling and control of a tilting rotor quadcopter with design and fabrication of two different prototypes. Future work should be directed towards the following directions:

- Future work could focus on developing modeling and the control techniques when all rotors can tilt around their axes independently in order to make the flight smoother and possibly faster in complicated maneuvers.
- Based on our experience with the second prototype, which is lighter and more practically applicable than the first one, and also by the experience our group had in the other projects

with 3D printed quadcopter frame, a third generation prototype of the quadcopter with tilting rotors can be fabricated by a combination of 3D printed parts and the carbon fiber materials to make the vehicle lighter, firmer and smaller.

- Such over-actuated systems promise to provide mechanisms to overcome wind disturbances in outdoor application more effectively. Further work is needed to develop control methods that can robustly reject such wind disturbances.
- In order to decrease the reaction time of the tilting mechanism, actuation system improvement as well as higher computational processor and better on-board sensors can be investigated.
- Further studies are required for understanding the time delay between the time of motor failure and when the new controller takes over the system. Furthermore, this logic can be implemented in the on board flight software for all the propellers.
- Implement nonlinear control theory to allow the prototype with one motor failure, to track complex trajectory.
- Experimental work for executing autonomous flight with tilting rotors also forms a future work. This would require developing auto-pilot from scratch since available auto-pilot systems are developed for traditional quadcopters that attempt to modify rotor speeds to make the frame horizontal when they receive IMU feedback that quad is tilted. Some progress in this respect has been made. The commands which are required to be sent to the servo motors with respect to the output of designed controller in this work has been modified in the code in two different auto pilot boards for the tilt rotor quadcopter. For the experiment related to the motor failure, the KK2.1 flight controller has been used. The experiments were done by taking off while the quadcopter had three working motors. This experiment can be performed as a future work in the way that starts with the quadcopter with all working motors. Subsequently, fault is induced in one of the motors mid-flight that requires switching to the failure mode control algorithm in an online fashion. This experiment would ensure that the transition between different control algorithms is smooth and does not lead to instability.

References

- [1] K. Ahmadi and E. Salari. Small dim object tracking using a multi objective particle swarm optimisation technique. *IET Image Processing*, 9(9):820–826, 2015.
- [2] J. Allen and B. Walsh. Enhanced oil spill surveillance, detection and monitoring through the applied technology of unmanned air systems. In *International oil spill conference*, volume 2008, pages 113–120. American Petroleum Institute, 2008.
- [3] M. H. Amoozgar, A. Chamseddine, and Y. Zhang. Experimental test of a two-stage kalman filter for actuator fault detection and diagnosis of an unmanned quadrotor helicopter. *Journal of Intelligent & Robotic Systems*, 70(1-4):107–117, 2013.
- [4] D. Andrea. *Battery Management Systems for Large Lithium Ion Battery Packs*. Artech house, 2010.
- [5] R. W. Beard, D. Kingston, M. Quigley, D. Snyder, R. Christiansen, W. Johnson, T. McLain, and M. Goodrich. Autonomous vehicle technologies for small fixed-wing uavs. *Journal of Aerospace Computing, Information, and Communication*, 2(1):92–108, 2005.
- [6] L. Besnard, Y. B. Shtessel, and B. Landrum. Quadrotor vehicle control via sliding mode controller driven by sliding mode disturbance observer. *Journal of the Franklin Institute*, 349(2):658–684, 2012.
- [7] O. Bilgen, K. Kochersberger, E. C. Diggs, A. J. Kurdila, and D. J. Inman. Morphing wing micro-air-vehicles via macro-fiber-composite actuators. In *Proceedings of the 48th AIAA/ASME/ASCE/AHS/ASC Structures, Structural Dynamics, and Materials Conference, Honolulu, HI, Apr*, pages 23–26, 2007.

- [8] M. Blanke, M. Staroswiecki, and N. E. Wu. Concepts and methods in fault-tolerant control. In *American Control Conference, 2001. Proceedings of the 2001*, volume 4, pages 2606–2620. IEEE, 2001.
- [9] S. Bouabdallah, P. Murrieri, and R. Siegwart. Towards autonomous indoor micro vtol. *Autonomous Robots*, 18(2):171–183, 2005.
- [10] W. L. Brogan. *Modern control theory*. Pearson Education India, 1974.
- [11] D. W. Casbeer, D. B. Kingston, R. W. Beard, and T. W. McLain. Cooperative forest fire surveillance using a team of small unmanned air vehicles. *International Journal of Systems Science*, 37(6):351–360, 2006.
- [12] A. Cavoukian. *Privacy and drones: Unmanned aerial vehicles*. Information and Privacy Commissioner of Ontario, Canada, 2012.
- [13] E. Cetinsoy. Design and control of a gas-electric hybrid quad tilt-rotor uav with morphing wing. In *Unmanned Aircraft Systems (ICUAS), 2015 International Conference on*, pages 82–91. IEEE, 2015.
- [14] H. Chao, Y. Cao, and Y. Chen. Autopilots for small unmanned aerial vehicles: a survey. *International Journal of Control, Automation and Systems*, 8(1):36–44, 2010.
- [15] D. A. Conner, B. D. Edwards, W. A. Decker, M. A. Marcolini, and P. D. Klein. Nasa/army/bell xv-15 tiltrotor low noise terminal area operations flight research program. *Journal of the American Helicopter Society*, 47(4):219–232, 2002.
- [16] S. Cousins. Exponential growth of ros [ros topics]. *IEEE Robotics & Automation Magazine*, 1(18):19–20, 2011.
- [17] P. Doherty and P. Rudol. A uav search and rescue scenario with human body detection and geolocalization. In *AI 2007: Advances in Artificial Intelligence*, pages 1–13. Springer, 2007.
- [18] C. P. Ellington. The novel aerodynamics of insect flight: applications to micro-air vehicles. *Journal of Experimental Biology*, 202(23):3439–3448, 1999.

- [19] A. T. Erman, L. v. Hoesel, P. Havinga, and J. Wu. Enabling mobility in heterogeneous wireless sensor networks cooperating with uavs for mission-critical management. *Wireless Communications, IEEE*, 15(6):38–46, 2008.
- [20] A. Freddi, S. Longhi, A. Monteriu, and M. Prist. Actuator fault detection and isolation system for an hexacopter. In *Mechatronic and Embedded Systems and Applications (MESA), 2014 IEEE/ASME 10th International Conference on*, pages 1–6. IEEE, 2014.
- [21] S. Griffiths, J. Saunders, A. Curtis, B. Barber, T. McLain, and R. Beard. Obstacle and terrain avoidance for miniature aerial vehicles. In *Advances in Unmanned Aerial Vehicles*, pages 213–244. Springer, 2007.
- [22] S. Grzonka, G. Grisetti, and W. Burgard. A fully autonomous indoor quadrotor. *Robotics, IEEE Transactions on*, 28(1):90–100, 2012.
- [23] C. Hancer, K. T. Oner, E. Sirimoglu, E. Cetinsoy, and M. Unel. Robust position control of a tilt-wing quadrotor. In *Decision and Control (CDC), 2010 49th IEEE Conference on*, pages 4908–4913. IEEE, 2010.
- [24] K. hmadi, A. Y. Javaid, and E. Salari. An efficient compression scheme based on adaptive thresholding in wavelet domain using particle swarm optimization. *Signal Processing: Image Communication*, 32:33–39, 2015.
- [25] G. M. Hoffmann, H. Huang, S. L. Waslander, and C. J. Tomlin. Quadrotor helicopter flight dynamics and control: Theory and experiment. In *Proc. of the AIAA Guidance, Navigation, and Control Conference*, volume 2, 2007.
- [26] M.-D. Hua, T. Hamel, and C. Samson. Control of vtol vehicles with thrust-tilting augmentation. *IFAC Proceedings Volumes*, 47(3):2237–2244, 2014.
- [27] A. S. Huang, E. Olson, and D. C. Moore. Lcm: Lightweight communications and marshalling. In *Intelligent robots and systems (IROS), 2010 IEEE/RSJ international conference on*, pages 4057–4062. IEEE, 2010.

- [28] V. Hugel, A. Abourachid, H. Gioanni, L. Mederreg, M. Maurice, O. Stasse, P. Bonnin, and P. Blazevic. The robocoq project: Modelling and design of a bird-like robot equipped with stabilized vision. In *Proceedings of the 2nd International Symposium on Adaptive Motion of Animals and Machines (AMAM)*, 2003.
- [29] A. Isidori. *Nonlinear control systems*, volume 1. Springer, 1995.
- [30] D. R. Jenkins, T. Landis, and J. Miller. American x-vehicles: An inventory-x-1 to x-50. 2005.
- [31] J. G. Kassakian, H.-C. Wolf, J. M. Miller, and C. J. Hurton. Automotive electrical systems circa 2005. *Spectrum, IEEE*, 33(8):22–27, 1996.
- [32] H. K. Khalil and J. Grizzle. *Nonlinear systems*, volume 3. Prentice hall New Jersey, 1996.
- [33] D. Kingston, R. W. Beard, and R. S. Holt. Decentralized perimeter surveillance using a team of uavs. *IEEE Transactions on Robotics*, 24(6):1394–1404, 2008.
- [34] A. Ö. Kivrak. Design of control systems for a quadrotor flight vehicle equipped with inertial sensors. *Atilim University, December*, 2006.
- [35] L.-C. Lai, C.-C. Yang, and C.-J. Wu. Time-optimal control of a hovering quad-rotor helicopter. *Journal of Intelligent and Robotic Systems*, 45(2):115–135, 2006.
- [36] D. Lee, H. J. Kim, and S. Sastry. Feedback linearization vs. adaptive sliding mode control for a quadrotor helicopter. *International Journal of control, Automation and systems*, 7(3):419–428, 2009.
- [37] D.-J. Lee, I. Kaminer, V. Dobrokhodov, and K. Jones. Autonomous feature following for visual surveillance using a small unmanned aerial vehicle with gimbaled camera system. *International Journal of Control, Automation and Systems*, 8(5):957–966, 2010.
- [38] V. Lippiello, F. Ruggiero, and D. Serra. Emergency landing for a quadrotor in case of a propeller failure: A pid based approach. In *Safety, Security, and Rescue Robotics (SSRR), 2014 IEEE International Symposium on*, pages 1–7. IEEE, 2014.

- [39] Y. Liu, Z. Pan, D. Stirling, and F. Naghdy. Control of autonomous airship. In *Robotics and Biomimetics (ROBIO), 2009 IEEE International Conference on*, pages 2457–2462. IEEE, 2009.
- [40] L. Ljung. System identification toolbox. *The MathWorks Inc., South Natick, MA, USA*, 1988.
- [41] R. Luxman and X. Liu. Implementation of back-stepping integral controller for a gesture driven quad-copter with human detection and auto follow feature. In *Computer Science, Computer Engineering, and Social Media (CSCESM), 2015 Second International Conference on*, pages 134–138. IEEE, 2015.
- [42] M. Mahmoud, J. Jiang, and Y. Zhang. *Active fault tolerant control systems: stochastic analysis and synthesis*, volume 287. Springer Science & Business Media, 2003.
- [43] M. D. Maisel, D. J. Julianetti, and D. C. Dugan. The history of the xv-15 tilt rotor research aircraft from concept to flight. 2000.
- [44] L. Meier, P. Tanskanen, F. Fraundorfer, and M. Pollefeys. Pixhawk: A system for autonomous flight using onboard computer vision. In *Robotics and automation (ICRA), 2011 IEEE international conference on*, pages 2992–2997. IEEE, 2011.
- [45] L. Meier, P. Tanskanen, L. Heng, G. H. Lee, F. Fraundorfer, and M. Pollefeys. Pixhawk: A micro aerial vehicle design for autonomous flight using onboard computer vision. *Autonomous Robots*, 33(1-2):21–39, 2012.
- [46] N. Michael, D. Mellinger, Q. Lindsey, and V. Kumar. The grasp multiple micro-uav testbed. *Robotics & Automation Magazine, IEEE*, 17(3):56–65, 2010.
- [47] T. Mikami and K. Uchiyama. Design of flight control system for quad tilt-wing uav. In *Unmanned Aircraft Systems (ICUAS), 2015 International Conference on*, pages 801–805. IEEE, 2015.
- [48] M. W. Mueller and R. D’Andrea. Stability and control of a quadrocopter despite the

complete loss of one, two, or three propellers. In *Robotics and Automation (ICRA), 2014 IEEE International Conference on*, pages 45–52. IEEE, 2014.

- [49] D. R. Nelson, D. B. Barber, T. W. McLain, and R. W. Beard. Vector field path following for miniature air vehicles. *Robotics, IEEE Transactions on*, 23(3):519–529, 2007.
- [50] A. Nemati, M. HZarif, and M. M. Fateh. Helicopter adaptive control with parameter estimation based on feedback linearization. *International Journal of Mechanical Industrial and Aerospace Engineering*, 2:229–234, 2007.
- [51] A. Nemati and M. Kumar. Modeling and control of a single axis tilting quadcopter. In *American Control Conference (ACC), 2014*, pages 3077–3082. IEEE, 2014.
- [52] A. Nemati and M. Kumar. Non-linear control of tilting-quadcopter using feedback linearization based motion control. In *ASME 2014 Dynamic Systems and Control Conference*, pages V003T48A005–V003T48A005. American Society of Mechanical Engineers, 2014.
- [53] A. Nemati and M. Kumar. Control of microcoaxial helicopter based on a reduced-order observer. *Journal of Aerospace Engineering*, page 04015074, 2015.
- [54] A. Nemati, R. Kumar, and M. Kumar. Stabilizing and control of tilting-rotor quadcopter in case of a propeller failure. In *ASME 2016 Dynamic systems and control conference*. American Society of Mechanical Engineers, 2016.
- [55] A. Nemati, N. Soni, M. Sarim, and M. Kumar. Design, fabrication and control of a tilt rotor quadcopter: Theory and experiments. In *ASME 2016 Dynamic systems and control conference*. American Society of Mechanical Engineers, 2016.
- [56] K. Nonami, F. Kendoul, S. Suzuki, W. Wang, and D. Nakazawa. *Autonomous Flying Robots: Unmanned Aerial Vehicles and Micro Aerial Vehicles*. Springer Science & Business Media, 2010.
- [57] B. Norton. *Bell Boeing V-22 Osprey: tiltrotor tactical transport*. Aerofax, 2004.
- [58] K. Ogata. *Modern control engineering*. Prentice Hall PTR, 2001.

- [59] K. T. Oner, E. Cetinsoy, M. Unel, M. F. Aksit, I. Kandemir, and K. Gulez. Dynamic model and control of a new quadrotor unmanned aerial vehicle with tilt-wing mechanism. *International Journal of Applied Science, Engineering & Technology*, 5(2), 2009.
- [60] W. R. Oney. High power density brushless dc motor, Feb. 5 1980. US Patent 4,187,441.
- [61] A. Oosedo, S. Abiko, S. Narasaki, A. Kuno, A. Konno, and M. Uchiyama. Flight control systems of a quad tilt rotor unmanned aerial vehicle for a large attitude change. In *Robotics and Automation (ICRA), 2015 IEEE International Conference on*, pages 2326–2331. IEEE, 2015.
- [62] C. Papachristos, K. Alexis, and A. Tzes. Hybrid model predictive flight mode conversion control of unmanned quad-tiltrotors. In *Control Conference (ECC), 2013 European*, pages 1793–1798. IEEE, 2013.
- [63] P. Pounds and R. Mahony. Design principles of large quadrotors for practical applications. In *Robotics and Automation, 2009. ICRA'09. IEEE International Conference on*, pages 3265–3270. IEEE, 2009.
- [64] P. Pounds, R. Mahony, and P. Corke. Modelling and control of a quad-rotor robot. In *Proceedings Australasian Conference on Robotics and Automation 2006*. Australian Robotics and Automation Association Inc., 2006.
- [65] L. Qing, C. Zhihao, Y. Jinpeng, S. Yun, and W. YingXun. Trajectory tracking control for hovering and acceleration maneuver of quad tilt rotor uav. In *Control Conference (CCC), 2014 33rd Chinese*, pages 2052–2057. IEEE, 2014.
- [66] M. Quigley, K. Conley, B. Gerkey, J. Faust, T. Foote, J. Leibs, R. Wheeler, and A. Y. Ng. Ros: an open-source robot operating system. In *ICRA workshop on open source software*, volume 3, page 5, 2009.
- [67] M. Radmanesh and M. Kumar. Grey wolf optimization based sense and avoid algorithm for UAV path planning in uncertain environment using a bayesian framework. In *2016 International Conference on Unmanned Aircraft Systems (ICUAS)*, pages 68–76. IEEE, 2016.

- [68] M. Radmanesh, M. Kumar, A. Nemati, and M. Sarim. Dynamic optimal UAV trajectory planning in the national airspace system via mixed integer linear programming. *Proceedings of the Institution of Mechanical Engineers, Part G: Journal of Aerospace Engineering*, page 0954410015609361, 2015.
- [69] M. Radmanesh, M. Kumar, A. Nemati, and M. Sarim. Solution of traveling salesman problem with hotel selection in the framework of MILP-Tropical optimization. In *2016 American Control Conference*. IEEE, 2016.
- [70] M. Radmanesh, M. Kumar, and M. Sarim. On the effect of different splines on way-point navigation of quad-copters. In *ASME 2016 Dynamic systems and control conference*. American Society of Mechanical Engineers, 2016.
- [71] M. Radmanesh, A. Nemati, M. Sarim, and M. Kumar. Flight formation of quad-copters in presence of dynamic obstacles using mixed integer linear programming. In *ASME 2015 Dynamic systems and control conference*, pages V001T06A009–V001T06A009. American Society of Mechanical Engineers, 2015.
- [72] M. Radmanesh and I. Samani. IUT MAV2013, Part I: Aerodynamic design of tailless wing and body configuration.
- [73] M. Radmanesh and I. Samani. IUT MAV2013, Part II: flight test results.
- [74] A. Rodić and G. Mester. The modeling and simulation of an autonomous quad-rotor microcopter in a virtual outdoor scenario. *Acta Polytechnica Hungarica*, 8(4):107–122, 2011.
- [75] J. Roldan, D. Sanz, J. del Cerro, and A. Barrientos. Lift failure detection and management system for quadrotors. In *ROBOT2013: First Iberian Robotics Conference*, pages 103–114. Springer, 2014.
- [76] M. Ryll, H. Bulthoff, and P. R. Giordano. Modeling and control of a quadrotor uav with tilting propellers. In *Robotics and Automation (ICRA), 2012 IEEE International Conference on*, pages 4606–4613. IEEE, 2012.

- [77] M. Ryll, H. H. Bulthoff, and P. R. Giordano. First flight tests for a quadrotor uav with tilting propellers. In *Robotics and Automation (ICRA), 2013 IEEE International Conference on*, pages 295–302. IEEE, 2013.
- [78] M. Ryll, H. H. Bülthoff, and P. R. Giordano. A novel overactuated quadrotor unmanned aerial vehicle: modeling, control, and experimental validation. *IEEE Transactions on Control Systems Technology*, 23(2):540–556, 2015.
- [79] E. Samiei, M. Nazari, E. Butcher, and H. Schaub. Delayed feedback control of rigid body attitude using neural networks and lyapunov–krasovskii functionals. In *AAS/AIAA Spaceflight Mechanics Meeting, Charleston, SC*, pages 12–168, 2012.
- [80] A. Sanyal, M. Izadi, G. Misra, E. Samiei, and D. Scheeres. Estimation of dynamics of space objects from visual feedback during proximity operations. In *AIAA/AAS Astrodynamics Specialist Conference, AIAA*, volume 4419, pages 4–7, 2014.
- [81] P. Segui-Gasco, Y. Al-Rihani, H.-S. Shin, and A. Savvaris. A novel actuation concept for a multi rotor uav. *Journal of Intelligent & Robotic Systems*, 74(1-2):173–191, 2014.
- [82] F. Senkul and E. Altug. Modeling and control of a novel tilt-roll rotor quadrotor uav. In *Unmanned Aircraft Systems (ICUAS), 2013 International Conference on*, pages 1071–1076. IEEE, 2013.
- [83] S. Sepasi, R. Ghorbani, and B. Y. Liaw. Soc estimation for aged lithium-ion batteries using model adaptive extended kalman filter. In *Transportation Electrification Conference and Expo (ITEC), 2013 IEEE*, pages 1–6. IEEE, 2013.
- [84] S. Sepasi, R. Ghorbani, and B. Y. Liaw. Improved extended kalman filter for state of charge estimation of battery pack. *Journal of Power Sources*, 255:368–376, 2014.
- [85] S. Shafiei and S. Sepasi. Incorporating sliding mode and fuzzy controller with bounded torques for set-point tracking of robot manipulators. *Elektronika ir elektrotechnika*, 104(8):3–8, 2015.

- [86] J.-J. E. Slotine, W. Li, et al. *Applied nonlinear control*, volume 199. Prentice-Hall Englewood Cliffs, NJ, 1991.
- [87] S. H. Strogatz. *Nonlinear dynamics and chaos: with applications to physics, biology, chemistry, and engineering*. Westview press, 2014.
- [88] E. Stura and C. Nicolini. New nanomaterials for light weight lithium batteries. *Analytica chimica acta*, 568(1):57–64, 2006.
- [89] A. Tayebi and S. McGilvray. Attitude stabilization of a vtol quadrotor aircraft. *IEEE Transactions on control systems technology*, 14(3):562–571, 2006.
- [90] H. P. Thien, T. Mulyanto, H. Muhammad, and S. Suzuki. Mathematical modeling and experimental identification of micro coaxial helicopter dynamics. *International Journal of Basic & Applied Sciences*, 12(2), 2012.
- [91] M. N. Thompson. Flight direction control system for blimps, May 25 1999. US Patent 5,906,335.
- [92] L. A. Zadeh and C. A. Deosar. *Linear system theory*. Robert E. Krieger Publishing Company, 1976.
- [93] Y. Zhang and J. Jiang. Bibliographical review on reconfigurable fault-tolerant control systems. *Annual reviews in control*, 32(2):229–252, 2008.
- [94] Q.-L. Zhou, Y. Zhang, C.-A. Rabbath, and D. Theilliol. Design of feedback linearization control and reconfigurable control allocation with application to a quadrotor uav. In *Control and Fault-Tolerant Systems (SysTol), 2010 Conference on*, pages 371–376. IEEE, 2010.